Evaluation and Optimisation of Traction System for Hybrid Railway Vehicles

By

Tajud Din

A thesis submitted to The University of Birmingham

for the degree of Doctor of Philosophy

Department of Electronic, Electrical and Systems Engineering

College of Engineering and Physical Sciences

University of Birmingham

August 2022

ABSTRACT

Over the past decade, energy and environmental sustainability in urban rail transport have become increasingly important. Hybrid transportation systems present a multifaceted challenge, encompassing aspects such as hydrogen production, refuelling station infrastructure, propulsion system topology, power source sizing, and control. The evaluation and optimisation of these aspects are critical for the adaptation and commercialisation of hybrid railway vehicles. While there has been significant progress in the development of hybrid railway vehicles, further improvements in propulsion system design are necessary.

This thesis explores strategies to achieve this ambitious goal by substituting diesel trains with hybrid trains. However, limited research has assessed the operational performance of replacing diesel trains with hybrid trains on the same tracks. This thesis develops various optimisation techniques for evaluating and refining the hybrid traction system to address this gap.

In this research's first phase, the author developed a novel Hybrid Train Simulator designed to analyse driving performance and energy flow among multiple power sources, such as internal combustion engines, electrification, fuel cells, and batteries. The simulator incorporates a novel Automatic Smart Switching Control technique, which scales power among multiple power sources based on the route gradient for hybrid trains. This smart switching approach enhances battery and fuel cell life and reduces maintenance costs by employing it as needed, thereby eliminating the forced charging and discharging of excessively high currents. Simulation results demonstrate a 6% reduction in energy consumption for hybrid trains equipped with smart switching compared to those without it.

In the second phase of this research, the author presents a novel technique to solve the optimisation problem of hybrid railway vehicle traction systems by utilising evolutionary and numerical optimisation techniques. The optimisation method employs a nonlinear

programming solver, interpreting the problem via a non-convex function combined with an efficient "Mayfly algorithm." The developed hybrid optimisation algorithm minimises traction energy while using limited power to prevent unnecessary load on power sources, ensuring their prolonged life. The algorithm takes into account linear and non-linear variables, such as velocity, acceleration, traction forces, distance, time, power, and energy, to address the hybrid railway vehicle optimisation problem, focusing on the energy-time trade-off. The optimised trajectories exhibit an average reduction of 16.85% in total energy consumption, illustrating the algorithm's effectiveness across diverse routes and conditions, with an average increase in journey times of only 0.40% and a 15.18% reduction in traction power. The algorithm achieves a well-balanced energy-time trade-off, prioritising energy efficiency without significantly impacting journey duration, a critical aspect of sustainable transportation systems.

In the third phase of this thesis, the author introduced artificial neural network models to solve the optimisation problem for hybrid railway vehicles. Based on time and power-based architecture, two ANN models are presented, capable of predicting optimal hybrid train trajectories. These models tackle the challenge of analysing large datasets of hybrid railway vehicles. Both models demonstrate the potential for efficiently predicting hybrid train target parameters. The results indicate that both ANN models effectively predict a hybrid train's critical parameters and trajectory, with mean errors ranging from 0.19% to 0.21%. However, the cascade-forward neural network topology in the time-based architecture outperforms the feed-forward neural network topology in terms of mean squared error and maximum error in the power-based architecture. Specifically, the cascade-forward neural network topology within the time-based structure exhibits a slightly lower MSE and maximum error than its power-based counterpart. Moreover, the study reveals the average percentage difference between the benchmark and FFNN/CNFN trajectories, highlighting that the time-based architecture exhibits lower differences (0.18% and 0.85%) compared to the power-based architecture (0.46% and 0.92%).

ACKNOWLEDGEMENTS

"No one has a problem with the first mile of a journey. Even an infant could do fine for a while. But it isn't the start that matters. It's the finish line."

Julien Smith (2010)

I would like to express my deepest gratitude to my supervisors, Dr Stuart Hillmansen and Prof. Clive Roberts, for their invaluable guidance, supervision, patience, and unwavering support throughout this research. Their wealth of knowledge and experience has been integral to the successful completion of this thesis and has greatly enriched my academic journey.

I am profoundly thankful to Dr Zhongbei Tian for his persistent guidance during my research, particularly for his tailored MATLAB tutorials that facilitated the development of the Hybrid Train Simulator. Additionally, I would like to extend my appreciation to Dr Robert Ellis and Mr Syed Kamil Hashmi for their expert advice and technical support during the early stages of my PhD.

My heartfelt thanks go to my parents and siblings for their unyielding belief in me and for providing outstanding support throughout my life and academic journey. I am especially grateful to my wife, Mrs Noreen Nisar, for her constant love and moral support. I also wish to acknowledge my wonderful sons, Muhammad Arham and Shahabud Din, and my angelic daughter, Anabiya Noor.

Lastly, I am deeply appreciative of all the individuals not mentioned above who have supported and guided me throughout my research. Their contributions have truly played a significant role in the successful completion of this thesis.

To my family,
for their eternal love and support.

TABLE OF CONTENTS

LIST OF TABLES

LIST OF FIGURES

LIST OF ACRONYMS

Term	Explanation
ACO	Ant Colony Optimisation
AC	Alternating Current
ANN	Artificial Neural Network
BP	Backpropagation
CFNN	Cascade Forward Neural Network
R	Correlation Coefficient
DEMU	Diesel Electric Multiple Unit
DE	Differential Evolution
DC	Direct Current
DP	Dynamic Programming
EMU	Electric Multiple Unit
FFNN	Feedforward Neural Network
FA	Firefly Algorithm
GE	Genetic Algorithm
HTS	Hybrid Train Simulator
ICE	Internal Cumbustion Engine
LB	Lower Bounds
MAE	Mean Absolute Error
MSE	Mean Square Error
OHTL	Overhead Trasnamission Line
STS	Single Train Simulator
UP	Upper Bounds

1 INTRODUCTION

1.1 Background

The idea of utilisation of better yet clean energy sources blended with reliability, efficiency, and availability is not new to this world. It is human nature to pursue better, which led us to the rise of hybrid transport vehicles utilising clean and environmentally friendly energy sources. Environmental concerns and rising prices of conventional fuels worked as a pinnacle of diversion towards developing new methods that can decrease the impact on fossil fuels and increase reliance on renewable energy sources. A hybrid vehicle is generally defined as one that operates on two or more power sources [1]. In a hybrid vehicle's typical design, the primary power source can be an internal combustion engine or fuel cell. At the same time, batteries and ultra-capacitors can be secondary power sources [2]. The advancement in the environmental sciences identified the damage which has been and can be caused by conventional energy sources and has panicked the modern world.

The theory of damaging the environment by using fossil fuels due to carbon dioxide & nitrogen dioxide emissions has become a hot topic among energy researchers and enthusiasts in the last decade. Fossil fuels do not only have environmental effects; they are also in limited supply. A rapid increase in energy demand for domestic, industrial and transport vehicles are causing the exhaustion of fossil fuel. It suggests that key energy providers and users such as governments, industrialists and transport sectors seek alternative and reliable energy sources to cut the use of conventional energy sources entirely. Or, in the worst case, to reduce the reliability of fossil fuels and switch to renewable energy sources available in abundance [3-5]. Worldwide energy consumption for residential and industrial sectors has increased gradually in the last decade and accounts for an average of 40–50% of total energy consumption [6]. Around 20% of energy is consumed by the transport sector, produced by fossil fuels and leaving a significant carbon

dioxide footprint. These emissions are mainly released during conventional fuel production for transport vehicles [7]. A recent study shows that the transport sector only produces a considerable 16.2% of emissions in Europe. The most significant contributor is road transport, with 11.9% emissions, aviation with 1.9% emissions, shipping with 1.7% emissions & and railway transport, with only 0.4% emissions [8]. Railway has the advantage of enormously low rolling resistance against traction, allowing railway vehicles to operate at a higher speed while consuming less energy [9].

In the railway transport sector, electricity and diesel fuel are the two primary sources which provide traction to trains. Electricity is a clean and cheap power source used widely in railway vehicles; it does not generate carbon dioxide emissions at the point of use; however, the electrification infrastructure is expensive and is not fully compatible with urban areas. Alternatively, diesel fuel provides continuous power and extraordinary range to railway vehicles at the cost of carbon emissions at the point of use and generation plants [10]. Worldwide, railway vehicles are the most efficient form of the transport system; however, to further reduce the effect of emissions on the environment, members of the International Union of Railways and Community of European Railway Infrastructures decided to reduce energy consumption by 30% and carbon dioxide emissions by 50% in 2030 [11].

These issues with conventional energy sources have been addressed, and hydrogen, as a renewable energy source, has been introduced into the transport industry. In the automotive industry, the combination of gasoline with hydrogen in vehicles has been developed to reduce energy consumption along with dependence on gasoline. These hybrid vehicles equipped with fuel cells produce nearly zero emissions at the point of use in some cases [12]. Researchers are conducting enormous research into using hybrid fuel cells that can generate a few to several kilowatts of power in transport vehicles such as cars, buses, rail vehicles, and ships [13, 14].

The main challenge is using two different power sources to achieve maximum efficiency with minimum energy consumption and cost-effective vehicle production. To achieve this, researchers have used different approaches to seek an optimal speed profile based on the key points of vehicle acceleration, cruising, coasting and braking [15]. Various algorithms can be implemented based on the deterministic system, but an optimal solution cannot be found [16]. Therefore, researchers have shifted their interest toward techniques and strategies based on optimisation algorithms despite the complexity of implementing them in real-time optimisation [17, 18], proving that optimisation-based techniques can produce an optimal or suboptimal solution in real-time [19, 20].

A hybrid energy management solution can be achieved using a numerical algorithm by defining and joining two consecutive constant speed points with a vehicle's traction, coasting and braking. Most researchers have used this approach to a maximum level to find the optimal switching points of different operations followed by optimal vehicle trajectories [21, 22]. Once these key switching points are found, the entire speed profile can be modified optimally, and it has been specifically proven that the optimal strategy exists and is exclusive [23, 24]. To extend the economic life cycle of power sources, a Fuzzy Logic Control strategy is ideal to distribute the exact amount of power from energy sources to fulfil traction power demand [25].

Despite the saturation in research for evolving energy-efficient driving techniques, most of this research work is based on computer simulations, providing only a few practical results [26]. In this modern era, where the transport system is fully automated with the aid of the Driver Advisory System (DAS), the majority of trains are still driven by humans [27] and so lack the performance of a fully optimal propulsion system. Recent implementations of DAS in intelligent railway operations prove the possibility of a successful linkage between theoretical optimisation techniques and real-time operation [11, 28].

It is crucial to optimise the propulsion system and associated power electronic devices installed

onboard to achieve an optimal trajectory and maximise the efficiency of a hybrid traction system. This also includes optimising an energy management strategy that controls energy and power flow through a hybrid traction system [29]. Energy management strategies for railway vehicles have been an active area of research for past decades and have been expanded since the rise of modern hybrid railway technologies [10]. Previous research approaches, and energy management strategies developed are based on mathematical models or the information obtained from vehicle operations static data [30].

There are specific approaches to developing an optimal control strategy for energy and power distribution in hybrid railway vehicles, including linear and dynamic programming [31]. Such techniques do not offer an online solution due to assumptions by the system that the algorithm has known the entire future trajectory. Thus, these algorithms' results can only be used for benchmarking performance for online energy and power control strategies [32]. Considering that the current state of a hybrid vehicle is known, by utilising numerical and metaheuristics optimisation techniques, optimising the operational parameters of individual components in the system can still be very beneficial with limited possibilities [33]. The rule-based strategies for hybrid energy management systems generally translate the driver input and determine the energy distribution between power sources [34].

On the contrary, energy management strategies based on optimisation algorithms utilise stochastic advance driving profiles to minimise energy consumption. They can also convert battery energy into comparable fuel consumption using an electronic collaborative manufacturing approach [35, 36]. This thesis will focus on various practical techniques for optimising hybrid railway traction systems and train trajectories. Train trajectory refers to the planned path or route of a train over a certain distance and time period. It includes information such as the train's speed, acceleration, deceleration, stopping points along the route, energy consumption and power demand. The trajectory is typically designed to optimise various

factors, such as energy consumption, travel time, safety, and passenger comfort. The optimal trajectory may vary based on factors such as the type of train, the track conditions, and the desired outcomes. Various case studies are also performed in this thesis to present the developed techniques as an application for hybrid railway vehicles.

1.2 Objectives

Based on the literature and the research gaps identified in Chapter 2 and Chapter 3, the objectives of the research work presented in this thesis are:

- To design and validate a hybrid train simulator tailored for the study of various propulsion systems and their impact on train movement dynamics.
- To investigate the optimal traction system and trajectory for hybrid trains.
- To investigate the possibility of enhancing the life of power sources and minimising energy consumption.
- To develop and evaluate artificial neural network algorithms for predicting the optimal trajectory of hybrid railway vehicles based on time and power considerations.

1.3 Original Research Articles

1) **T. Din**, Z. Tian, S. Bukhari, S. Hillmansen, and C. Roberts, " *Prediction of the Optimal Hybrid Train Trajectory by Using Artificial Neural Network Models*," IEEE Transactions on Intelligent Transportation Systems, **Submitted.**
2) **T. Din**, Z. Tian, S. Bukhari, S. Hillmansen, and C. Roberts, *" Hybrid railway vehicle trajectory optimisation using a non-convex function and evolutionary hybrid forecast Algorithm*," IET, Intelligent Transport Systems, **Submitted.**
3) **T. Din**, Z. Tian, K. Li, S. Hillmansen, and C. Roberts. (2021) "*Operation and energy evaluation of diesel and hybrid trains with smart switching controls*," Control Engineering Practice, vol. 116, p. 104935, Doi.

4) **T. Din**, S. Hillmansen. (2018), "*Energy consumption and carbon dioxide emissions analysis for a concept design of a hydrogen hybrid railway vehicle*," IET Electrical Systems in Transportation, vol. 8, pp. 112-121, Doi.

1.4 Thesis Structure

The detailed structure of this thesis is set out as follows:

5) Chapter 1 illustrates the detailed background of the research rationale, objectives, and thesis design.
6) Chapter 2 reviews conventional and hybrid railway traction and power supply systems. This Chapter provides a comprehensive technical background behind the hybrid vehicle design demonstrated in Chapter 4.
7) Chapter 3 provides a comprehensive review of the various optimisation techniques. In this Chapter, numerical optimisation, dynamic programming and metaheuristics are discussed. The optimisation techniques presented in this Chapter are used to develop a hybrid optimisation algorithm presented in Chapter 6.
8) Chapter 4 presents the development of a hybrid train simulator. It describes the literature review behind the modelling and simulation of a hybrid traction power system. The simulator is developed by utilising a time-step-based approach to replicate train movement. The HTS developed in this research will carry out all case studies in Chapters 5, 6 and 7.
9) Chapter 5 illustrates the study of hybrid train trajectories. In the case study, automatic switching of power sources is introduced and simulated over a specific route to demonstrate its appropriateness as a hybrid train application. Afterwards, a charging strategy and energy time trade-off for given case studies are presented.
10) Chapter 6 presents the development of a hybrid optimisation algorithm to optimise the traction system of hybrid trains, thus, enhancing the lifetime of power sources and

reducing maintenance costs and energy consumption. The developed optimisation algorithm reflects the techniques discussed in Chapter 3 and a case study demonstrating the application to the hybrid train optimisation problem.

11) Chapter 7 presents the development of two artificial neural networks based on the time and power architectures to predict the optimal trajectory for hybrid railway vehicles centred on the traction power of a hybrid train for any given route.
12) Chapter 8 concludes the main contributions and future work of the research carried out in this thesis.

2 A REVIEW OF RAILWAY TRACTION SYSTEM

2.1 Introduction

Generally, a mechanism that provides propulsion to a vehicle such that the tractive and driving forces are achieved through various devices such as steam engines, internal combustion engines, electric motors etc., is known as a traction system. Like most other vehicles, a railway tractions system provides mechanical power, which is then translated into kinetic and potential energy to overcome the resistive forces against the train [37].

There are specific distinctive requirements for the design approval of a successful train traction system. They are given as follows [38-40]:

- A traction system must be capable of initiating and hauling a designated load over any given route within the recommended timeframe.
- A traction system must have a long service life with minimal maintenance cost.
- A traction system must be fuel-efficient.
- A traction system must be environmentally friendly with lower carbon footprints.

This Chapter introduces three standard railway traction systems: electric, diesel-electric, and hybrid. The AC and DC electric traction system is widely used in the railway industry due to its highly efficient performance with modern power electronics. Both systems required different transmission systems scaled with multiple power control electronics to produce a smooth uninterruptable power supply for the network. Diesel-electric traction systems are still feasible and commonly used on routes that are not covered by electrification. The hybrid traction system has seen rapid development in the past few years. Although most work has been done on hybridisation and using energy storage devices, energy consumption can be reduced along with minimising carbon emissions. Yet, it requires additional development [41, 42].

2.2 Railway Traction System

2.2.1 Electric Traction System

Von Siemens introduced Electric traction for railway vehicles for the first time in 1879 by demonstrating an electric locomotive powered by conventional third rail at an exposition in berlin [43, 44]. At the early stages of the development of the electric traction system, locomotives were equipped with DC motors and were powered by low voltage DC power through the third rail due to their minimal torque control attributes. Subsequently, a high-voltage AC transmission power network is also adopted by electric traction systems due to its integral tractive qualities of induction motors and the complexity of providing power via a DC power network [45]. With the passage of time and development in power electronics, electric traction systems achieved a milestone by implementing an industrial-grade 25kV single-phase transmission network with 50-60 Hz frequency to power railway vehicles in the 1950s [44].

DC traction systems in modern railway systems are equipped with transformers and rectifiers to draw power from local distribution networks [46]. The benefits of using a DC power supply system are control equipment's reduced size and weight and the easy-to-control traction equipment installed onboard. Generally, a traction system for a DC railway is powered with a 600V or 1.5kV DC power supply fed through conductors along the tracks. This system incurs high losses of electrical current due to the flow of higher currents through supply circuits. DC traction systems are ideal for regional railway lines, metros and light railway vehicles [47]. An AC power supply commonly powers high-speed or mainline trains via overhead transmission lines. These transmission lines are located at a certain height from the tracks. The benefit of using an AC power supply system is fewer electrical losses due to higher voltage and less current. The AC traction system also required fewer substations for distribution of power along tracks than the DC power network. Figure 1 presents the general illustration on electric traction system.

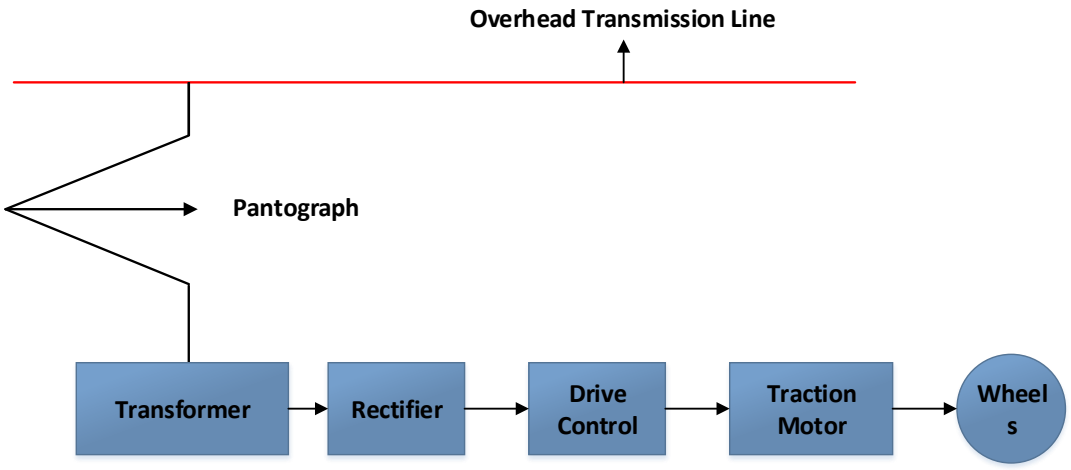

Figure 1: Typical electric traction system illustration

2.2.2 Diesel and Diesel-Electric Traction System

The diesel engine was introduced in 1892 by Rudolph diesel [48]. In the early days of diesel engine development, the diesel engine was considered an application to be used in automobiles complementing the idea of operating a single rail carriage without a locomotive [49]. Multiple gasoline-powered transmission systems were tried, including direct mechanical and electric transmission systems. However, including petrol engines that proved to be inconsistent and not powerful enough, the diesel engine developed for railway vehicles was also a failure [50, 51]. Due to the direct connection between conventional diesel engines and railway vehicle wheels, it is found that diesel engines do not perform well at low speeds, which makes the whole transmission system undesirable [52].

Modern railway vehicles equipped with diesel engines generally transfer power via an electric transmission system due to their high efficiency and accessibility[53]. Modern electric traction systems are equipped with a diesel engine which is used to drive an electric generator. The electric generator produces electric power, which is then transferred to the traction motors installed onboard to move the wheels. Diesel-electric traction systems are inefficient compared to their latest counterparts and less potent while bearing high maintenance and operating costs compared to electric traction systems. The diesel and diesel-electric traction systems are

significant sources of carbon emissions and noise pollution in the railway industry [54]. Figure 2 presents the typical illustration of a diesel-electric traction system.

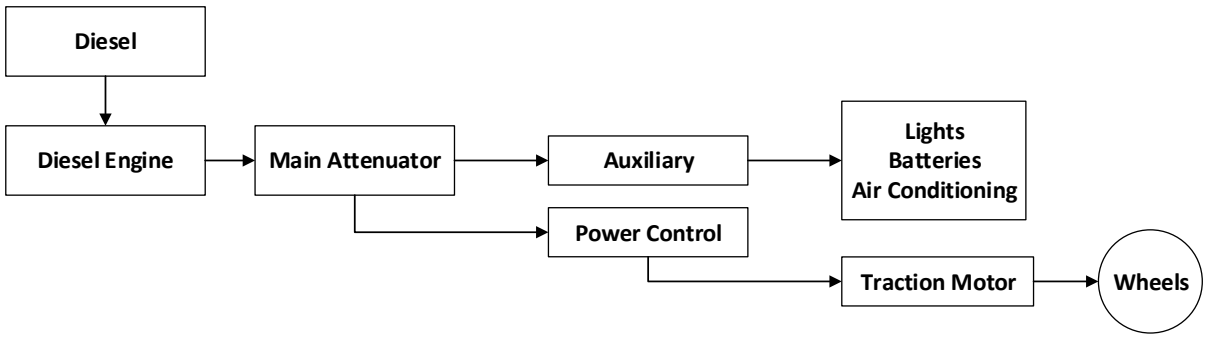

Figure 2: Typical illustration of a Diesel-Electric traction system

Despite its drawbacks, the diesel-electric traction system is more widely used in the British railway sector than the electric tractions system, where only 38% of the railway tracks are electrified [55]. Diesel-Electric traction systems also eliminate the dependency on electrical power, which tends to operate on non-electrified railway tracks. Thus, eliminating the chances of becoming non-operational during the failure modes or maintenance events associated with the electrical transmission network. Diesel-electric traction systems redundant the capital investment required to install and maintain the fixed power supply network considering short-term gains. Railway vehicles equipped with diesel-electric traction systems can provide efficient energy consumption at various speeds when an appropriate power management strategy is applied [41, 56, 57].

2.2.3 Hybrid Tractions System

Generally, a hybrid railway vehicle can be defined as a railway vehicle equipped with two or more power sources on board [58]. A hybrid propulsion traction system comes with various configurations, such as a fuel cell with batteries storage or supercapacitors onboard, a diesel engine with batteries storage onboard or a conventional bi-mode configuration with pantograph and diesel engine onboard [59]. Modern railway systems are widely adopting hybrid traction systems. There are certain advantages of hybrid traction systems over conventional traction

systems, and government legislation recommends railway manufacturers focus on hybrid traction systems for railways. Figure 3 presents the typical model of a hybrid train equipped with a hydrogen fuel cell and a battery pack.

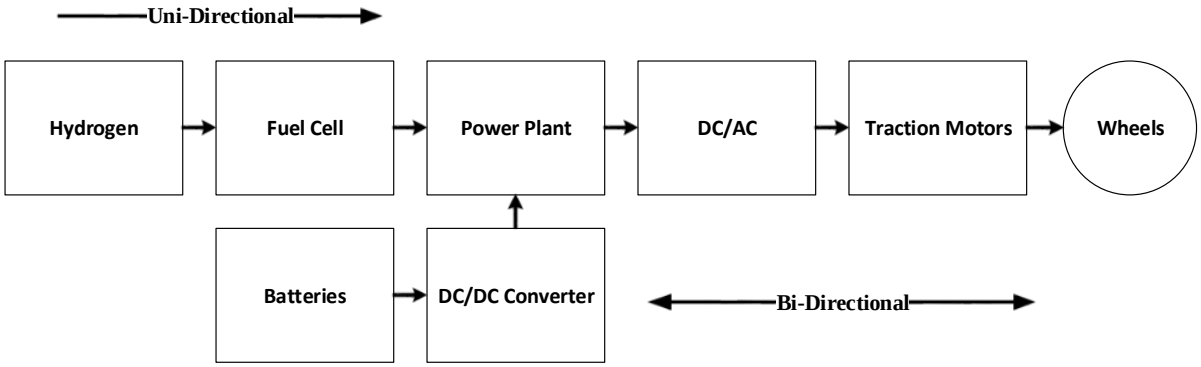

Figure 3: Typical illustration of a hybrid hydrogen train

Hybrid railway vehicles equipped with hydrogen fuel and battery storage have immense advantages. These hybrid vehicles do not produce carbon emissions at the point of use which is incredibly environmentally friendly, thus fulfilling the government's global warming legislation in certain countries [60]. Such hybrid trains are equipped with a regenerative braking system that captures energy while braking during the journey and stores it in onboard energy storage systems that can later be used for traction [61]. Bi-mode trains equipped with electric and diesel traction systems are designed for the high-speed railway system without compromising speed at any track region with or without electrification. Hybrid railway vehicles offer a wide range of efficient energy consumption and power management [62]. Examples of such energy and power management strategies are further discussed in this thesis's Chapters 5,6, and 7.

2.2.4 Traction Drives

Railway vehicles are often equipped with electric traction motors, which generally consist of two types. They are classified as AC and DC motors. Both motors have subclasses with various operating configurations applied according to their railway application [63]. Since successful

development in power electronics, the power supply to electric traction drives is suitably smoothed to achieve maximum efficiency.

Modern DC traction motors are regulated via different voltage supplies. The internal resistance was shorted in series or excited separately to increase the terminal voltage of the DC motors used in railway applications in the early days. A camshaft controller device is used to achieve this, which is still actively used in some railway applications [64]. In modern railway applications, such a task can be completed by using a modern DC-DC chopper converter that regulates a fixed voltage into multiple desired voltages [47].

Alternatively, an AC traction motor with the fundamental capability of regeneration, precipitous speed and torque attributes is considered an appropriate final drive for railway traction applications [65]. This superiority of AC motors over DC motors is achieved mainly by removing the commutator and utilising modern power electronics, which benefit from increased power density and low maintenance [66]. However, AC motors functionality is still complex regarding variable voltages and frequency modulation. However, the advanced power electronic inverter IGBT (Insulated Gate Bipolar Transistor) resolves the issue due to its high-frequency modulation, voltage and current transmission [67].

2.3 Power Supply and Energy Storage System

2.3.1 Hydrogen Fuel Cell

Fuel cells can be defined as a system to convert electrochemical energy into electricity and heat with high efficiency and low toxic emissions [68]. The general structure of a fuel cell is composed of two electrodes: an anode where the fuel oxidation takes place and a cathode where oxidation-reduction takes place. The electrodes are separated by an electrolyte capable of conducting ions, excluding electrons. During the reaction, the electrons released at the anode migrate towards the cathode through a segregated circuit where another semi-reaction occurs.

As a result of this reaction at the cathode, an electric current is generated [69]. Unlike the conventional internal combustion engines that run on gasoline fuels, a fuel cell uses hydrogen as a fuel. Hydrogen is an abundant renewable energy source on Earth [10]. The economic extraction and distribution of hydrogen is currently a substantial challenge. In modern times, various technologies are demonstrated for the extraction of hydrogen. Among these technologies, hydrogen extraction by steam reforming of natural gases is considered extremely cost-efficient, effective, and large-scale use [70]. A chemical reaction that occurs during steam reformation can be expressed by Equation (1.1).

$$CH_4 + 2H_20 + (ENERGY) \rightarrow 4H_2 + CO_2 \quad (1.1)$$

Although the utilisation of hydrogen does not release any carbon emission at the point of its use, it does produce carbon dioxide gas during its production by stream reformation. Alternatively, hydrogen can be made by electrolysis of water, which will avoid the release of any carbon emissions. The positive effect of electrolysis is that the energy required for electrolysis can be achieved by any other renewable energy source, such as solar power, wind power or hydropower [14]. The electrolysis process can be expressed by Equation (1.2)

$$H_20 + (ENERGY) \rightarrow H_2 + \frac{1}{2}O_2 \quad (1.2)$$

Typically, water is oxidised at the anode during electrolysis, producing oxygen, electrons and protons. They circulate cathode, where they are split to form H_2 gas and release negatively charged hydroxide ions which move towards the anode to form O_2 [71, 72]. Figure 4 presents a graphical illustration of a reaction at the anode and cathode in the fuel cell.

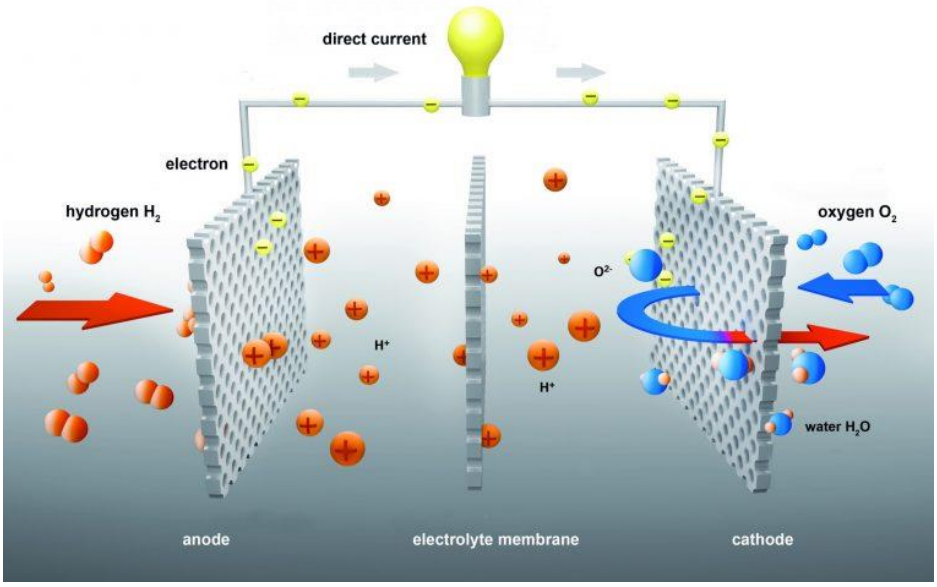

Figure 4: A graphical representation of a reaction at the anode and cathode in a hydrogen fuel cell [73]

Various research presented that fuel cell is a viable power source for railway vehicles [10, 14, 16, 43, 74, 75]. The first development of hydrogen-powered railway vehicles is traced back to 2002, a mining locomotive developed by vehicles projects inc. It was equipped with a 17 kW fuel cell [13]. The demonstration and evaluation successfully laid down a future for hydrogen-powered railway vehicles. At present several demonstrations and hydrogen-powered trains are in service. However, in 2018 Alstom introduced a new hydrogen-powered train known as Coradia iLint, which is being used as a commercial passenger train in Germany and will soon be available in different variants in Poland and Sweden [76].

2.3.2 Traction Batteries

Traction batteries are one of the most anticipated energy storage systems implemented in railway vehicles with advancements in battery technologies [77]. The battery serves many purposes in railway vehicles. Their primary goal in hybrid railway vehicles is to support another power source onboard the train to meet peak power demand. Apart from this, electric trains equipped with batteries provide accessibility to tracks where electrification is impossible.

Similarly, diesel trains equipped with batteries benefit from saving the energy produced by regenerative braking [78]. There are various types of conventional batteries that are used in railway vehicles.

Lead-acid battery (LA): Lead-acid batteries were developed in 1859 by Gaston Plante, a French physicist [79]. It is considered one of the oldest and most successful variants of battery in history. Lead-acid batteries have been improved over time. Although the battery's chemistry has been the same since its invention, few modifications have been made to increase the efficiency and performance of the battery [80]. Lead-acid batteries provide reliable high power for both stationary and mobile applications and still hold the largest share in the market among all battery variants [81].

Nickel-cadmium battery (NiCad): Nickel-cadmium batteries were invented by Swedish engineer Waldemar Junger in 1899 [82]. Compared to lead-acid batteries, nickel-cadmium batteries are utilised in many portable electric devices such as cameras, wireless phones, shavers and other instruments of the same category [83]. They are low-cost and enormously robust. Other advantages of these batteries are their low charging time and regular operation in low temperatures where certain batteries do not operate normally [84]. However, Nickel-cadmium batteries come with the disadvantage of having a very high memory effect and low energy density & specific energy [85].

Nickel–metal hydrate battery (NiMH): Nickel–metal hydrate batteries were introduced in 1990 by the Japanese company Sanyo [86]. Technically, they are similar to the nickel-cadmium battery in chemistry. However, the energy density is appreciably higher compared to NiMH batteries. They were initially used in the first generation of electric and hybrid cars, latter they were replaced with lithium-ion batteries [86].

Lithium-ion battery (Li-ion): A Japanese company known as Sony practically introduced lithium-ion batteries in 1991 [84]. Li-ion batteries are considered to be revolutionalised variant of batteries. The chemistry of Li-ion batteries is entirely different from other types of batteries. It is due to the battery's cathode being made of lithiated metal oxide, and the anode is made of graphite carbon with a layering structure [80]. Some advantages of Lithium-ion batteries are that they do not suffer from memory effects, hold higher energy density and can be used in railway applications. Li-ion batteries operate well within -20C to 60C compared to conventional batteries [87].

2.3.3 Ultra-Capacitors

Ultra-capacitors have been commercially available and underdeveloped since 1990 for vehicle applications [88]. They work on the same principle as any regular capacitor, storing energy between two metal plates in an electric field, unlike batteries which store energy in a chemical reaction [89]. However, ultra-capacitors have a substantially higher energy density but are lower than batteries. Extensive research has been done on ultra-capacitors, which use pseudo capacitive in one electrode and microporous carbon in another [90-92]. This technique immensely increased the energy density of ultra-capacitors. Ultracapacitors, unlike batteries, have a higher life cycle and can sustain deep charging and discharging process. They are more efficient than batteries due to their terminal voltage adjustment by the amount of energy stored and low internal resistance. A light rail vehicle is considered to go through three hundred thousand charging cycles, which is hard to handle by a battery. Therefore, ultracapacitor becomes handy with their extended charging and discharging cycles [93]. Ultracapacitors are an ideal energy source for railway vehicles because they absorb higher inrush currents during regenerative braking, reducing unnecessary stress on batteries [94].

2.3.4 Flywheels

Flywheels are an innovative energy storage technology that has recently gained attention for its potential application in railway systems. They are mechanical devices that store kinetic energy through a rotating mass, which can be quickly released when needed to provide instantaneous power. The fundamental principle behind flywheels relies on the conservation of angular momentum, enabling the conversion of electrical energy into mechanical energy and vice versa [95]. Railway systems can benefit from flywheels, as they can efficiently capture and store regenerative braking energy during deceleration and release it during acceleration or uphill travel, improving overall energy efficiency [96]. Integrating flywheels in railways can reduce energy consumption, minimise peak power demands, and decrease wear on mechanical components [97]. Moreover, flywheels have a fast response time and a long operational life, making them suitable for the demanding operational conditions of railway systems [98].

Several research projects and pilot installations have demonstrated the feasibility and advantages of flywheel technology in railway applications. For instance, the Gyrobus project in Switzerland successfully employed a flywheel energy storage system for an electric bus, showcasing its potential for public transportation [99]. In conclusion, flywheels have promising potential as an effective energy storage solution in the railway industry. Further research and development efforts are required to optimise their integration with existing railway systems and maximize the benefits they can offer in terms of energy efficiency, cost reduction, and environmental sustainability.

2.3.5 Discussion

Various power sources and energy storage devices used in railway vehicles, including hydrogen fuel cells, traction batteries, ultra-capacitors, and flywheels, are discussed in this Section. Each energy storage device has its advantages and disadvantages, influencing its suitability for specific railway applications. Following is a brief comparison of these devices:

Hydrogen Fuel Cells: They are efficient and produce zero emissions at the point of use, but hydrogen's economical extraction and distribution remain a significant challenge. Additionally, carbon emissions are produced during hydrogen production through steam reformation, although electrolysis of water can be a cleaner alternative.

Traction Batteries: Different battery chemistries, such as lead-acid, nickel-cadmium, nickel-metal hydride, and lithium-ion, offer varying levels of energy density, specific energy, life cycle, and operational temperature range. Lithium-ion batteries are currently the most preferred choice due to their higher energy density, no memory effect, and wider operating temperature range.

Ultra-Capacitors: They possess a lower energy density than batteries but have a higher life cycle and can sustain deep charging and discharging processes. Ultra-capacitors are suitable for railway vehicles that require frequent charging and discharging cycles, such as capturing regenerative braking energy and reducing stress on batteries.

Flywheels: These innovative energy storage devices store kinetic energy through a rotating mass and can quickly release it when needed. Flywheels can efficiently capture regenerative braking energy and have a fast response time and long operational life. However, further research and development efforts are required to optimise their integration with existing railway systems.

In conclusion, the choice of energy storage device for railway vehicles depends on the specific application requirements, such as power demand, energy density, life cycle, and operational conditions. By understanding the characteristics and limitations of each device, railway engineers can make informed decisions in designing and implementing sustainable and efficient railway transportation systems.

2.4 Parameters Affecting the Life and Performance of Power Sources in Railway Vehicles

The performance and lifespan of various power sources in hybrid railway vehicles, including diesel engines, batteries, fuel cells, traction drives, and power electronics, are crucial for overall system efficiency and operational costs. Several factors impact their longevity and reliability. This Section discusses the key parameters influencing these power sources' degradation and performance decline.

Diesel Engines: The life of a diesel engine depends on factors such as fuel quality, lubrication, maintenance, and operating conditions. Regular maintenance, including oil and filter changes, is essential for engine longevity [100]. Additionally, using high-quality fuels and lubricants can reduce internal wear and extend the engine's life [101].

Batteries: Battery life is affected by factors such as operating temperature, depth of discharge (DoD), state of charge (SoC), charge/discharge rates, and cycling [102]. Implementing energy management strategies that balance these factors can prolong battery life and maintain system efficiency.

Fuel Cells: The life of fuel cells is influenced by factors such as temperature, humidity, and contamination [103]. Proper water and thermal management are crucial for maintaining performance and extending the life of fuel cells. Furthermore, using high-quality hydrogen and ensuring proper air filtration can prevent contamination-related degradation [104].

Traction Drives: The life of traction drives is affected by factors such as loading, temperature, and vibration [105]. Proper maintenance, including lubrication and regular inspection of bearings and gearboxes, can extend the life of traction drives. Additionally, implementing strategies to minimize mechanical stress and thermal loads can improve reliability [106].

Power Electronics: The life of power electronics is influenced by factors such as temperature, electrical stress, and mechanical stress [107]. Ensuring proper thermal management and protection against over-voltage and over-current conditions can prolong the life of power electronics components. Furthermore, designing power electronics with appropriate mechanical robustness can improve their resistance to vibrations and mechanical stresses [108].

In conclusion, understanding and managing the parameters affecting the life of various power sources in hybrid railway vehicles is crucial for optimising system performance, efficiency, and cost-effectiveness. Developing and implementing smart energy management strategies that take these factors into account can significantly enhance the operational life and reliability of power sources, leading to more sustainable and efficient railway transportation systems.

2.5 Summary

The author presents an extensive review of railway traction systems, traction drives, power supplies, and energy storage alternatives in this Chapter. Both electric and hybrid traction systems are identified as captivating and offering substantial potential in railway applications compared to traditional railway traction systems. The discourse on traction drives indicates that contemporary AC motors are widely employed in railway applications due to their robust and uncomplicated design and energy regeneration capabilities. Efficient energy consumption, onboard energy regeneration in hybrid trains, and zero carbon emissions at the point of use render these systems a more viable and sustainable solution for modern railway systems. Currently, hydrogen is the most suitable renewable alternative to conventional gasoline fuels employed in fuel cells. Technological advancements have demonstrated that fuel cells are more efficient than diesel engines, particularly when integrated with onboard energy storage devices to compensate for energy density. In terms of onboard energy storage options and other power sources, modern lithium-ion batteries have proven to be more potent, reliable, and cost-effective for railway applications.

Despite the extensive literature review on railway traction systems, traction drives, power supplies, and energy storage alternatives, several research gaps and opportunities for future work have been identified. The following gaps indicate the potential for further advancements in hybrid railway vehicle Optimisation, enhancing their performance, sustainability, and efficiency.

Optimisation of Energy Management Strategies: While existing research on hybrid railway vehicles has focused on the design and implementation of various energy storage and power supply alternatives, there is a need for more comprehensive research on the Optimisation of energy management strategies to ensure the efficient utilization of multiple energy sources.

Comprehensive Performance Evaluation of Hybrid Railway Vehicles: Limited studies have been conducted to evaluate the overall performance of hybrid railway vehicles across different operational conditions and scenarios. Future research should focus on the development of performance evaluation frameworks and methodologies that consider various factors, such as energy consumption, emissions, and reliability.

Influence of Operational Parameters and Constraints: There is a need to study the impact of different operational parameters and constraints on the energy consumption, emissions, and overall performance of hybrid railway vehicles. Such research would help identify the most critical factors affecting the performance of these vehicles and guide the development of more effective Optimisation algorithms and energy management strategies.

Addressing these research gaps and opportunities will contribute to the ongoing efforts to improve the performance, sustainability, and efficiency of hybrid railway vehicles. By focusing on these areas, future research can support the development of more advanced and environmentally friendly railway transportation systems.

3 REVIEW OF OPTIMISATION TECHNIQUES

3.1 Introduction

In recent decades, the railway transport system was traditionally designed to operate on conventional fuel sources such as diesel and electricity [109]. Modern legislation against carbon dioxide emissions makes it hard to operate railway vehicles on gasoline. In the past, railway operators and governments tried to resolve it with the electrification of railway tracks, but the major challenge it faced was the high cost of electrification and consequent grid stability issues in urban areas [110]. Nevertheless, owing to the swift expansion of renewable energy systems and the political shift towards clean energy, the railway industry has also directed its attention towards hybrid propulsion systems, enabling railway vehicles to utilise renewable energy sources. Contrary to light road vehicles, designing and operating hybrid trains present more complexity. Hybrid propulsion systems, which comprise hydrogen fuel cells combined with batteries, are increasingly popular in the pursuit of decarbonising railway operations. Such systems are particularly prevalent on lower-traffic density routes where electrification is not deemed viable [111].

Numerous researchers have proposed various configurations for hybrid propulsion systems, and each design varies according to train operating companies' requirements. In one of the proposed configurations, batteries are the primary power source where the fuel cell is used to charge the batteries and provide backup power if required according to the power demand. Another proposed configuration is where the fuel cell is the main power source, and batteries store regenerative power onboard, thus extending the range [112, 113]. Previous studies involving hybrid trains equipped with hydrogen fuel cells and batteries are ideal for routes with frequent stops and minimal gradient of any significance [10, 41]. Due to their suitability for urban, suburban, and military transportation, hybrid propulsion systems are considered an

aspiration for future railway transportation [114]. It has been proven that hybrid vehicles do not put excessive load on the grid due to hydrogen production at times of surplus power which is saved to use later. This method can also help in the reduction of grid fluctuation and helps in controlling the intermittence of renewable systems [115, 116]. Hybrid transportation systems are a multidimensional issue that can be addressed by various aspects such as hydrogen production, refuelling station infrastructure, propulsion system topology, power source sizing, and control. Evaluating and optimizing these aspects is important for adapting and commercialising hybrid railway vehicles [117, 118].

Optimisation in the energy systems field often refers to finding one optimal solution to minimise or maximise the objective function [119]. The optimisation is the process of finding the conditions, i.e., the values of variables, that give the minimum or maximum of the objective function [120]. Optimisation can also be referred to as an improvement. However, both words do not have the same meaning and should be used with care [121]. The general Optimisation problem exists to resolve the minima and maxima of an objective function under specified constraints. Mathematically the objective function can be stated as follows:

$$f(x) = Extreamum$$

w.r.t $$x = x_1 + x_2 + x_3, \cdots, x_n$$

Subject to $$h_i(x) = 0 \qquad i = 1,2,3, \cdots, I$$

$$g_j(x) \leq 0 \qquad j = 1,2,3, \cdots, J$$

In the above Equation $f(x)$ is an objective function to be optimised, $g_j(.) j = 1,2,3, \dots, J$ is an inequality constraint function, $h_i(.)\ i = 1,2,3, \dots, I$ is an equality constraint function, and x is the vector of the independent variables. During the minimization process, the objective function $f(x)$ is also referred to as the "cost function", and during maximization, it is referred to as the "fitness function" [122].

In Chapter 3, $f(x)$ is considered a cost function to be minimised. To simplify, as mentioned in Chapter 2 about the effect of power demand division among power sources on total fuel consumption. Therefore, in this case, the objective function to be minimised is the total fuel consumption, while other immediate constraints should be applied to act as constraints. This study focuses on the identification of utilisation of energy between multiple power sources, i.e. x in the Equation mentioned above, to minimize the total fuel consumption.

Optimisation algorithms have developed rapidly in the past couple of decades, increasing their identification categories. However, they are mainly divided into two main classifications. The first category is numerical optimisation, presented in Section 3.2, and the second category is metaheuristics, shown in Section 3.3. Along with these main categories, the author also employs some modern optimisation techniques to develop a hybrid optimisation algorithm for hybrid railway vehicles, which are categorically discussed in Sections 6 and 7.

3.2 Numerical Optimisation

Numerical optimisation is widely used in power systems where complex problems and large data sets correlate [123]. The attributes of the objective function and comparative constraints intensely affect the numerical optimisation algorithms. Majority of numerical optimisation algorithms workaround on derivative information of the objective functions. It's been noted that numerical optimisation solutions are often predictable due to their deterministic nature of searching pattern and the strategies it implements to solve a problem [69]. Generally, one possible solution is chosen by numerical optimisation at the start of the iterative procedure of solving the problem, which provides only a sub-optimal solution for the non-convex objective function [124].

To solve an optimisation problem via a numerical optimisation algorithm, an initial vector x_0 is required. The algorithm's performance depends on the selection of starting point as it will be

considerably affected by x_o. The algorithm will produce a set of the solution presented as $\{x_j\}_j^{\infty}$. Eventually, given that $|f(x_j) - f(x_{j+1})| \leq n$ is reasonably smaller than the subjectively selected small value, or if there is no decrease attained by generated solution, the optimisation algorithm will be terminated.

In the problem mentioned above, the optimisation algorithm will decide how to generate (x_{j+1}) from the initial vector (x_j) for $j = 0,1,2,\cdots$. The results produced by the objective function (I) at (x_j) or also the results generated by initial iterations $x_0 + x_1 + x_2,\cdots, x_{j-1}$ are used to generate the new optimal solution. The optimal solution produced should be able to reduce the value of the objective function as a result of a limited number of iterations presented as $f(x_j) < f(x_{j-n})$ where $n = 1,2,3,\cdots, j-1$. Usually, line search and trust region are the two most common methods used to select the next candidate point in numerical optimisation algorithms [125].

3.2.1 Line Search Strategy

Based on the simple divide and conquer strategy, line search algorithms try to find all possible solutions from predetermined sets by splitting the problem into more minor problems that are easier to solve. It should be noted that this strategy is very effective, however, given that not every problem is easy to be divided and later combine, thus making the use of the line search strategy limited [123, 125].

In the line search strategy, each iteration generates a search direction x_j and then decides how long to continue the search in the given direction. The exact step size could be very time-consuming during the computation process; therefore, to minimise time consumption, a decent predefined step length will be sufficient [126]. The iteration is presented in Equation (3.1)

$$x_{j+1} = x_j + s_j l_j \tag{3.1}$$

where s_j is the direction of search and l_j is the step length. A suitable and decent selection of step length and direction should be performed to achieve an optimal line search strategy.

The direction $s_j^T \nabla f_j < 0$ of function $f(x)$ is considered to be the proper direction for most of the line search optimisation algorithms. Search direction can also be presented in the form of Equation (3.2).

$$s_j = -N_j^{T-1} \nabla f_j \tag{3.2}$$

where N_j is a symmetric nonsingular and significant positive matrix. ∇ is the first-order partial result of f_j. The line search strategy is further divided into three subcategories based on a different selection of search direction s_j.

Steepest Descent Method: Also known as the "gradient decent method" or "saddle point method", it is the primary type of line search strategy [127]. In this method, N_j is the positive identity matrix I and can be presented as:

$$s_j = -\nabla f_j \tag{3.3}$$

$$x_{j+1} = x_j - \nabla f_j l_j \tag{3.4}$$

Newton's Method: Newton's method is the simplest method for finding the minima and maxima of any univariate function $f(x)$ and is equivalent to finding the roots of its gradient. In newton's method N_j is exact Hessian $\nabla^2 f_j(x_j)$ and the result is zero at minimum or maximum. Newton's method can be presented in the form of

$$s_j^p = -\nabla^2 f_j^{-1} \nabla f_j \tag{3.5}$$

s_j^p may not always be an effective direction since the Hessian matrix $\nabla^2 f_j$ may not always be a significant positive matrix. Equation (3.6) denotes the quadratic function in terms of Δx.

$$\nabla f(x + \Delta x) = \nabla f(x) + \nabla^2 f(x) \nabla x \tag{3.6}$$

where ∇x is a small change in design and $\nabla^2 f$ is the Hessian of the optimisation function (x). According to second-order Taylor's expansion of $\nabla f(x)$ in Equation (3.6). By setting Equation (3.6) to zero, the minima and maxima of the objective function can be obtained. There are two essential conditions to keep x^* as a local minimizer of f and $\nabla^2 f(x)$ being continuous and existing. They are presented as $f(x^*) = 0$ by setting the derivative to zero and $\nabla^2 f(x^*)$ exact minimiser in semi-positive scalar quantity. Thus, providing us with the iterations:

$$s_j = -\frac{\nabla f_j(x_j)}{\nabla^2 f_j(x_j)} \tag{3.7}$$

$$x_{j+1} = x_j - \frac{\nabla f_j(x_j)}{\nabla^2 f_j(x_j)} l_j \tag{3.8}$$

Quasi-Newton Method: Originally developed for positive definite quadratic functions, the quasi-newton method overcomes the issues the original newton method lacks. In quasi-newton method N_j approximates the Hessian $\nabla^2 f_j(x_j)$ and the matrix is updated for every iteration during the optimisation process. For the Quasi-Newton method, the Taylor series can be approximated as:

$$f(x_j + \Delta x) \approx f(x_j) + \nabla f(x_j)^T \Delta x + \frac{1}{2} \Delta x^T N_j \Delta x \tag{3.9}$$

The gradient for optimisation function $f(x)$ can be approximated as:

$$\nabla f(x + \Delta x) \approx \nabla f(x) + \nabla^2 f(x) \Delta x \tag{3.10}$$

It should be noted that the Hessian matric $\nabla^2 f(x)$ may not be the positive matrix. The following iterations will be achieved by setting the above approximation of the gradient to zero.

$$s_j = -\frac{\nabla f_j}{N_j} \tag{3.11}$$

$$x_{j+1} = x_j - \frac{\nabla f_j}{N_j} l_j \tag{3.12}$$

In the quasi-newton method, the derivation of updating procedures is also known as the "secant" Equation [128].

The above-mentioned line search methods focus on the choice of direction s_j at each iteration, as described in [125]. Thus, substituting $s_j^T \nabla f_j$ into Equation (3.13) gives:

$$s_j^T \nabla f_j = \nabla f_j N_j^{-1} \nabla f_j < 0 \tag{3.13}$$

By finding the minimum of $f(x_j + s_j l_j)$ the step length l_j can be determined. It should be noted that the step length is a symmetrical and positive scalar quantity, and to maintain the decent direction l_j is considered to be a positive value. In Equation (3.13), at each iteration s_j is an adequate or decent direction. In the practical optimisation process, finding the absolute minimum of $f(x_j + s_j l_j)$ is computationally costly and needless; therefore, the step length is usually predetermined after certain conditions [129].

3.2.2 Trust Region Strategy

In trust region strategy, a model function $f'(x)$ is constructed by using the information gathered during the process to approximate the behaviour near the current iterative point x_j of the original objective function $f(x)$. The model function $f'(x)$ often does not show an ideal approximation of original function $f(x)$ when there is a long step length between x & x_j, the search is restricted to a newly defined small region around x_j. This newly defined small region is known as the "Trust Region".

The model function $f'(x)$ is usually presented in the form of a quadratic function given in Equation (3.14).

$$f_j'(x_j + l) = f_j + l^T \nabla f_j + \frac{1}{2} l^T N_j l \tag{3.14}$$

where f_j is a scalar function and ∇f_j is a vector objective function. N_j is the Hessian matrix for function f_j. To agree with the first order at the initial iteration x_j, the f_j and ∇f_j are selected to be the function and gradient values at the point x_j. Equation (3.14) is the second-order Taylor Series question of the function f_j while removing the elements comprehending higher derivatives order than 2. Once the trust region and model function are both defined, the desired step l_j is obtained by using Equation (3.15).

$$\min_{l_j} f_j'(x_j + l_j) \tag{3.15}$$

As mentioned before, a trust region with a large range could result in an unnecessary decrease of objective function $f(x)$; therefore, the $(x_j + l_j)$ in Equation (3.15) is declared with the predefined trust region. The trust region can be defined as:

$$\|l_j\|_2 \leq \Delta r_j \tag{3.16}$$

where $\Delta r_j \geq 0$ is a scalar quantity and is also referred to as the trust-region radius.

3.2.3 Summary

In conclusion, both strategies differ from each other concerning the direction and length of the step. In the Line Search strategy, the optimisation algorithm finds the direction s_j initially and afterwards solve $f(x_j + s_j l_j)$ to find the step length l_j. However, finding direction initially is not essential in the Trust Region strategy and does not follow a fixed search pattern. Therefore, it is determined once the step length is found. By utilising Equation (3.16) during the minimisation process, the algorithm will try to identify the maximum step length initially, which is Δr_j and denotes the trust region. Afterwards, it will find the data sets of direction and step length with the most significant reduction of $f(x)$. The trust region will be further shortened if the solution is not optimal in the optimisation process.

3.3 Metaheuristics

3.3.1 Introduction

Numerical optimisation and dynamic programming offer guaranteed optimal solutions for a given problem with finite sizes occurrence. However, the applications with combinative optimisation where the set X is discrete or just as limited, heuristic information is generally used to find optimal solutions at a relatively low computational cost [130]. Such algorithms are usually addressed as metaheuristics. Metaheuristic algorithms avoid the convulsion of local solutions as their flexible nature is very useful in covering a more comprehensive range of optimal solutions in the shortest possible time. Local and global solution strategies characterize metaheuristics. They can be defined as the solution method for a sub-optimal solution that creates a process that cannot be stuck in local optima and perform a robust search of the solution. i-e. a global solution at a moment that is better than or equal to any feasible solution [131, 132].

Metaheuristics are used as general-purpose algorithms that can be applied to various optimisation problems with comparatively fewer variations. The standard methodology of metaheuristics algorithms defines the excellent move from one solution to another at each iteration step of the process, creating or destroying a new solution until the optimal solution is achieved[133, 134]. Over the past years, a variety of successful metaheuristic algorithms have been developed, such as the Genetic algorithm [133-135], Simulated Annealing [136, 137], Guided Local Search [138, 139], the Ant Colony Algorithm [140, 141], Scatter Search [141, 142], Differential Evolution [143, 144] etc.

Metaheuristics are identified into two categories, i-e. constructive and local search-based, in other words, population-based search and single-point search [145]. Single-point search methods tend to present a solution at each iteration of the optimisation algorithm, such as Tabu search and Simulated Annealing. On the other hand, the population-based search method

generates a cluster of feasible solutions known as the population at each process iteration. The Ant Colony Optimisation and Genetic Algorithms exemplify a population-based search.

Metaheuristic algorithms work regardless of the gradient or Hessian matrix of the objective function. This property of metaheuristics gives objective function the ability not to be necessarily constant or differentiable and can have limitations. Metaheuristics are suitable to search for a local optimum for non-convex objective function due to their various abilities to overcome the local optima.

In this Section, the author introduced three metaheuristic algorithms: Genetic Algorithm, Ant Colony Optimisation and Differential Evolution.

3.3.2 Genetic Algorithm:

Genetic Algorithms are inspired by Darwin's theory of evolution [146, 147]. Specifically based on the biological evolution process mentioned in [148]. The genetic algorithm is based on population and constructive metaheuristics. This algorithm has a probable solution to a definite problem on a simple chromosome-like data structure, where every solution communicates with the chromosome, and each constraint characterises a gene. The genetic algorithm utilises an iterative and stochastic operation that works on a population of one or more than one individuals in the system. The genetic algorithm works in five basic steps [149]. Initially, an objective function is encoded with the chromosomes, laying a foundation for the evolution process [147, 150]. In the second step, a fitness function or selection criteria are established. In the third step, an individual population is created [151]. In the fourth step, the evolutionary process iteratively begins during production. The final step decodes the results to achieve the optimal solution. This allows each iteration to present a feasible solution to a given problem, and each iteration is assigned comparatively to the optimal solution. Table 1 shows the pseudo-code for the genetic algorithm.

Table 1: Pseudocode for the genetic algorithm

Genetic Algorithm
// Objective function as an input *P^* //initialisatoin of papulation* *Evaluate (P^*) // computes fitness function* *A_{fo} //Find-Optimal value of (P^*)* ***While x** < maximum iteration or conditions not met **do*** *P_x^* // Mutation of (P^*) during the fourth step* *Evaluate (P_x^*) // computes fitness function* *P^{x+1} // Replacement* ***end while*** *// Optimal solution as an output*

3.3.3 Ant Colony Optimisation:

The ant colony optimisation (ACO) is based on a metaheuristic population-based search method primarily for combination optimisation inspired by the idea of ant foraging and pheromone interaction in building favourable paths [152]. The ACO was first introduced by MIT researcher Marco Dorigo [153]. The ACO algorithms utilise the idea of constructing solutions by probabilities, forming local decisions in sequential order and following the path of the graph. To achieve a low-level solution, it is essential to use the history of past searches in the ACO algorithm. Furthermore, to produce high-level solutions, the ACO adopts a population framework and Monte Carlo-style randomization based on the operation of the calculation performed in the past [154, 155].

Typically, the ACO algorithm can be applied to any combinatory problem. It is an artificial ant that forms a construction operation for defining a complete solution by adding individual elements into a limited solution. Theoretically, in ACO, a constructive graph G = (V, E) can be created from the pool of all feasible solutions where the set of edges E connects to each element in the set of vertices V. During this process, each artificial ant is capable of dealing with constraints and creates solutions while crossing from vertex to vertex along the edges of the graph. Each edge between two vertices is comprised of two sets of information; pheromone information and heuristic information. The pheromone information is a long-term memory

bank of artificial ants that stores the searching history of the process and updates iteratively. On the other hand, heuristic information is a perspective of artificial ants that is directly proportional to the cost of the edge.

Equation (3.17) can be used to illustrate the selection of the subsequent positions during the transversion of ants from vertex to vertex along the edge.

$$p_{ij}^{x} = \begin{cases} \dfrac{\tau_{i,j}^{\alpha}\eta_{i,j}^{\beta}}{\sum_{x_{i,v}} \in M(s^{p})^{\tau_{i,j}^{\alpha}\eta_{i,j}^{\beta}}}, & if \sum_{x_{i,v}} \in M(s^{p}) \\ 0, & otherwise \end{cases} \tag{3.17}$$

where $M(s^{p})$ is the following feasible location of the ant n at vertex i. v is the vertex that hasn't yet select by the ant n. τ is the amount of pheromone accumulated along the edge, η is the suitability of the evolution via edge i,j. α and β are the constraints used to control the comparative importance of pheromone against appropriateness [150]. After initialisation, the ACO algorithm iterates over three main functions given below [156].

1. **Construction**: Each artificial ant builds numerous solutions during this step by mobilizing each vertex in the current region sequentially until a complete solution is constructed. Different ACO algorithms support a variety of rules for the selection of vertex. However, all of them are stimulated by the foraging framework of ants stated in Equation (3.17).
2. **Local Search Function**: The local search function is considered once the construction step is executed. Ideally, the function helps improve the solutions achieved in previous actions and makes the next step more decisive.
3. **Update Function**: The algorithm will balance the pheromone levels associated with each edge accordingly during this step. It will increase the pheromones values for the solution with the best quality and attracts more ants to follow. Furthermore, the pheromone values will be reduced for the wrong or optimal local solution, decreasing the popularity of corresponding edges due to the forgetful nature of some ants. The update function's sole

purpose is to make the optimisation process further efficient by drawing more ants with favourable solutions. Table 2 presents the Pseudo-code for Ant Colony Optimisation.

Table 2: Pseudo-code for Ant Colony Optimisation

Ant Colony Optimisation
// Optimisation Objective Function as an input
Implementing Optimisation Parameter // Initialisation of pheromone tracks
While *set conditions are not met,* ***do***
Construction
Local Search Function
Update Function
end while
// Optimal solution as an output

3.3.4 Differential Evolution:

Differential evolution (DE) is a promising algorithm based on evolutionary techniques known as population-based optimisation. DE was first developed in the 1990s by Price and Storn [157]. The idea behind its development was to produce a natural way of handling continuous variables in the setting of an evolutionary algorithm. DE uses continuous variables rather than discrete variables as compared to other evolutionary algorithms. One major characteristic of DE is that mutations in the algorithm are also established from the group and mating. The rise in mutations is associated with weighted differences in the population members, which forms a type of population-derives-noise [158].

DE algorithm is generally adopted to solve the minimum optimisation problem with the dimensional variables. In the process, at each iteration, the DE will construct a population with the size of S. The population at nth iteration is shown as $p_n = \{Y_{1,n}, Y_{2,n}, Y_{3,n}, \dots, Y_{S,n}\}$. Individual $x(x \in \{1,2,3, \dots, S\}$ at nth iterations represented by a d dimensional vector$Y_{j,n} = y_{j,1,n}, y_{j,2,n}, \dots, y_{j,d,n}$. Mutation, crossover, and selection operations are performed in sequence during this iterative process of DE [159].

There are three significant operations performed during the differential evolutionary algorithm.

1. **Initialisation**: During this stage of operation, the DE will generate the initial population using any generation method. The general utilization function can be written as follows:

$$x_i = (x_1, x_2, \ldots v_{(Nj)} \in P,\ x_i = \begin{matrix} x_{i1} \\ x_{i2} \\ x_{in} \end{matrix} \tag{3.18}$$

where:

x_i is the initial value of the ith component of the population P. Nj represents a different number of vectors x at each iteration. Each vector will go through numerous steps in each generation to produce a new, marginally distinct population.

2. **Mutation Operation**: The mutation function produces a mutation vector at each iteration. This function impacts the performance of DE substantially. A new population trail is built in this stage by using the following Equation (3.19).

$$v_{i,n} = (x_{r1,n}, F_i \times (X_{(r2,n)} - X_{(r3,n)} \tag{3.19}$$

where:

$v_{i,n}$ are the mutation vector, and $r1, r2, r3$ are randomly selected from the population. F represents the weight of generations.

3. **Crossover Operation**: When the mutation vectors are produced in this stage, the crossover operation is applied to the original and mutated vectors to form a new trail vector. The crossover operation can be shown by Equation (3.20).

$$U_{i,n} = \begin{cases} V_{i,n} & if\ random\ number < CR_j \\ X_{i,n} & Otherwise \end{cases} \tag{3.20}$$

where:

$U_{i,n}$ is the nth component of the trailing vector. CR_j is the cross-over speed.

4. **Selection Operation**: In this stage, a better vector is chosen from the original vector once the trailing vector has been achieved, which will survive until the next generation by the

selection operation. The selection of the best vector relies on the input vector, which yields the lowest output. It is then compared with the old population vector X_i and the newly generated trail vector U_i and the better vector is carefully chosen for the new generation of the population. The crossover operation can be shown by Equation (3.21).

$$X_{i,n+1} = \begin{cases} U_{i,n} & if\ fU_{i,n} < fX_{i,n} \\ X_{i,n} & Otherwise \end{cases} \quad (3.21)$$

where:

$fU_{i,n}$ and $fX_{i,n}$ presents the value of the objective function for the trail vector and parent vector, respectively. Table 3 shows the Pseudo-code for Differential Evolution Optimisation.

Table 3: Pseudo-code for Differential Evolution

Differential Evolution
// Optimisation Objective Function as an input
Initialisation Operation
While *set conditions are not met,* ***do***
Mutation Operation
Crossover Operation
Selection Operation
end while
// Optimal solution as an output

3.3.5 Discussion:

In this Section, metaheuristics were introduced, and their characteristics were evaluated. It is concluded that metaheuristics can be characterized into different categories. Following are the rudimentary properties of metaheuristics optimisation algorithms.

- Metaheuristics algorithms tend to have a higher level of strategies for conducting the search process.
- Metaheuristics algorithms are mainly used to overcome shortages created by non-metaheuristic algorithms, such as to explore the search region at a significantly higher rate to find the closest optimal solution available.

- Metaheuristic algorithms are not dependent on specific problem statements as they can solve various problems.
- A primary function of evolution that is relevant to the objective function is required.
- Metaheuristic algorithms are equipped to access the criteria for selection and accept the solution.
- For such algorithms, usually, termination criteria must be set.

3.4 Mayfly Algorithm

The Mayfly algorithm is an evolutionary form of particle swarm optimisation introduced by Konstantinos Zervoudakis and Stelios Tsafarakis in late 2019 [160]. The mayfly algorithm incorporates the critical advantages of the genetic algorithm (GE), firefly (FA) and particle swarm algorithms (PSO) collectively [161]. The particle swarm optimisation algorithm is vulnerable to being stuck in a local optimum while solving high-dimensional complex problems [162]. These vulnerabilities are addressed in mayfly algorithms that efficiently optimise operation across small and large-scale data sets. The term mayfly is derived from the palaeoptera class of insects that mainly appears in the United Kingdom during May every year. During the life cycle of these insects, the juvenile mayflies take several years to grow as aquatic leprechauns until they are seemingly able to the surface as an adult mayflies. The male adult mayflies attract female mayflies by flying a few meters above the water's surface and performing a marital dance. The movement of dances replicates up and down movements creating a specific pattern which is an inspiration for the movement of variables and constraints in mayfly algorithm [163].

The mayfly algorithm models the matting process of mayflies. During the process, it assumes that after hatching, the mayfly becomes an adult, and the healthiest one will survive, ignoring the life expectancy. Mathematically, the location of each mayfly represents the possibility of achieving a suitable solution space. A certain amount of male and female mayflies is generated

randomly, implying that the initial position of search parameters is selected randomly in the search space. And is shown by the positioning vector $L = (l_1, l_2, l_3, \dots, l_n)^p$. The objective function tests the operational performance of this vector. To update the position of mayflies, the speed vector $S = (s_1, s_2, s_3, \dots, s_n)^p$ is utilised, which describes the movement pattern of mayflies on social and individual movement practices. The search parameters update their position based on their own individually tested position. The mayfly algorithm consists of three main components, which are described below.

3.4.1 Movement of male mayflies

Since it has been established that male mayflies update their position according to social or individual experiences, it can be expressed mathematically as:

$$l_i^{t+1} = l_i^t + s_i^{t+1} \tag{3.22}$$

where l_i^t is the position of the i^{th} mayfly within the range of r_{min} and r_{max}. l_i^{t+1} and s_i^{t+1} is the position and speed of mayflies, respectively, in the next time step. Due to the nuptial dance of male mayflies a few meters above the water surface, mayflies do not achieve high speeds and move at a constant pace. Their speed can be expressed as:

$$s_{ij}^{t+1} = s_{ij}^t + k_1 exp^{\alpha d_i^2} \times (lbest_{ij} - l_{ij}^t)) + k_2 exp^{\alpha d_2^2} \times (gbest_j - l_i^t)) \tag{3.23}$$

where k is constant for favourable attraction used to scale the shares of both cognitive and social elements. α is the limiting factor of the distance between two mayflies. d presents the cartesian distances between the mayfly position with $lbest$ the best current position and $gbest$ is the j^{th} position component of the fittest male mayfly. To solve the minimisation problem, the current best position $lbest_{ij}$ at next time step can be calculated as:

$$lbest_{ij} = \begin{cases} l_i^t, & f(l_i^{t+1}) < f(lbest_i) \\ lbest_i, & f(l_i^{t+1}) \geq f(lbest_i) \end{cases} \tag{3.24}$$

To define the quality of the optimal solution, $lbest_{ij}$ can be used as an objective function. As mentioned in Equation (3.23), the cartesian distances (d_1 and d_2) between the present and previous best position of mayflies can be expressed as:

$$\|l_i - L_j\| = \sqrt{\sum_{j=1}^{n}(l_{ij} - L_{ij})^2} \tag{3.25}$$

where l_{ij} presents the location of j^{th} element of i^{th} mayfly and L_i is either $lbest_i$ or $gbest_i$. To continue achieving optimal results, the fittest mayflies must continue the nuptial dance in up and down movements, and in doing so, the healthiest mayfly must produce a variance within their speed that provides an additional random feature to the algorithm, which can mathematically be written as:

$$l_{ij} = s_{ij}^t + \delta * \mathrm{R} \tag{3.26}$$

where δ is the nuptial dance coefficient, and R is the additional random value within the range of $(-1,1)$.

3.4.2 Movement of female mayflies

Comparatively, female mayflies have a different pattern of movement. Biologically adult mayflies only survive for one to seven days only. Therefore, the female mayflies are slightly faster in finding the fittest male mayflies to mate and reproduce. The velocity of the female mayfly is directly proportional to the speed of the male mayfly they want to breed. Given that q_i^t is the current location of the i^{th} female mayfly in the search region at a time step t, the position of the female mayfly will change by the addition of q_i^{t+1} to the current location and can be expressed mathematically as:

$$q_i^{t+1} = q_i^t + s_i^{t+1} \tag{3.27}$$

It is possible to randomise the attraction process of male and female mayflies. However, in this case, it is implemented as a predetermined process based on fitness function; thus best female attracts the best male mayfly, and the second-best female attracts the second-best male mayfly. The facilities during the attraction process can be calculated by Equation (3.28):

$$s_i^{t+1} = \begin{cases} s_{ij}^t + k_2 exp^{\alpha d_{mf}^2} \times (l_{ij}^t - q_{ij}^t), & f(q_i) > f(l_i) \\ s_{ij}^t + \vartheta \times r, & f(q_i) \leq f(l_i) \end{cases} \quad (3.28)$$

where q_{ij}^t presents the position and s_{ij}^t presents the speed of i^{th} female mayflies in the j^{th} dimension at the time step t. The distance between male and female mayflies is shown by d_{mf}^2. ϑ is the walk coefficient chosen randomly and is used by the female mayfly when she is not attracted by any male mayfly. Therefore, it flies erratically across the search regions within the range of $(-1,1)$ and is represented by r in Equation (3.28).

3.4.3 Matting of mayflies

The crossover operator covers the matting process between male and female mayflies. From the mayfly's population, one male and one female parent mayfly are selected in the same behaviour as they were attracted to each other. The selection process is generally based on cost function or randomised. Afterwards, the selected mayflies breed with each other in a pattern of the first best female breeds, the first best male mayfly, and so on. As a result, offspring are produced, which are expressed in Equations (3.29) and (3.30):

$$\delta_1 = \partial \times male + (1 - \partial) \times female \quad (3.29)$$

$$\delta_2 = \partial \times male + (1 - L\partial) \times female \quad (3.30)$$

where ∂ presents the random value in a given range, δ_1 and δ_2 represents the offspring 1 and 2, respectively. Male and female present parents mayflies and the initial speed of offsprings are set to zero.

3.4.4 Discussion

This Section presents a contemporary optimisation algorithm called the Mayfly Algorithm. The Mayfly Algorithm employs a population-based approach, integrating features from other notable metaheuristic algorithms. It mimics the behaviour of adult mayflies, encompassing processes such as crossover, mutation, swarming, nuptial dance, and random walk. A key aspect of the Mayfly Algorithm is the use of distinct Equations for each male and female population, enhancing exploration capabilities. The foundation of the Mayfly Algorithm will be utilised in Section 6 to develop a hybrid optimisation algorithm tailored explicitly for hybrid railway vehicles, as proposed by the author in this thesis. The overall flowchart of the Mayfly algorithm process is presented in Appendix A, Figure 34.

3.5 Dynamic Programming

Dynamic programming is an exhaustive search and appropriate method for solving a wide range of search and discrete multi-stage decision optimisation problems. It was initially developed in 1950 and later refined by American mathematician Richard Bellman [164, 165]. Dynamic programming works on an old strategic technique known as divide and conquer. The original problem must be divided into isolated sub-problems and solved by each subproblem recursively. The optimal solutions to subproblems can produce an optimal solution to the actual problem [166].

3.5.1 Mathematical Presentation

The objective function for the dynamic programming method can be presented for the "n" decision process as:

$$k(f_1, f_2, \ldots, f_n) = M_1(f_1) \bullet M_2(f_2) \bullet \ldots \bullet M_n(f_n) \tag{3.31}$$

And the sub cost function can be presented as:

$$M_i = j_m(x_i) \bullet j_p(x_i, f_i) \tag{3.32}$$

where:

f_i is the decision made by the algorithm at time i;

x_i presents the system state at the time i and is allocated by the decision set $(f_1, f_2, \ldots, f_{i-1})$;

j_m is the cost function of the system and is generated due to the system's state x_i;

j_p presents the system shift function due to the system state x_i and f_i;

$(\bullet)$ presents the associatory binary operation of the algorithm, such as the addition or multiplication operation.

Dynamic programming aims to minimize the objective function k by utilising the set of decisions $\{f_1, f_2, \ldots, f_n\}$. If Δ_i presents the processed decision calculations at the nth stage, F^* signifies the optimal decision set $\{f_1^*, f_2^*, \ldots, f_n^*\}$ solved by the objective function presented in Equation (3.31) at its maximum output and O^*denotes the minimum output of the objective function.

$$O^* = k(F^*) = k(f_1^*, f_2^*, \ldots, f_n^*) \tag{3.33}$$

To find F^* multiple methods can be applied. However, the most natural way would be using the "Brute Force" method. The brute force algorithm can find all possible combinations of possible solutions at every stage and choose the most optimal solution produced by each combination. Implementing this method to substantial problems can cause excessive computational complications. However, for minor problems, it's very cost-effective and possible.

The ideal way would be to divide the problem into small problems. Then solve each problem by initially optimizing the sub-objective function and then achieving the optimal solution for the entire problem. The problem has various stages of decision-making. It is instinctive to divide the problem into steps to ease decision-making.

$$O^* = min_{(f_1,f_2,\dots,f_n)\in\Delta}\{k(f_1,f_2,\dots,f_n)\} = min_{f_1\in\Delta_1}\{min_{f_2\in\Delta_2}\{\dots\{min_{f_n\in\Delta_n}\{k(f_1,f_2,\dots,f_n)\}\dots\}\} \quad (3.34)$$

where:

$\Delta = \Delta_1 \times \Delta_2 \times \dots \Delta_n$ and $f_i \in \Delta_i$ are presented as sequential decision processes[166].

In dynamic programming, the decision-making process is entirely based on previous decisions made by the algorithm, i-e.

$$\Delta_i = f_\Delta(\Delta_1, \Delta_2, \dots \Delta_{(i-1)}) \quad (3.35)$$

Equation (3.35) above states that the stages in the decision process are defined by the decision made by the algorithm in the past. Equation (3.34) presents that each minimum function can be established to find an optimal solution to the sub-problem.

$$min_{(f_i\in\Delta_i}\{k(f_1,f_2,\dots,f_{i-1},f_i,f_{i+1},\dots,f_n)\} = min_{f_i\in\Delta_i}\{k(f_1,f_2,\dots,f_{i-1},f_i,f_{i+1}^*(f_i),\dots,f_n^*(f_i))\} \quad (3.36)$$

In Equation (3.36) above, minimisation processes at the "ith" stage are shown, which are used to find the optimal solution strategy to minimize the cost incurred due to the decision set $(f_i, f_{i+1}, \dots, f_n)$ and f_i is shown as the cost-to-go function [167]. Assuming that the function $f(x_i)$ represents the solution for the cost-to-go function where $(f_i, f_{i+1}, \dots, f_n)$ are yet to be produced subsequently, and $f_{(x_i)}^*$ implies the optimal solution to the objective function. We have:

$$f_{(x_i)}^* = min_{\Delta_i}\{min_{\Delta_{i+1}}\{\dots\{min_n\{M_i(x_i,f_i) \bullet M_{i+1}(x_{i+1},f_{i+1}) \bullet \dots \bullet M_n(x_n,f_n)\}\}\dots\}\} \quad (3.37)$$

Substituting Equation (3.31) into (3.34) will give:

$$O^* = min_{f_1\in\Delta_1}\{min_{f_2\in\Delta_2}\{\dots\{min_{f_n\in\Delta_n}\{k(f_1,f_2,\dots,f_n)\}\}\dots\}\} \quad (3.38)$$

$$= min_{f_1 \in \Delta_1} \{M_1(x_1, f_1) \bullet min_{f_2 \in \Delta_2} M_2(x_2, f_2) \bullet \ldots \bullet$$

$$min_{f_n \in \Delta_n} \{M_n(x_n, f_n)\} \bullet\}\} = min_{f_1 \in \Delta_1} \{M_1(x_1, f_1) \bullet f^*(x_1)\}$$

Since $O^* = f^*(x_1)$ in the above Equation (3.38) can be solved iteratively.

3.5.2 Elements of Dynamic programming

Typically dynamic programming can be applied to any optimisation problem, which must present two essential elements, i.e. overlapping subproblems and optimal substructure [168].

3.5.3 Overlapping Sub-problems

Overlapping sub-problems can be defined as the process in which the algorithm solves the same sub-problem repeatedly to solve a given problem is said that the given problem has overlapping sub-problems.

Dynamic programming adopts the general methodology of solving the problem by creating sub-problems, solving each sub-problem only once and storing the results into the lookup table where the solution to the problem can be obtained. This method eliminates the possibility of solving the same problem repeatedly. Hence, reducing the computation time. The storing process in dynamic programming is called memoisation [169].

3.5.4 Optimal Sub-Structure

The optimal substructure is when a problem exhibits an optimal solution to the problem, which contains the optimum solution to the sub-problems, regardless of initial conditions and choices made over the periods of solving the problem.

In a problem where the optimal solution of sub-problems is the optimal solution to the original problem, it satisfies the principle of the optimal substructure. This dynamic programming property is based on the bellman principle of optimality [164]. Dynamic programming methodology is based on the sequence problem solving linked with the previous optimal solution to the sub-sequence. This bottom-up approach precedes dynamic programming to

move forward from small sub-problems to bigger sub-problems to achieve a solution to the given problem.

3.5.5 Discussion

It is concluded that dynamic programming solves the problems in a bottom-up fashion, where the simple problems will be initially solved before they move to complex problems. Solving complex problems usually takes exponential time to find the optimal solution. To rectify this issue, dynamic programming provides an excellent solution. Dynamic programming offers a guaranteed solution to combinatory optimisation problems with limited sizes occurrences.

3.6 Hypothesis Development

The existing literature offers a wealth of information on energy-saving strategies for railway systems, with a focus on optimising train driving profiles to reduce traction power and energy consumption or maximize the energy recovered through regenerative braking systems. However, there is a noticeable gap in the literature regarding the optimisation of hybrid train trajectories, particularly when considering the complex interplay between linear and non-linear constraints of hybrid railway vehicles and the proper distinction between different power sources.

Based on the in-depth analysis of the literature in Chapters 3, 6 and 7, it is evident that previous research has explored optimisation, railway traction, and power supply simulation to a significant extent. However, the techniques employed in these studies are often conventional or rules-based, which may not be suitable for modern hybrid railway systems. This suggests a need for dedicated optimisation techniques that can effectively handle the linear and non-linear data sets associated with hybrid train operations.

In light of these research gaps, this thesis proposes the following hypothesis:

A system-level Optimisation approach can be developed and applied to enhance the energy efficiency of hybrid railway vehicles, leading to improved operational performance and environmental sustainability.

To address this hypothesis, the following research objectives are proposed:

- Develop a simulation tool to evaluate the energy consumption and power demand of hybrid railway vehicles, taking into account the unique characteristics and constraints of these systems.
- Model the hybrid railway vehicle traction system, focusing on the interactions between different power sources and energy storage devices, as well as the effects of various operational parameters on system performance.
- Investigate modern optimisation algorithms and artificial neural networks for their applicability to hybrid train energy optimisation while also considering the potential adaptation of previous Optimisation techniques used for conventional railways.
- Conduct case studies to demonstrate the feasibility and effectiveness of the proposed system-level Optimisation approach for hybrid railway vehicles, highlighting the energy efficiency improvements that can be achieved through this methodology.

By addressing these research objectives, this thesis aims to make a significant contribution to the field of hybrid railway vehicle Optimisation, offering novel insights and practical solutions for enhancing the energy efficiency, operational performance, and environmental sustainability of these systems.

3.7 Summary

This Chapter reviewed the optimisation techniques such as numerical optimisation, metaheuristic algorithms, mayfly algorithm, and dynamic programming techniques. A detailed introduction to numerical optimisation is introduced in Section 3.2. The research highlights

that the numerical optimisation technique is ideal for solving non-linear optimisation problems by utilising true region and line search strategies. Section 3.3. illustrates the metaheuristics focusing on genetic algorithms, ant colony optimisation and modern differential evolution optimisation. It is concluded that dynamic programming can solve huge optimisation problems due to its characteristic of breaking down problems into subproblems and solving them subsequently. This technique is prevalent in modern optimisation algorithms.

The comprehensive review of optimisation techniques presented in this Chapter, including numerical optimisation, metaheuristic algorithms, the mayfly algorithm, and dynamic programming techniques, reveals several research gaps and opportunities that can be further explored to enhance the optimisation of hybrid railway vehicles and are mentioned as follows:

Hybrid Optimisation Techniques: Although various optimisation techniques have been individually explored, there is potential for research on developing and implementing hybrid optimisation techniques that combine the strengths of multiple approaches. This could lead to more effective and efficient optimisation algorithms for hybrid railway vehicle energy management and operational performance.

Adaptation of Optimisation Techniques for Hybrid Railway Vehicles: Many optimisation techniques have been widely used in other fields, but their direct application to hybrid railway vehicle optimisation may require further refinement and adaptation to address the unique characteristics and constraints of railway systems. Future research should focus on tailoring these techniques to better suit the specific requirements of hybrid railway vehicles.

Comparison and Benchmarking of Optimisation Techniques: Limited studies have been conducted to compare and benchmark the performance of different optimisation techniques in the context of hybrid railway vehicle optimisation. This could provide valuable insights into

the most suitable Optimisation methods for various scenarios and problem formulations, guiding researchers and practitioners in selecting the best approach for their specific needs.

Scalability of Optimisation Techniques: As hybrid railway vehicles become more complex and incorporate a greater number of energy sources, storage devices, and subsystems, the scalability of existing optimisation techniques should be investigated. Future research should aim to develop optimisation algorithms capable of handling large-scale and high-dimensional optimisation problems while maintaining computational efficiency.

Real-Time and Adaptive Optimisation: In real-world railway operations, various factors, such as traffic conditions, passenger demand, and energy availability, can change dynamically. Developing optimisation techniques that can adapt to these changes in real-time would significantly enhance the performance and reliability of hybrid railway vehicles. This requires research on real-time optimisation algorithms and adaptive energy management strategies that can respond effectively to dynamic operating conditions.

By addressing these research gaps and opportunities, future work can contribute to the development of more advanced optimisation techniques specifically tailored to the needs of hybrid railway vehicle optimisation. This will ultimately lead to improved energy efficiency, operational performance, and environmental sustainability of railway transportation systems.

4 DEVELOPMENT OF A HYBRID TRAIN SIMULATOR

4.1 Introduction

Simulation is generally defined as a method of replicating the behaviour of an event or operation via a suitably comparable situation or mechanism, typically for research or training purposes [170]. Technology has significantly evolved in recent decades, and modern computer technology allows access to any outcome of research or training operation with different scenarios. Simulations also provide a sustainable and cost-effective technique and information beforehand to engage in the physical development of any project. Various researchers have investigated railway systems via train movement simulators. Such as a general purpose model based on the algebraic structure to describe train movement was developed by Taylor and Petersons in 1982 [171]. Later, in 1995, Leachman and Dessouky introduced a simulator to analyse the traffic congestion on the railway track from downtown Los Angelos to San Pedro Bays [172]. A most recent multiple train simulator developed by Ning is capable of analysing various train movements on different railway lines with different singling systems, traction performance and speed limits [173].

Previous railway trajectory simulation studies [174-178] are usually based on conventional railway vehicle models and movements. Most of the designed simulations only consider the linear components of modelling the vehicle. Thus, making them incompetent to simulate a hybrid railway vehicle. This Chapter presents the development of a hybrid train simulator. It is an expanded version of the studies that resulted in the paper "*Operation and energy evaluation of diesel and hybrid trains with smart switching controls*," published in Control Engineering Practice, for which the author was the primary contributor and the lead author.

A Hybrid Train Simulator (HTS) based on the time domain has been developed in MATLAB. The simulator can analyze hybrid train movements on various railway routes with traction

performance, customized speed limits and multiple power sources. The HTS scales multiple power sources according to journey requirements and real-time energy demand

The hybrid train simulator (HTS) is developed using Lomonoff's Equation [41]. The detailed schematic of HTS is shown in Figure 5.

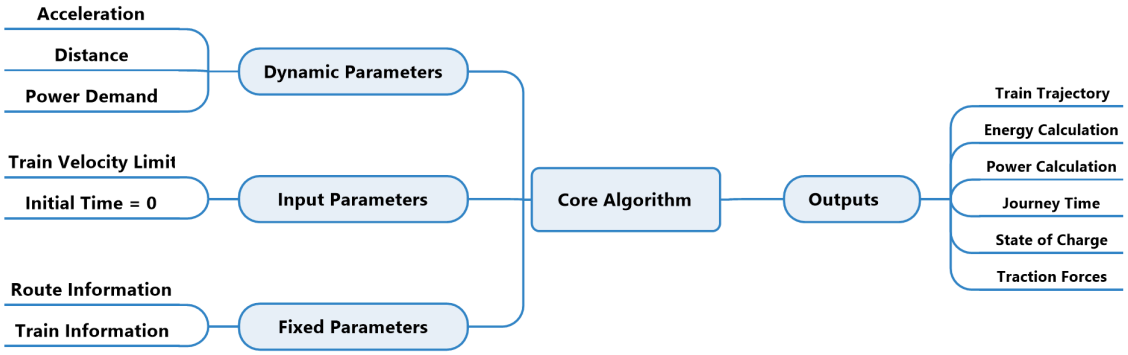

Figure 5: Block diagram of hybrid train simulator (HTS)

The hybrid train simulator process is broken down into four Sections.

1. **Journey Profile:** The journey profile includes track information, the geographical position of the train, speed limits and the station's location. The journey information is stored in the lookup tables and retrieved before the simulation is initiated. Journey profile components are considered as the fixed input parameters.

2. **Operating Control Input:** The HTS obtains the acceleration and power demand of the train from the information saved in the journey profile, then injected with control input "driving style" during the train journey at each step of the simulation process. These parameters are considered dynamic due to their adaptive nature.

3. **Core Algorithm:** The core algorithm performs the main calculations and obtains the state change based on the present state, and so on, until the final condition is met.

4. **Outputs:** The results achieved from the core algorithm are stored in the output block. These results are saved at each time step incorporating every state of the train during the journey. The output block produces results such as energy consumption, power demand,

traction forces, journey time and train trajectory, state of charge of the battery and hydrogen levels at various stages of electric components onboard the train.

4.2 Vehicle Modelling

Applying the fundamental physics law of vehicle motion is crucial for any train movement simulation. Lomonosoff's Equation is widely used in the simulation of railway vehicle motion, based on Newton's second law [47]. The complete differential Equation describing the train moment can be written as [179]:

$$M_t(1+\lambda)\frac{d^2s}{dt^2} = T_{effort} - \left[C\left(\frac{ds}{dt}\right)^2 + B\left(\frac{ds}{dt}\right) + A\right] - M_t\, g\sin(\alpha) \tag{4.1}$$

4.2.1 Adhesion

Adhesion can be defined as a constraint of tractive effort generated by the powered axles. The adhesion of resistive forces also plays a vital role in vehicle dynamics and shall be deemed before calculating the tractive force. On a flat track, the adhesion limit assuming the maximum accessible tractive effort is shown in Equation (4.2)

$$Tractive\ effort_{max} = \mu M_t g \tag{4.2}$$

where μ is the friction coefficient, M_t is the total mass of the train, and g is the gravitational acceleration. If the coefficient of friction value drops excessively low, an adverse wheel slip may occur, which will cause a wastage of energy and prevent increasing the train speed [53]. Previous studies [180-182] performed using full-scaled and scaled roller rig shows that the coefficient of friction μ does not differ for a clean and dry wheel surface. The μ will drop excessively to a low level and will be maintained with the increase in speed of the train if the surface of the track or wheel is covered with oil. However, the μ will decrease with the train's speed if the surface of the track or wheel is covered by water.

Increasing the number of motor-powered axles is common among train manufacturers To achieve maximum tractive force [183]. Equation (4.3) shows the maximum acceleration on a flat track.

$$\frac{s}{t^2} = \mu g k_d \tag{4.3}$$

where μ is the coefficient of friction, g is gravitational acceleration, s is distance, t is time and k_d is the ratio between motor-powered axles and the total number of axles.

It is important to understand that the friction coefficient is generally considered independent of the vehicle's speed. However, realistically a slight decrease occurs at high speeds of vehicles [184].

4.2.2 Resistance

Multiple resistive forces counter the train's movement at a levelled track [185, 186]. The overall resistance of a train on a flat track is presented in Equation (4.4)

$$R = Cv^2 + M_t(A + Bv) + \frac{D}{r} \tag{4.4}$$

where A, B, C & D are empirical constants associated with rolling resistance. M_t is the mass of the train, v is the velocity of the train, and r represents the radius of track curvature. The constants mentioned in Equation (4.4) can be calculated by using empirical methods. It is observed that the term $\frac{D}{r}$ used to calculate the curvature of the track has lesser-known effects when the train speed is less than 200 km per hour [187]. Therefore, the effect of mass and the rise in resistance anticipated to track curvature is negligible and can be presented as:

$$R = Cv^2 + Bv + A \tag{4.5}$$

where v is the speed of the train and the constants C, B, A are also referred to as the Davis coefficients [187].

4.2.3 Vehicle Traction Design

The force required to carry the load is known as tractive effort. Tractive effort is a complicated non-linear function of the coordinates that characterise the vehicle's speed, which is apprehended in the contact of the wheel and track surface. Tractive effort depends on the driving torque of the traction motor via a mechanical reducer which creates driving torque on the tooth gear and is located at the axle of the wheelset. Tractive effort for a traction motor can be written as:

$$T_k = T_{effort} * \mu * \eta_k \tag{4.6}$$

where T_{effort} is a tractive effort, T_k is a torque on the tooth gear, η is the transmission ratio and η_k is the efficiency of the tooth gear.

4.2.4 Force Due to Gradient

Force due to gradient is an essential component in vehicle design. It shows the effect of the gradient profile of a route and the acceleration due to gravity. If the vehicle moves uphill, it obtains a negative gravity acceleration element against the direction of vehicle movement. However, when a vehicle moves downhill, it obtains a positive acceleration element [173]. Force due to gravity can be written as:

$$F_g = M_t g sin(\alpha) \tag{4.7}$$

where M_t is the total mass, and α is slope angle.

4.2.5 Effective Mass

The moment of inertia, also known as the rotational allowance, is one of the crucial properties used in developing a vehicle. It measures vehicle resistance to angular acceleration, which increases with accelerated train mass and is shifted by the gear ratio and wheel diameter. The calculation of inertial properties is based on the actual weight and dimensions of various parts of the vehicle [188]. To improve the accuracy of vehicle simulation, the moment of inertia is

considered in the calculation of effective mass by using rotary allowance. Effective mass can be calculated by:

$$M' = M_t(1 + \lambda) + M_{load} \tag{4.8}$$

where M_{load} is passenger load, and λ is a rotary allowance.

4.2.6 Modes of movements

Four typical movement modes are considered in the development of HTS [189] [190]. They are presented below:

- **Acceleration Mode:** High power is used to move the train from low speed to high speed, overcome the effects of resistance and gravity, and accelerate it to the required rate.
- **Cruising Mode:** Moderate power keeps the train at a constant speed. In this mode, train acceleration is zero.
- **Coasting Mode:** Power is shut down in this mode; speed from the first two modes moves the train while the route's resistance and gradient help the train's movement. In the case of an uphill route, the train will slow down to the point where the braking event will take place, while in the case of a steep downhill route, the train will still accelerate unless intervened.
- **Braking Mode:** In this mode, a braking event occurs, where service brakes are applied to reduce the train speed from higher velocity to stand still.

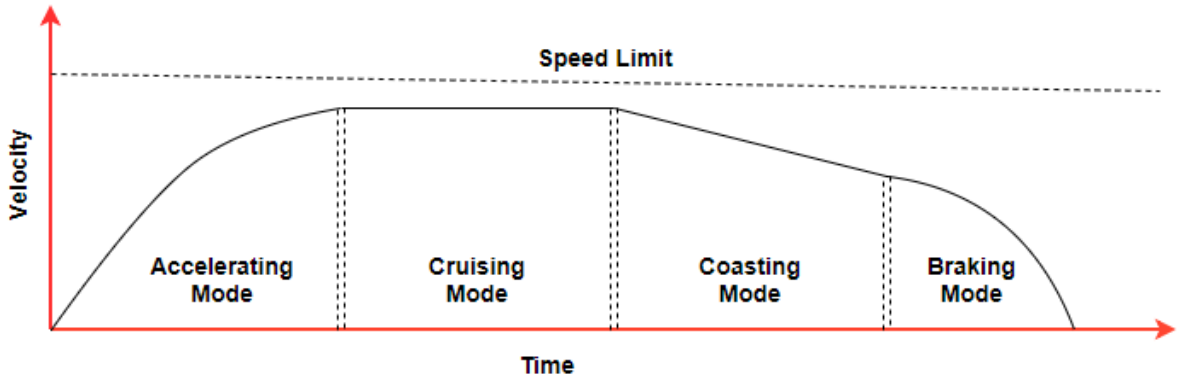

Figure 6: Four modes of movement of the vehicle

4.3 Simulator I/O Description

Various factors are considered in selecting driving control modes, such as the maximum train speed, target speed, track speed limit, headway distance, and train journey timetable. HTS is based on various input parameters, some are fixed, and some are dynamic. Route data is a fixed parameter consisting of information such as the gradient of the route, track speed limits and position of stations. Train characteristics are also a fixed parameter, consisting of general information about the train, such as weight, maximum speed, power sources, etc. Acceleration and distance are dynamic parameters, although the distance is already given in route information and can be used in the simulation. However, to satisfy the condition of working in the time domain, the distance from the route file is only used for reference points and calculated again in real-time during the simulation. Acceleration changes correspond to the train velocity and gradient and the selection of train movement mode. Train speed is a standalone input parameter that affects the Optimisation of a train journey. The speed values will change according to the track speed limit and approach to the nearest station. The dynamic parameters change from time to time and calculate further required information, such as the amount of energy used by the train to complete the journey, journey time and many more.

4.3.1 Simulation Design

HTS uses numerical integration to compute outputs. Initially, the simulator reads route and vehicle information and calculates the dynamic parameters for each step that form the vehicle course. Considering the time scale of the simulation, a small time-step Δt in milliseconds for each iteration of calculation can produce a more precise result but will take an immense amount of computation time [173, 191]. Considering this, in HTS, the time step Δt is set to 1 second. By using any personal computer, generating 6000 iterations based on 1-second time-step is easy and quick compared to 6000000 iterations for 100 minutes journeys based on a one-millisecond time-step. The results generated, such as time taken to complete the journey,

energy consumption, train velocity, acceleration, distance, traction forces, braking and traction power, are stored in an array at each step and used in the next time step.

If the train moves one time-step Δt from $Step_1$ to $Step_2$ with an acceleration rate a, the train velocity v_2 can be calculated by the following Equation (4.9).

$$v_2 = v_1 + (a \times \Delta t) \tag{4.9}$$

The basic concept of a vehicle accelerating between initial and final velocities is used to calculate the train's acceleration. Acceleration is calculated using Equation (10) by solving the Equation of train motion concerning the velocity with an initial and final speed as the assimilation limits.

$$a = Force_T / M' \tag{4.10}$$

where $Force_T$ is traction force and M' is the effective mass of the train.

In HTS simulation, the train is set to accelerate at given speed limits using maximum accessible acceleration. To determine the maximum achievable acceleration, a threshold v_{max} is set for the current speed limit v_{limit}. Equation (4.11) is used to apply the threshold limit on speed.

$$v_{max} = v_{limit} - C \tag{4.11}$$

where C is an arbitrary constant value in m/s.

Two simple rules are introduced in the simulation to achieve a steady approach to speed limits.

- If acceleration is above the maximum limit, it will be truncated.
- If the acceleration is below a threshold speed, it will be equal to maximum acceleration.

To achieve truncation of acceleration, velocity difference is calculated by using Equation (4.12).

$$\Delta v = v_{limit} - v \tag{4.12}$$

where Δv is the difference between the current speed and speed limit, maximum acceleration is calculated by using Equation (4.13).

$$a_{max} = a'_{max} - \frac{\Delta v}{v_{limit} - v_{max}} \quad (4.13)$$

where a'_{max} is the initial maximum acceleration. The train will operate in cruising mode if Δv and maximum acceleration is zero.

Distance d_2 is calculated by using Equation (4.14). Since the time step for each calculation in simulation is set to 1 second, the time was calculated using Equation (4.15).

$$d_2 = (\Delta t \times v_1) + d_1 \quad (4.14)$$

$$t_2 = t_1 + \Delta t \quad (4.15)$$

The total energy consumed by the train traction system can be calculated by using Equations (4.16) and Equation (4.17)

$$E_{Total} = \frac{1}{2} + M_t * \Delta v^2 + \int_{v_1}^{v_2} R - \Delta h M_t g \quad (4.16)$$

$$E_2 = (P_t \times \Delta t) + E_1 \quad (4.17)$$

where M_t is the total mass of the train, $\Delta v^2 = (v_2^2 - v_1^2)$, v_1 is train speed at the current position of distance and v_2 is train speed at the next position of distance. Δh is the difference between the track gradient at the current step and the next step. R represents train resistance calculated by Equation (4.5), and g is the gravitational acceleration.

Total Power can be calculated by (4.18).

$$P_t = F_t v \quad (4.18)$$

where P_t is total power. F_t is traction forces applied during the motion of the train, and v is the speed of the train.

4.3.2 Automatic Smart Switching Control

The idea of implementing the smart switching technique is to evaluate the effect of power demand on power sources. The goal of smart switching is to avoid excessive use of power sources and to use the relevant power source only when required according to the power demand and track terrain. It is also considered to charge the battery with only regenerative

braking. This will restrict the fuel cell to provide only traction power and power required for onboard auxiliaries. This strategy will rid the fuel cell of being a utility for charging the battery during the journey. The HTS use the route's gradient as a reference to switch power sources. When the track is levelled, the train will only use power from the battery. During elevation, both the battery and the fuel cell will start providing the power, while moving downhill, the train will use power from only the fuel cell. Total power is calculated by Equation (4.19) when the route's gradient is equal to zero.

$$P_{t,i} = P_b - P_{aux} \tag{4.19}$$

where P_b is battery power and P_{aux} is auxiliary power used to power onboard auxiliaries such as air conditioning, door operation, lighting and providing power for users to charge their gadgets. When the gradient is greater than 0, the total power is calculated by Equation (4.20).

$$P_{t,i} = P_b + P_f - P_{aux} \tag{4.20}$$

where $P_b \; and \; P_f$ are battery power and fuel cell power, respectively. When the gradient is less than 0, the total power is:

$$P_{t,i} = P_f - P_{aux} \tag{4.21}$$

Figure 7 shows the flowchart for the core algorithm of the HTS. The simulator reads the data from input files such as train position, speed limit, gradient, station location and dwelling time at each station. At time = 1 second, HTS finds the speed limit and gradient at the current step. The simulator will choose the appropriate power according to the gradient and start calculating velocity, traction, resistance and acceleration. Matching the speed limit from the input file, at each time step simulator will choose the required mode for speeding from lower train movement to higher or vice versa. Acceleration mode is used to speed up the train. Once the speed limit is achieved, HTS will choose cruising mode. When HTS detects the braking point, it will use coasting mode until the train arrives at the braking point, where HTS will apply braking mode, which will stop the train at the station. At the end of each time step, it calculates

power and energy consumption, separated according to different power sources with respect to route gradient. This process ends once the train arrives at the final station. All results are saved in appropriate arrays, and various graphical results are generated.

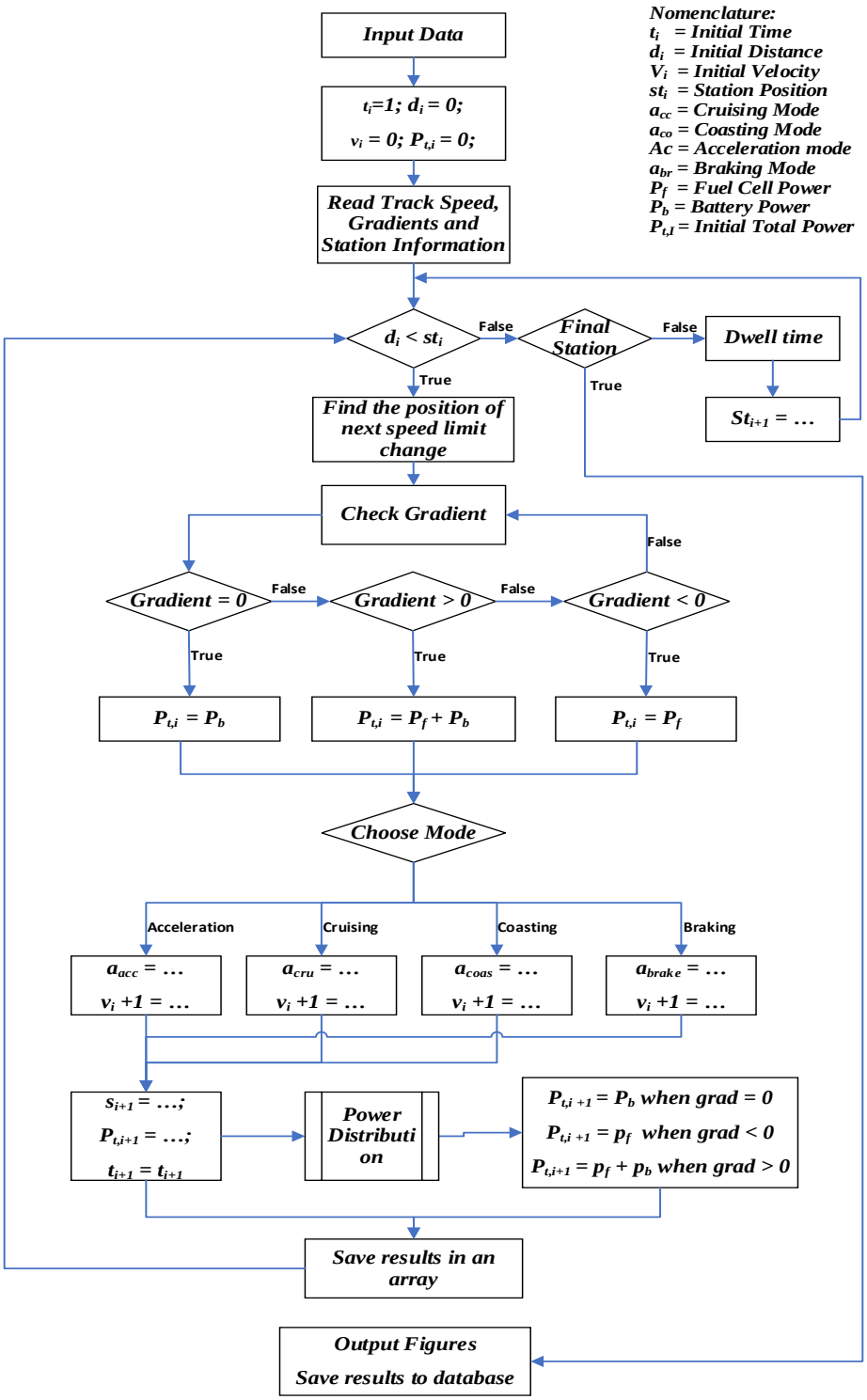

Figure 7: Flow chart of Hybrid Train Simulator

4.4 Validation of Hybrid Train Simulator

The hybrid train simulator was validated based on the validation techniques proposed by [179]. An experiment was designed to generate test scenarios to achieve energy consumption, journey time, and distance travelled by train to validate HTS. The test was performed on all four modes of movement (acceleration, cruising, coasting and braking). Tests were also conducted with both zero and constant gradients to isolate any programming errors and further investigate them. The HTS is validated against the Matlab-based single train simulator (STS) developed by Dr Stuart Hillmansen [77] at the University of Birmingham. The main characteristics of HTS and STS are illustrated in Table 4.

Table 4: Characteristics of HTS and STS

Parameters	**HTS**	**STS**
Number of Trains	Single	Single
Calculation Step	Time	Distance
Calculation from Acceleration	Velocity, Distance	Velocity, Time
Integration Method	Euler, Midpoint	Euler
Power Sources	Multiple	Single
Power Scaling	Automatic	-
Power Sources Switching	Smart	-

A British class 150 diesel multiple-unit train model was used during the experiment for both analytical and simulation tests. The main characteristics of the British class 150 train are presented in Table 10. Although a hybrid train simulator can analyse multiple power sources at once, due to the lack of this ability in STS, HTS was kept to a single power source mode during the validation process. The length of the test route was set to 4 km. Since STS work in the distance domain and HTS works in the time domain, the STS was configured with a distance step of 1 meter, while HTS was configured with a time step of 1 second.

Accelerating: During the acceleration phase of the simulation, constant power was provided by both simulators, and the train accelerated from 0 to 29.5 m/s. The test results presented in Table 5 indicate that both simulators have exceeded the analytical solution. Considering this,

the STS is in error by 2 meters which impacts the final time calculation by 0.52 seconds compared to the 1.24 seconds error of HTS. Alternatively, the HTS simulation significantly impacts distance calculation by the error of 10 meters. Since both simulators are microscopic and have comprehensive route geometry, such minute errors do not affect the final solution at full-scale trajectory calculations. They can be neglected or otherwise compensated based on the application of the simulator.

Table 5: Results of acceleration at zero and 1% gradient test

	0 Gradient					
	Distance (m)	**Difference** (m)	**Time** (s)	**Difference** (s)	**Energy** (kWh)	**Difference** (kWh)
Analytical	896	-	62.24	-	9.19	-
STS	894	-2	62.76	0.52	9.31	0.12
HTS	886	-10	64	1.76	9.45	0.26
	1% Gradient					
Analytical	911	-	63.98	-	9.46	-
STS	914	3	64.07	0.09	9.51	0.05
HTS	917	6	66	2.02	9.84	0.38

Cruising: During the cruising phase train cruised for 1,261 analytical meters. The results show that STS is in error by 0.1 seconds and HTS by 0.28 seconds, respectively, as shown in Table 6. In cruising mode, both simulators can calculate approximately within the same range of parameters (distance), given that the cruising distance or the time is multiple of the simulation step size.

Table 6: Results of cruising at zero and 1% gradient test

	0 Gradient					
	Distance (m)	**Difference** (m)	**Time** (s)	**Difference** (s)	**Energy** (kWh)	**Difference** (kWh)
Analytical	1261	-	45.19	-	2.51	-
STS	1262	1	45.29	0.1	2.59	0.08
HTS	1263	2	45.47	0.28	2.78	0.27
	1% Gradient					
Analytical	1509	-	54.19	-	3.47	-
STS	1506	-3	54.25	0.06	3.50	0.03
HTS	1507	-2	53	-1.19	3.44	-0.03

Coasting: Coasting mode is often used to optimise railway trajectories by applying various ranges of optimal coasting velocities or coasting points along the route. They are generally greater than zero; otherwise will result in errors. During the validation process, in both simulations, the train costs from the speed of 29.5 m/s to 0 m/s. The results indicate a similar pattern of errors in the distance, as shown in previous test results. However, HTS results are improved by showing negligible error in time consumed during the coasting mode. The STS carries an error of 3 meters, and HTS is in error by 0.07 seconds, as shown in Table 7.

Table 7: Results of coasting at zero and 1% gradient test

	Distance (m)	**Difference** (m)	**Time** (s)	**Difference** (s)	**Energy** (kWh)	**Difference** (kWh)
0 Gradient						
Analytic	1328	-	51.67	-	-	-
STS	1325	-3	51.95	0.28	-	-
HTS	1335	7	51.60	-0.07	-	-
1% Gradient						
Analytic	1077	-	41.95	-	-	-
STS	1079	2	42.07	0.12	-	-
HTS	1072	-5	42	0.05	-	-

Braking: In this validation experiment, during the braking phase of a simulation, the train brakes from 29.5 m/s to 0 m/s with a variable braking power restricted to the maximum available braking power. The results indicate that the electric brakes significantly impacted the train's stop-off time and distance. It is also possible to apply manual constant braking power subject to maximum available braking power to stop the train. However, the results presented in Table 8 show improved results compared to the previous phases of the experiment. Therefore, the application of constant power braking was ignored in the validation process.

Table 8: Results of braking at zero and 1% gradient test

	Distance (m)	Difference (m)	Time (s)	Difference (s)	Energy (kWh)	Difference (kWh)
0 Gradient						
Analytic	515	-	44.13	-	4.71	-
STS	519	4	44.48	0.35	4.9	0.19
HTS	516	1	44.91	0.78	5.19	0.48
1% Gradient						
Analytic	503	-	42.91	-	4.69	-
STS	501	-2	43.04	0.13	4.79	0.10
HTS	504	1	43.15	0.24	4.96	0.27

The results of validation experiments indicate that both simulators performed calculations within the range of ±5% error. At some phases of the investigation, the errors that appeared were negligible while performing full-scale train trajectory simulations due to their minute size. It is also observed that a respective calculation step in both simulators can significantly impact the precision of results. Given the nature of research work and validation against a proven Single train simulator and based on experiment results Hybrid train simulator is considered authentic and accurate for this research.

4.5 Summary

This Chapter delves into the development of the hybrid train simulator (HTS), which is integral to the research presented in this thesis. The comprehensive review of the mathematical modelling of hybrid railway vehicles is based on the Equations of motion, taking into account the constraints imposed by the route and driver on the train. By developing the HTS, the author has successfully achieved one of the primary objectives: creating a hybrid train movement simulator.

Section 4.2 provides a detailed analysis of the general physical dynamics of the hybrid train, which is crucial for advancing railway vehicle development. Section 4.3 depicts the simulator's input and output design structure, which relies on a time-step approach for train modelling and power and energy management systems.

Section 4.3.2 introduces a novel feature: the Automatic Smart Switching of power sources installed onboard hybrid railway vehicles. This innovative mechanism ensures an efficient and seamless transition between energy sources. Section 4.4 presents the validation process for the HTS by comparing its performance to a Matlab-based single-train simulator developed at the University of Birmingham. Both simulators yield experimental results within an acceptable error margin of ±5%.

The Hybrid Train Simulator (HTS) serves as a pivotal component in the forthcoming chapters of this thesis, contributing significantly to the exploration and development of various aspects of hybrid train systems.

In Chapter 5, the HTS is employed to examine the practical application of automatic smart switching of power sources. This investigation delves into the intricacies of efficiently managing multiple power sources, such as internal combustion engines, electrification, fuel cells, and batteries, to optimise energy consumption and performance in hybrid train systems.

Chapter 6 details the integration of the HTS with a sophisticated hybrid optimisation algorithm, which is designed to determine an optimised hybrid train trajectory. This process involves the careful consideration of numerous factors, including velocity, acceleration, traction forces, distance, time, power, and energy, to achieve a well-balanced energy-time trade-off without significantly compromising journey duration. This balance is crucial in creating sustainable transportation systems that can successfully navigate the complexities of modern urban rail transport.

In Chapter 7, the HTS will generate a comprehensive dataset of hybrid train trajectories, which will serve as the foundation for predicting optimal trajectories using artificial neural networks (ANNs). The application of ANNs in this context allows for the efficient analysis of large datasets, enabling the identification of key patterns and trends that contribute to the

optimisation of hybrid railway vehicles. By leveraging the capabilities of the HTS, this chapter aims to demonstrate the potential for ANNs to predict hybrid train target parameters proficiently, thereby contributing to the overall goal of enhancing energy and environmental sustainability in urban rail transport.

5 ENERGY EVALUATION OF HYBRID TRAINS WITH SMART SWITCHING CONTROLS

5.1 Introduction

Previous studies presented the impact of the route and its gradient on vehicles [192-194]. However, there has not been yet done to scale the power source according to the route's gradient and required journey time. To address this issue, a technique of smart switching control is implemented in this Chapter which will help in scaling and using the power sources based on the gradient of the route. The smart switching controls are discussed elaborately in Section 4.3. It is an expanded version of the studies that resulted in the paper "*Operation and energy evaluation of diesel and hybrid trains with smart switching controls*," published in Control Engineering Practice, for which the author was the primary contributor and the lead author.

A generic route representing a typical British cross-country route and a typical vehicle that operates on such routes is used in the simulation in this Chapter. The simulation will present the benchmark results based on the rated values of the power sources simulated in a realistic environment and the optimised simulation where the power source values will automatically switch according to the route's gradient to achieve the most energy-efficient trajectory.

5.2 Route Configuration

Camp Hill Line in Birmingham was one of the final main lines introduced to the town during the ‘Railway Mania’ of 1830–1850. Motivations for restoring services to the line are to reduce congestion in the area, provide clean air and offer a greater transport infrastructure for the 2022 Commonwealth Games. Three stops are made between the origin and destination; the route length is 11.2 km, and the return journey is 22.4 km, as in Table 9. Additionally, a 60 mph speed limit [147] is imposed on this line. Electrification infrastructure is close to Birmingham

city centre, with 1.36 km of overhead electrification. The point of electrification has been confirmed using Google Earth and railway track diagrams [195].

Table 9: Camphill Line Route Specifications

Parameter	Value
Route Name	Camp Hill Line
Route Length	11.2 km
Track Speed Limit	60 mph
Service Operation	Under Renovation
Stations	8

5.3 Vehicle Configuration

The British Rail Class 150, also known as “Sprinter”, built by British Railway Engineering Limited York during 1984–1987 [10], was used in this simulation. The Sprinter has a very generic body frame with a rigid design. It has had a successful tenure of 33 years in service without any major setbacks or design flaws. The body frame and chassis design make it ideal for modification and retrofitting. Considering the conversion of the Sprinter after the removal of engines, transmission system, fuel tank and exhaust systems, it will provide enough space to accommodate fuel cells, batteries and hydrogen tanks without exceeding the original weight of the Sprinter [10]. Table 10 shows the specifications of a British Rail class 150 DMU [10].

Table 10: British Class 150 Train Specifications

Parameter	Value
Tare mass	76.5 t
Starting tractive effort	37.52 kN
Maximum acceleration	0.5 m/s2
Maximum speed	121 km/h
Davis Equation	R = 1.5 + 0.006v + 0.0067v2
Diesel engine power	426 kW
Auxiliary power	28 kW
Diesel tank capacity	1500 L
Energy available in diesel tank	14910 kWh

5.4 Benchmark Diesel Train Simulation

The train was simulated with the original equipment manufacturer's configuration in this benchmark simulation. This configuration comes with 425 kW diesel engine power and 14,910 kWh energy in diesel fuel. The efficiencies applied in the benchmark simulation are 92.6% for the traction package, 95.6% for the diesel engine drive shaft to traction package and 29% for the diesel engine, as in Table 11 [7].

Table 11: Efficiencies applied during benchmark diesel train simulation

Parameter	Efficiency
Traction Package	92.6%
Drive Shaft	95.6%
Diesel Engine	29%

The dwelling time at each station is 60 seconds, while the turnaround time at the starting station (Kings Norton Station) and the terminus station (New Street Station) is 3 minutes. The benchmark diesel train required 36 minutes to complete the 22.40 km journey, including the turnaround time. During the journey, the train attained a maximum velocity of 96.56 km/h with an acceleration rate of 0.49 m/s2.

Detailed simulation results for the diesel class 150 train are presented in Table 12. The results indicate that the train consumed 273 kWh of energy, with an average power of 91 kW at the wheels. 28 kW of power was dedicated to the train's onboard auxiliaries. Being a diesel multiple unit, the British Class 150 lacks modern power electronic equipment on board, and power is transmitted mechanically to the wheels via the driveshaft. The driveshaft produces 347 kW of power to the wheels from the diesel engine power plant. To generate 79 kWh of energy at the power plant, the diesel engines consumed 24 litres of diesel fuel. Onboard auxiliaries consumed an additional 19 kWh of energy, with the remaining energy being transmitted to the wheels via the driveshaft.

Table 12: Simulation Results for Diesel Class 150 Train

Parameter	Value
Power	
Engine rated power	426 kW
Total power at wheels	347 kW
Average traction power at wheels	91 kW
Auxiliary power	28 kW
Energy	
Energy at wheels	54 kWh
Energy at the driveshaft	59 kWh
Auxiliary energy	19 kWh
Power plant output energy	76 kWh
Diesel engine output energy	79 kWh
Energy contained in diesel	273 kWh
Journey time	36 min
Max velocity reached	96.56 km/h
Max acceleration reached	0.49 m/s2

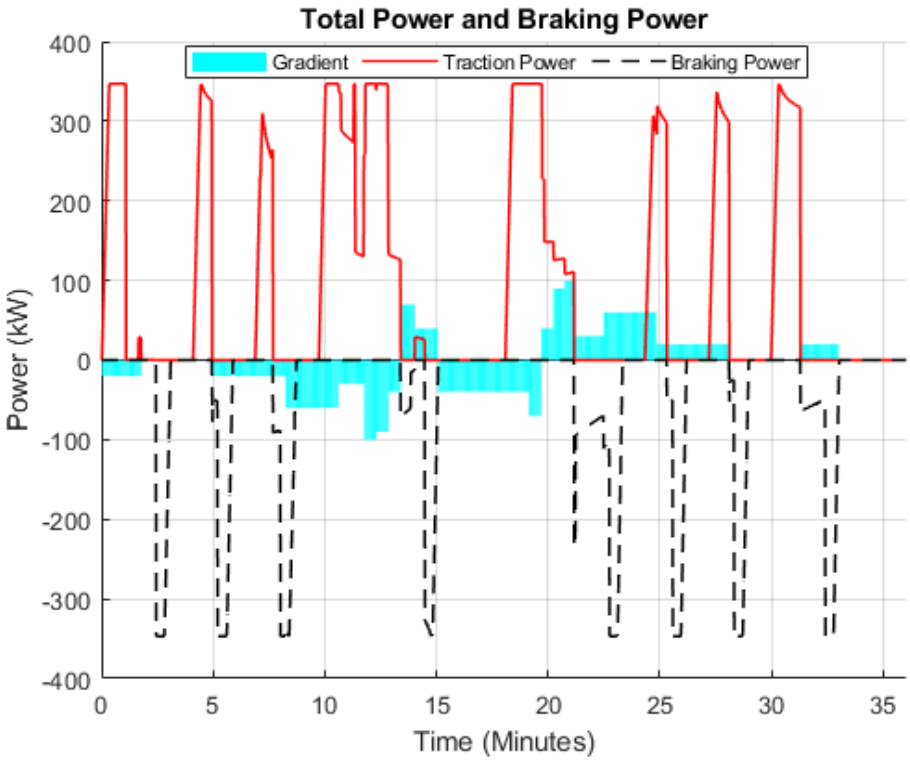

Figure 8: British Class 150 train traction and braking power demand

With 14910 kWh of energy from diesel fuel, the train can complete approximately 63 journeys without requiring refuelling. Each trip consumes roughly 24 litres of diesel, calculated using a lower heating value of 42.78 MJ to convert kWh energy to litres of diesel. Figure 8 illustrates

the traction and braking power demand throughout the journey and the route gradient. Future simulations of hybrid trains will examine the power demand changes based on the route's gradient in greater detail.

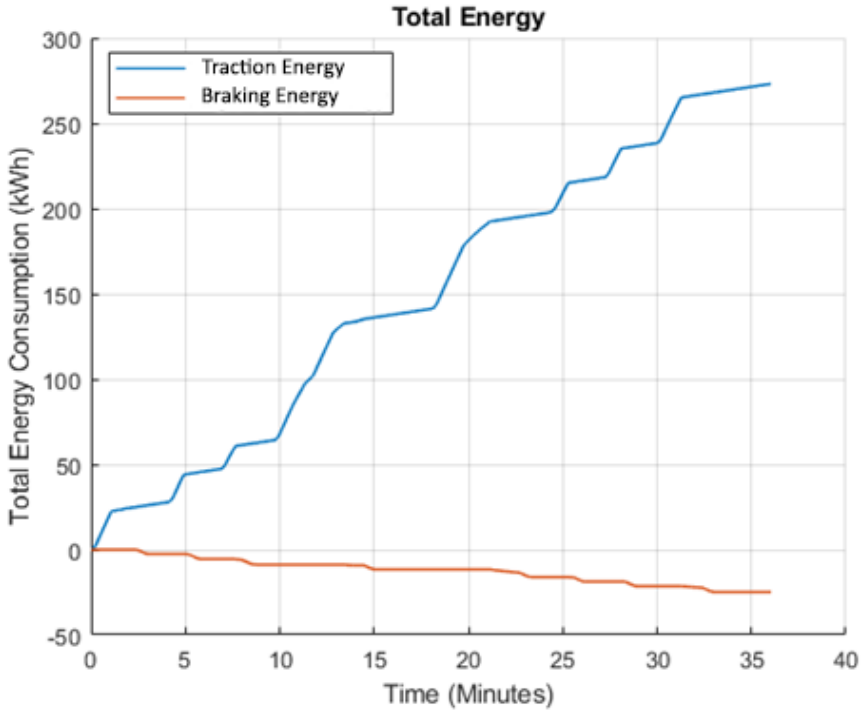

Figure 9: British Class 150 train energy consumption during the journey

Figure 9 displays the diesel train's energy consumption during a single return journey, noting that the benchmark diesel train is not equipped with regenerative or rheostatic brakes. Instead, braking energy is dissipated through mechanical brakes, such as disc or drum brakes. These brakes utilise friction to decelerate or stop the train, with the kinetic energy of the moving train converted to heat energy and dissipated into the environment. Nevertheless, the HTS has calculated the amount of regenerative energy that could be captured if the train were outfitted with regenerative braking.

5.5 Benchmark Hybrid Train Simulation

The hybrid benchmark train simulation simulated the train with a customized configuration. The diesel engine was replaced with a 200 kW fuel cell and 60.12 kWh battery. This replacement directly affected the train's weight by removing the engine, diesel fuel tank and

transmission system, including the driveshaft and alternator. Approximately 7 tonnes were removed and exchanged with the components necessary to operate hybrid trains. The replacement parts were a fuel cell, coolant and air subsystem, traction batteries, traction motor, power electronics and radiators. The extra weight added to the hybrid train was 4.5 tonnes. This made the final weight of the hybrid train 72.4 tonnes. The efficiencies applied in optimised simulations are presented in Table 13.

Table 13: Efficiencies Applied During Benchmark Hybrid Train Simulation

Parameter	Efficiency
Drive train	90.3%
Traction motor	95%
DC-BUS/IGBT	97.5%
Fuel cell	50%
Battery	87%

The energy flow system adopted in both hybrid trains is presented in Figure 10. The form of electricity used to move the train and overcome friction and gravitational forces is known as traction energy [11, 47]. Traction energy is collected from both hydrogen and battery.

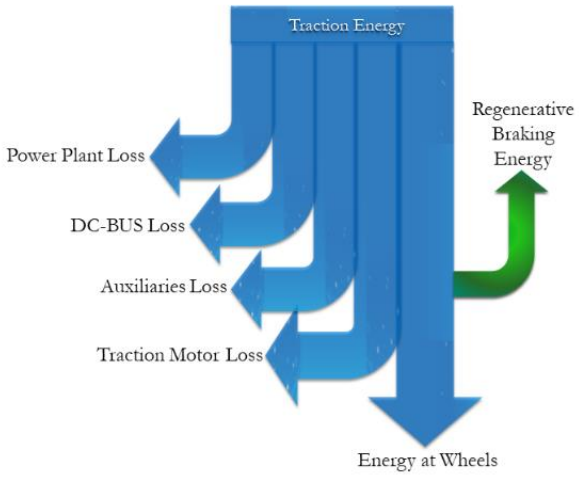

Figure 10: Generic traction energy flow diagram

The benchmark hybrid train was fitted with two power sources. However, the automatic switching between them was not enabled. Table 14 presents detailed results from the

benchmark hybrid train simulation. The train completed the journey in 38.37 min, consuming 99 kWh of energy. This is 64% less than the energy consumed by the diesel version, at the cost of a 6% increase in journey time. Since in the benchmark hybrid train simulation, the auto-switching between power sources was off, the traction power at the wheel was constant and supplied according to the traction power demand of the train. Figure 11 shows the hybrid benchmark train's traction and braking power demand.

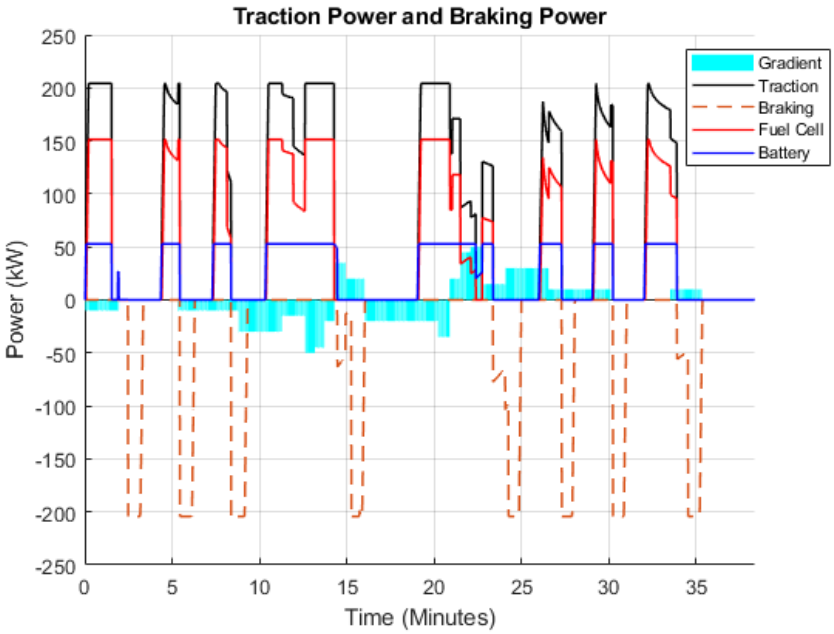

Figure 11: Hybrid benchmark train traction and braking power demand

The hybrid train is equipped with ten carbon fibre tanks to store hydrogen. Each tank holds 7.4 kg of hydrogen, which provides 2266 kWh of total energy. The battery levels are kept between 20% and 80% to maximize battery life and reduce maintenance costs. Figure 12 presents the energy utilised by the benchmark hybrid train during one return journey.

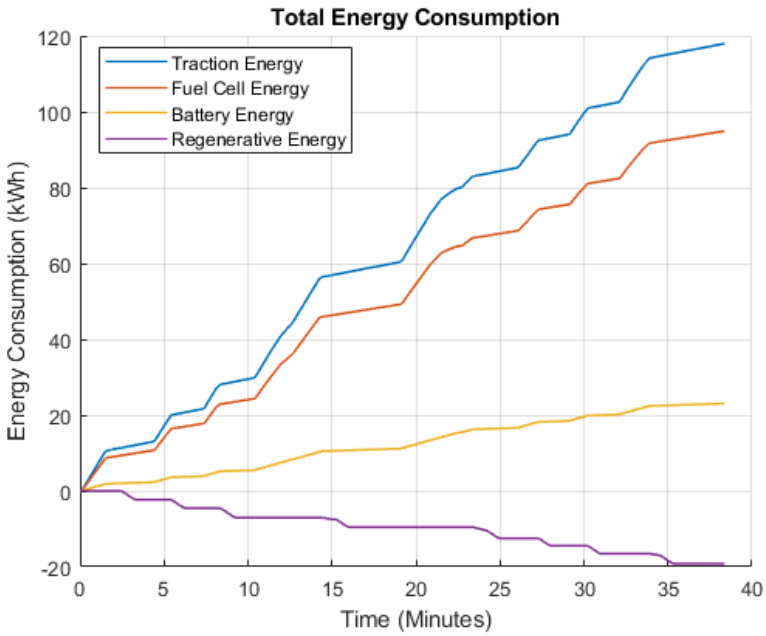

Figure 12: Benchmark hybrid train total energy consumption

Further calculations show that, during each journey, 23 kWh of energy is discharged from the battery, and 19 kWh of energy is recharged to the battery by regenerative braking since the battery is only charged once via the fuel cell when its charge level drops to 20%. Each return journey reduces battery charge by 8%, providing battery operation for nine return journeys only. After nine trips, the battery must be recharged up to 80% again. The state of charge of the battery used in the hybrid benchmark train is shown in Figure 13.

To charge the battery to 80% requires 1.44 kg of hydrogen. There are several charging strategies that can be adopted to maintain the battery's state of charge. One option is to recharge the battery fully via the fuel cell after each journey, consuming 0.12 kg of hydrogen and eliminating the nine-return journey range for battery operation. This strategy will provide a range of approximately 23 return journeys.

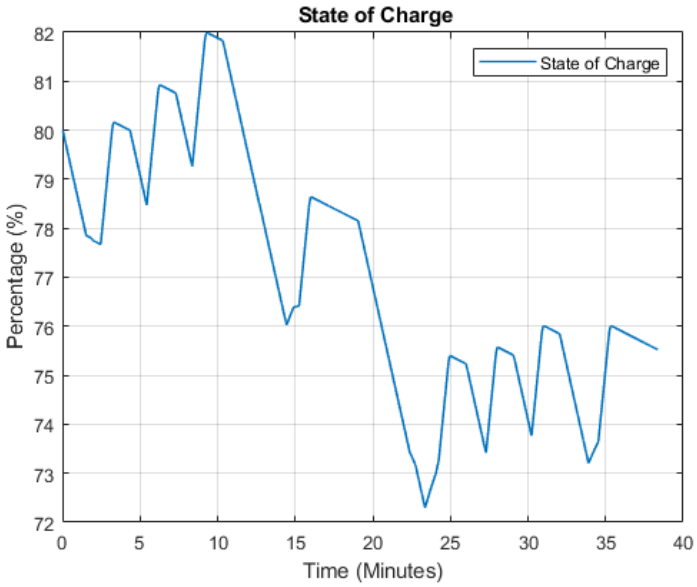

Figure 13: Benchmark hybrid train battery state of the charge against time

Alternatively, the battery can be charged up to 80% using 1.44 kg of hydrogen, which provides a range of around 26 return journeys. The railway operating companies can tailor the charging strategy choice based on their timetable and traffic management needs. The charging time required to charge the battery from 20% to 80% capacity is estimated to be 55 minutes, based on the battery's specifications and assuming 10% losses during the charging process.

Table 14: Simulation Results of Benchmark Hybrid Train

Parameter	**Value**
Power	
Fuel cell power	200 kW
Battery power @1-C rating	60 kW
Auxiliary power	28 kW
Fuel cell power at wheels	151 kW
Battery power at wheels	53 kW
Average traction power at wheels	155 kW
Energy	
Fuel cell energy at wheels	31 kWh
Battery energy at wheels	14 kWh
Total energy at wheels	46 kWh
Fuel cell energy at traction motor	33 kWh
Battery energy at traction motor	15 kWh
Total energy at traction motor	48 kWh
Fuel cell energy at DC-BUS	34 kWh
Battery energy at DC-BUS	15 kWh

Total energy at DC-BUS	49 kWh
Aux energy at DC-BUS from fuel cell	14 kWh
Auxiliary energy at DC-BUS from battery	5 kWh
Total auxiliary energy at DC-BUS	18 kWh
Fuel cell output energy for traction & aux	47 kWh
Battery output energy for traction & aux	20 kWh
Total output energy for traction & aux	68 kWh
Energy contained in hydrogen	95 kWh
Energy contained in battery	23 kWh
Regenerated energy saved in battery	19 kWh
Total energy required for a return journey	99 kWh
Hydrogen required for one return journey	2.85 kg
Hydrogen required to charge battery up to 80%	1.44 kg
Journey time	38.37 min
Max velocity reached	89.34 km/h
Max acceleration reached	0.49 m/s2

5.6 Optimised Hybrid Train Simulation

In the optimised simulation, the hybrid train was simulated with a similar configuration as the hybrid benchmark train simulation, with the same efficiencies applied. However, the essential element in this simulation was the automatic switching between power sources according to the track's gradient. Table 15 presents detailed results from the optimised hybrid train simulation. The results indicate that the Optimised Hybrid train required 99 kWh energy to complete the journey with 155 kW average power at the wheels. According to Table 15, 2.85 kg of hydrogen was used to produce 95 kWh of energy for the traction and onboard auxiliaries. 28 kW power from the fuel cell was dedicated for auxiliaries only and the rest for the train traction. The battery provided 23 kWh of energy for train traction during one return journey. Power and energy from the fuel cell and battery pack were transmitted via DC-BUS to the traction motor and wheels. Since the hybrid train was equipped with a regenerative braking system, it produced 19 kWh of energy via regeneration and was sent to the battery pack to recharge batteries.

In the Optimised simulation, the train took 44 min to complete one return journey. A significant increase of 14.5% in journey time compared to the benchmark hybrid train and a 22% increase

compared to the diesel benchmark train was observed. The increase in journey time is due to the reduction in traction power.

In the benchmark simulation, the traction power was constant according to the power demand of the train throughout the journey. However, in the Optimised simulation where auto-switching between power sources was enabled, the traction power decreased on flat terrain where only the battery provided traction power. On downhill terrain, just the fuel cell was providing traction power. This decrease in traction power slows down the train for a short period to cope with the power demand of the track terrain. When the train was moving uphill, both the fuel cell and battery provided traction power; therefore, it did not cause any increase in journey time.

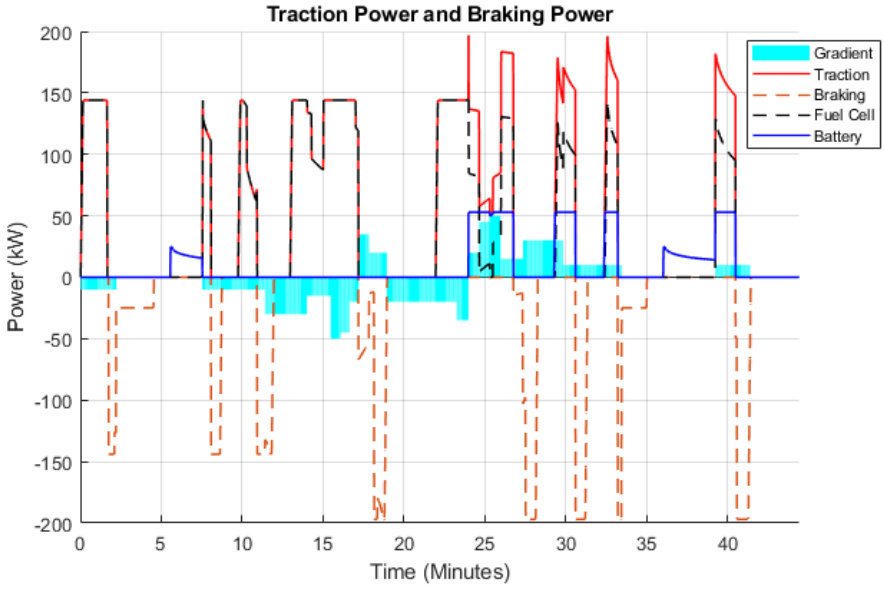

Figure 14: Optimised hybrid train simulation power demand

Figure 14 shows the traction power and braking power demand of the optimised simulation plotted over the track gradient to visualize the auto-power switching. Since both power sources were used according to the gradient of the track, excessive and constant use of power sources was discarded. This strategy could enhance the operating life of power sources while ensuring their reliability by improving the consistency of power sources; the time and costs used on

maintenance can be reduced [196]. Hybrid trains are more suitable for cross-country routes where traffic is less congested and less time-sensitive. They are also beneficial in keeping the area green as a hybrid train with fuel cell and battery combination has zero emission of carbon dioxide gas at the point of use compared to diesel trains [197]. It should be noted that the route used in this study was a test route. There is a possibility that there might be a more suitable route available for the technique of automatic switching of power sources.

The train consumed 93 kWh of energy in the optimised simulation to complete one return journey. This is 6% less than the energy consumed by the hybrid benchmark train and 66% less than the diesel benchmark train. The hydrogen and battery control strategy was kept similar to the control strategy used in the hybrid benchmark simulation. The detailed results of the simulation show that the train utilised 92 kWh of energy from hydrogen and 16 kWh of energy from the battery; this is 30% less than the 23 kWh used from the battery in the hybrid benchmark simulation to the train spending a short period on flat terrain. It was also observed that the energy regeneration rate fell to 15 kWh compared to 19 kWh in the hybrid benchmark simulation; the logical reason for this decrease is the reduction in braking power demand according to the track's gradient. Figure 15 illustrates the utilization of energy during the Optimised hybrid train simulation.

In the optimised hybrid train simulation, battery charge reduces by 2% during each return journey, providing an astonishing operation of 31 return journeys on one charge. After 31 journeys, the battery must be recharged up to 80% again to make the train ready for a further 31 journeys, subject to the availability of hydrogen. Hydrogen consumption is also slightly reduced to 2.77 kg per return journey in the Optimised simulation. Charging the battery to an 80% charge level will require 1.44 kg of hydrogen, making the hydrogen consumption for the first Optimised journey 4.21 kg. The above results project that the Optimised hybrid train can achieve 26 return journeys on one hydrogen gas refill, similar to the benchmark hybrid train.

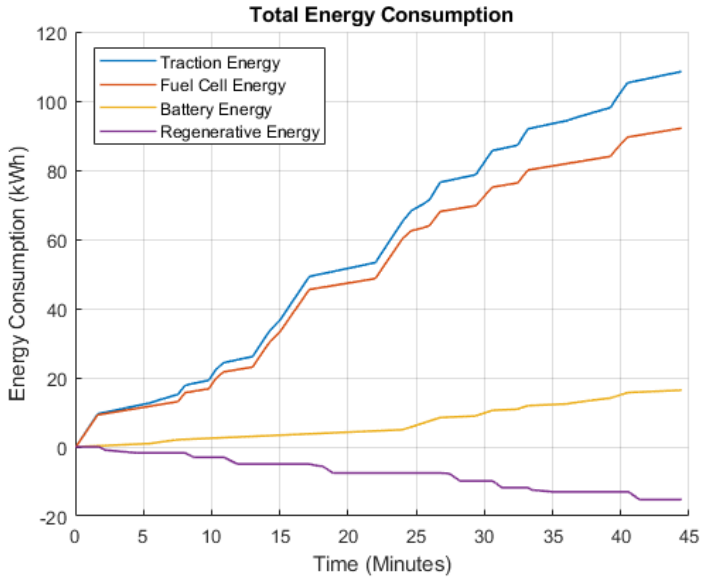

Figure 15: Optimised hybrid train simulation energy consumption

The Optimised hybrid train can also adopt the strategy of charging the battery after each return journey. It will require 0.03 kg hydrogen to top the battery up to 80% after one return journey. This strategy will provide an unlimited range for train operation but will be restricted by hydrogen gas storage onboard, limiting its range to 26 return journeys. Figure 16 presents the state of charge of the Optimised hybrid train.

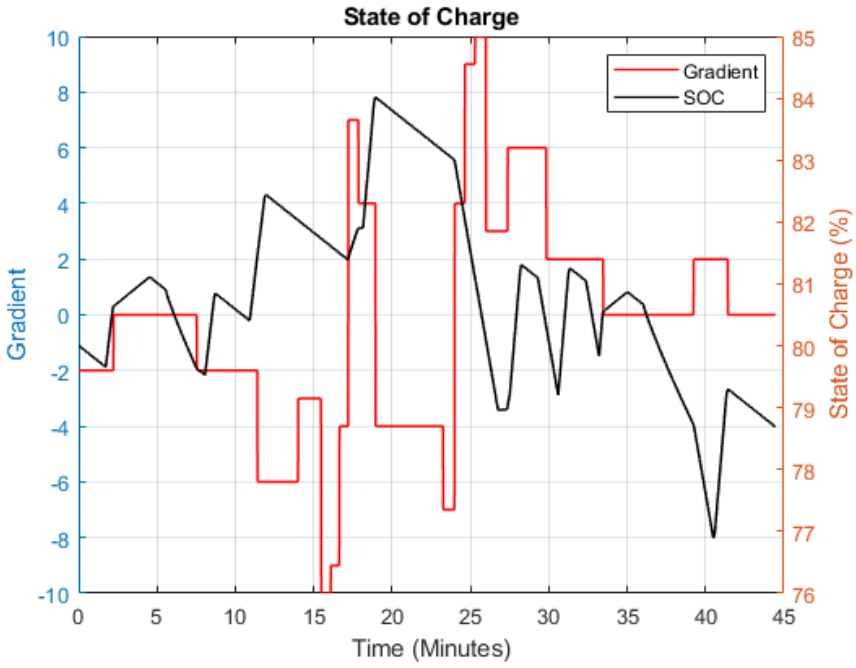

Figure 16: Optimised hybrid train simulation state of charge

Table 15: Simulation Results of Optimised Hybrid Train

Parameter	Value
Power	
Fuel cell power	200 kW
Battery power @1-C rating	60 kW
Auxiliary power	28 kW
Fuel cell power at wheels	144 kW
Battery power at wheels	53 kW
Average traction power at wheels	126 kW
Energy	
Fuel cell energy at wheels	29 kWh
Battery energy at wheels	7 kWh
Total energy at wheels	36 kWh
Fuel cell energy at traction motor	31 kWh
Battery energy at traction motor	7 kWh
Total energy at traction motor	38 kWh
Fuel cell energy at DC-BUS	32 kWh
Battery energy at DC-BUS	8 kWh
Total energy at DC-BUS	39 kWh
Aux energy at DC-BUS from fuel cell	15 kWh
Auxiliary energy at DC-BUS from battery	7 kWh
Total auxiliary energy at DC-BUS	21 kWh
Fuel cell output energy for traction & aux	46 kWh
Battery output energy for traction & aux	14 kWh
Total output energy for traction & aux	60 kWh
Energy contained in hydrogen	92 kWh
Energy contained in battery	16 kWh
Regenerated energy saved in battery	15 kWh
Total energy required for a return journey	93 kWh
Hydrogen required for one return journey	2.77 kg
Hydrogen required to charge battery up to 80%	1.44 kg
Journey time	44 min
Max velocity reached	88.87 km/h
Max acceleration reached	0.49 m/s2

5.7 Battery Charging Strategies

The above simulations illustrate that the battery will only be charged via regenerative braking during the journey, disregarding the integration of a system that could charge the batteries during the journey or while the train is stationary at stations. This strategy is adopted to dedicate fuel cell usage only for traction during the journey. This will relieve the fuel cell's excessive

use and compromise traction power. Although, the simulation presents the hydrogen amount required to recharge the batteries at a certain level. Charging the batteries during the journey will directly affect traction power by redirecting a certain amount of power towards the batteries. This will reduce the wheels' traction power, slowing down train acceleration while increasing journey time. Alternatively, batteries can be charged at stations while the train is stationary. This will also increase the journey time, affecting the train timetable. In conclusion, the selection of battery charging strategies solely depends on train operators according to their train operating schedules.

5.8 Energy-Time Trade-off

Energy consumption is crucial for the modern railway industry [173]. In general, if the train's speed is increased, it will cut the journey time short. However, increasing speed will also increase energy consumption and fuel costs. In such sophisticated cases, the trade-off between energy consumption and the journey time is accordingly taken into consideration [198, 199]

The following mathematical Equations can articulate energy usage:

$$E_{total} = f(a, V_t) \; if \; T_{min} \leq T_{total} \leq T_{max} \tag{5.1}$$

$$T_{total} = g(a, V_t) \tag{5.2}$$

where T_{min} and T_{max} are the minimum and maximum allowed scheduled journey times.

The above simulation results show that the energy consumption can be traded off against journey time for a less dense route where speed is not essential. Energy trade-off can be further optimised by an Optimisation algorithm, which will be further discussed in Chapter

5.9 Operational Performance Evaluation

In terms of the battery charging strategies, the above simulations illustrate that the battery was only charged via regenerative braking during the journey, which disregards the integration of a system that could charge the batteries during the journey or while the train is stationary at

stations. This strategy is adopted to dedicate fuel cells only for traction during the journey. This will relieve the fuel cell's excessive use and compromise traction power. Although, the simulation suggests the hydrogen amount required to recharge the batteries at a certain level. Charging the batteries during the journey will directly affect traction power by redirecting a certain amount of power towards the batteries. This will reduce the wheels' traction power, slowing down train acceleration while increasing journey time. Alternatively, batteries can be charged at stations while the train is stationary. This will also increase the journey time, which may affect the train timetable. In conclusion, the selection of battery charging strategies solely depends on train operators according to their train operating schedules.

Based on comparative analysis, as shown in Table 16, diesel trains consume more energy with 29% engine efficiency than hybrid trains with 50% efficiency of fuel cell and 87% of battery charging and recharging cycle. The hybrid trains, installed with carbon fibre tanks to store more hydrogen gas, can travel a longer distance with no correlation to their mass.

Moreover, the Optimised traction system configuration with automatic switching is based on the best terrain selection for railway routes, followed by designing a customised switching protocol and marking the best switching points according to the route's gradient. It is also concluded that energy consumption can be traded off against journey time for a less dense route where speed is not essential. This trade-off will ultimately impact the lifetime of power sources, subsequently increasing their operational life and reducing maintenance costs.

The case study concludes that an efficient traction system with auto-switching mode for urban and cross-country mid-range rail routes is feasible, cost-efficient and environmentally friendly where speed and time restrictions are not obligatory.

Table 16: Overall Comparison between Diesel Benchmark and Hybrid Trains

Parameter	Benchmark diesel	Benchmark hybrid	Optimised hybrid
Power			
Diesel engine power	426 kW	-	-
Fuel cell power	-	200 kW	200 kW
Battery power @1-C rating	-	60 kW	60 kW
Auxiliary power	28 kW	28 kW	28 kW
Engine power at wheels	347 kW		
Fuel cell power at wheels	-	151 kW	144 kW
Battery power at wheels	-	53 kW	53 kW
Average traction power at wheels	91 kW	155 kW	126 kW
Energy			
Total energy at wheels	54 kWh	46 kWh	36 kWh
Total energy at driveshaft	59 kWh	-	-
Total energy at traction motor	-	48 kWh	38 kWh
Total energy at DC-BUS	-	49 kWh	39 kWh
Total auxiliary energy	19 kWh	18 kWh	21 kWh
Total output energy for traction & aux	79 kWh	68 kWh	60 kWh
Regenerated energy saved in battery	-	19 kWh	15 kWh
Total energy required for a return journey	273 kWh	99 kWh	93 kWh
Diesel required for one return journey	23 L	-	-
Hydrogen required for one return journey	-	2.85 kg	2.77 kg
Range of train (return journeys)	63	26	26
Journey time	36 min	38.37 min	44 min
Max velocity reached	96.56 km/h	89.34 km/h	88.87 km/h
Max acceleration reached	0.49 m/s2	0.49 m/s2	0.49 m/s2

5.10 Summary

This Chapter presents a comprehensive hybrid train modelling approach and the development of a time-domain train simulator for simulating hybrid train trajectories. A case study highlights automatic smart switching between multiple power sources based on the route's gradient, enabling an efficient propulsion system that provides economical use of multiple power sources. This consequently eliminates unnecessary strain on power sources, extending their lifetime and reducing maintenance costs [7, 200-204].

The case studies showcase a control strategy where the traction system can be configured according to the terrain of the area where the train operates. This approach significantly

improves battery and fuel cell life and reduces maintenance costs by using power sources on a need basis and eliminating forced charge and discharge of excessive-high currents [205, 206]. By utilising fewer power sources, the wear and tear on these power sources are minimised, ultimately prolonging their lifetime. However, the study reveals that this system configuration might not support long-haul journeys.

The simulation results indicate a 6% reduction in energy consumption for a hybrid train equipped with auto-switching features compared to a benchmark hybrid and a 65% reduction compared to a diesel train. Results also show a significant increase in journey time for both hybrid trains compared to the diesel benchmark train due to the reduction in traction power. The optimised hybrid train takes 44 minutes to complete the journey, the benchmark hybrid train takes 38.37 minutes, and the diesel train takes 36 minutes. Although journey time is crucial for train operating companies, the novel traction system control strategy provided here is route-specific and may be acceptable for less dense routes. Alternatively, journey time could be improved by installing more powerful traction power sources, balancing the energy-time trade-off. Simulation results have also indicated a significant increase in journey time for both hybrid trains compared to the diesel benchmark train. This is logically correct due to the clear reduction in traction power in hybrid trains. In some cases, journey time matters for the train operating companies, but in this case, since the author is providing a novel traction system control strategy specific to one route, the journey time can be approved for less dense routes as provided by simulation. Alternatively, it can be improved by installing more powerful traction power sources.

6 SINGLE TRAIN TRAJECTORY OPTIMISATION BASED ON EVOLUTIONARY ALGORITHM

6.1 Introduction

Over the past several decades, railway transport systems have predominantly relied on conventional fuel sources, such as diesel and electricity, to power their operations [109]. However, recent legislation targeting carbon dioxide emissions has increasingly challenged the use of gasoline as a fuel source for railway vehicles. To address this issue, railway operators and governments have attempted to electrify railway tracks, only to face significant obstacles like exorbitant costs and grid stability concerns, particularly in urban areas [110]. As renewable energy systems rapidly expand and political focus shifts towards clean energy, the railway industry has turned to hybrid propulsion systems that harness renewable energy sources for powering railway vehicles [74]. In the context of sustainable travel models, Transit-Oriented Development (TOD) has emerged as a key strategy for encouraging environmentally friendly and efficient transportation systems. The existing literature highlights the importance of TOD in sustainable urban planning and its role in promoting the use of energy-efficient public transportation solutions [207, 208]. Unlike conventional railway vehicles, hybrid trains are inherently complex in terms of design and operation. The combination of hydrogen fuel cells and batteries in hybrid propulsion systems is gaining popularity as a means of decarbonising railway operations, particularly on less densely trafficked routes where electrification is not economically viable [111].

The challenges of hybrid transportation systems are multifaceted and include aspects such as hydrogen production, refuelling station infrastructure, propulsion system topology, power source sizing, and control mechanisms. A thorough evaluation and optimisation of these aspects are crucial for facilitating the adoption and commercialisation of hybrid railway

vehicles [117, 118]. Optimisation in energy systems typically involves identifying a single optimal solution to minimise or maximise an objective function [6], which is the process of determining the conditions or variable values that result in the minimum or maximum of the function [120]. It is important to note that 'optimisation' and 'improvement' are not synonymous and should be used judiciously [209]. The general optimisation problem seeks to find the minima and maxima of an objective function subject to specified constraints.

Advancements in hybrid railway system technology have spurred significant research on optimising hybrid trains, such as developing energy management strategies for balancing battery charge and discharge rates, minimising hydrogen consumption and reducing fuel ageing costs. These strategies are scalable and adaptive for conventional and bi-mode trains [210-212]. However, despite the extensive research on trajectory optimisation for conventional trains, there is a gap in the literature concerning hybrid railway vehicles. Existing methods and algorithms may not be directly applicable to hybrid trains due to the complexity and unique characteristics of their propulsion systems. Hybrid railway vehicles involve the integration of multiple power sources, such as batteries and hydrogen fuel cells, which present additional challenges in optimising energy management and train dynamics.

In addressing the research gap, this Chapter proposes a hybrid optimisation algorithm that utilises a non-convex objective function and considers both linear and non-linear constraints, ultimately offering a more tailored and efficient solution for the hybrid railway vehicles co-optimisation problem. The algorithm focuses on identifying the best dataset, considering variables such as time, distance, energy consumption, power distribution, traction forces, acceleration, and velocity. By employing non-convex optimisation techniques, the need to convert non-linear datasets into linear datasets is circumvented, avoiding unnecessary noise and computational stress that often arise from such conversions. Consequently, the proposed method aims to maximise algorithm efficiency and deliver more accurate results for hybrid

railway vehicle optimisation. This innovative approach holds the potential to contribute significantly to the development of sustainable and efficient hybrid railway systems, paving the way for further advancements in the field of green transportation technologies.

The proposed optimisation algorithm offers several notable contributions to hybrid railway vehicle optimisation and energy management. These contributions can be summarised as follows:

- The development of a hybrid optimisation algorithm tailored specifically for hybrid railway vehicles, employing a non-convex objective function. This algorithm is capable of improving the efficiency of energy management systems in hybrid trains while simultaneously optimising their trajectories.

- The proposed hybrid optimisation algorithm has implications for the advancement of driving profile and guidance systems, paving the way for more efficient and sustainable hybrid railway traction systems.

- The study also contributes to the broader field of evolutionary optimisation processes for hybrid railway traction systems, providing a solid foundation for future research and development in this area.

This Chapter is an expanded version of the studies that resulted in the paper *" Hybrid railway vehicle trajectory optimisation using a non-convex function and evolutionary hybrid forecast Algorithm*," submitted to be published in IET, Intelligent Transport Systems, for which the author was the primary contributor and the lead author.

The structure of this Chapter is as follows. Section 6.2 presents the literature review and briefly introduces the hybrid railway systems. Section 6.3 proposes the mathematical model of a hybrid railway vehicle in detail, including the proposed optimisation algorithm model. Section 6.4 presents a case study employing the proposed hybrid optimisation algorithm for hybrid

railway vehicles, where the existing hybrid train configuration is optimised. Finally, Section 6.5 concludes this Chapter and discusses future research directions.

6.2 Hybrid Train Trajectory Optimisation Problem Formulation

6.2.1 Hybrid Railway System

A hybrid railway vehicle can generally be described as a railway vehicle equipped with two or more onboard power sources [58]. Hybrid propulsion traction systems come in various configurations, including a fuel cell combined with battery storage or supercapacitors, a diesel engine with battery storage, or a conventional bi-mode design featuring a pantograph and diesel engine onboard [59]. Modern railway systems have increasingly embraced hybrid traction systems due to their advantages over conventional traction systems and governmental legislation driving railway manufacturers to prioritise hybrid traction systems. Figure 17 provides a graphical illustration of the hybrid railway vehicle used in this study.study.

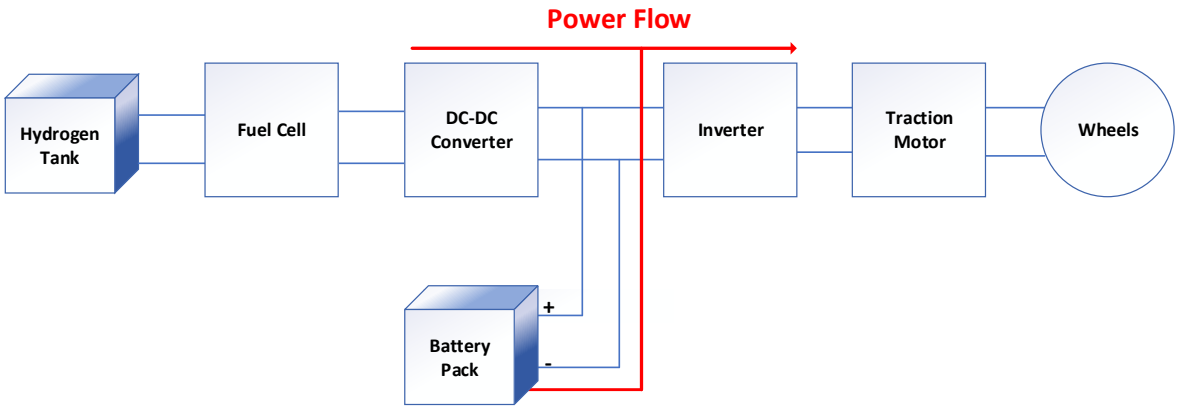

Figure 17: Hybrid railway vehicle equipped with hydrogen fuel cell and battery propulsion system

6.2.2 Optimisation Problem Identification

A hybrid train's journey, encompassing either a return or one-way trip, is referred to as a hybrid train trajectory. Like conventional railway vehicles, modern hybrid trains also face certain deficiencies. The hybrid railway system is presently grappling with the challenge of efficiently integrating multiple power sources on board while concurrently optimising the energy

management system, taking into account the ergonomic utilisation of these power sources. By effectively addressing these concerns, a hybrid train can attain optimal energy consumption, efficient power distribution, and economical use of power sources.

Trajectory optimisation for railway vehicles has garnered significant attention in the literature, particularly concerning conventional trains. In a study conducted by [213], the authors formulated an optimal control problem aimed at minimising the energy consumption of a train travelling between two stations. They employed a continuous-time optimal control approach and resolved the problem using a direct transcription method in conjunction with non-linear programming. Similarly, in a study by [214], the authors proposed an optimisation approach based on dynamic programming for train trajectory optimisation in the context of energy conservation. They examined the influence of various factors, including train mass, traction resistance, and track gradient, on the optimised trajectory.

In recent years, numerous optimisation techniques have been deployed to tackle the train trajectory optimisation problem. For instance, [215] utilised a model predictive control (MPC) strategy to optimise train trajectories while taking into account energy efficiency and travel time. The authors demonstrated that the MPC-based approach could optimise both the energy consumption and travel time of high-speed trains. Another study by [216] implemented a genetic algorithm to optimise the train speed profile and minimise energy consumption for regional trains subject to a fixed travel time constraint. A variety of energy management optimisation methods have been proposed and explored, including state machine strategies, fuzzy logic control, equivalent consumption minimization strategies, and more [217, 218]. Contemporary research predominantly focuses on fixed power demand [219]. One study [211] leverages the convexity of the specific consumption curve to enhance fuel economy and designs a scalable energy management strategy based on a suggested power-demand curve.

Another study [220] employs an online extremum-seeking method to estimate the maximum efficiency and power points of a fuel cell.

In the context of fixed-speed trajectories for fuel cell hybrid trains (FCHTs) [221], researchers have divided the trajectory into four states: traction, braking, coasting, and station parking. They then distribute power between the fuel cell and supercapacitor (SC) using a multi-mode equivalent energy consumption method. Building on this work [222], researchers have extended the approach to multiple fuel cells, splitting power among them through an equivalent fitting circle method and optimizing SC power output via an equivalent energy consumption method.

Yan et al. [223] optimised the speed trajectory to minimise energy consumption and determined a hybrid system control strategy based on minimum hydrogen consumption. Another study [224] proposed a rule-based energy management strategy to maximise regenerative braking energy recovery. A different method [225] used the motor characteristic curve, supercapacitor capacity, maximum acceleration, and other information to obtain the braking process speed trajectory, ensuring that the supercapacitor captures more regenerative braking energy. However, this method does not account for fuel cell efficiency. Sequential optimisation was applied in [226] to enhance fuel efficiency potential, developing a speed-smoothing strategy first, followed by battery charge optimisation based on the smoothed speed profile. Yet, train control strategies that directly impact traction energy demand are not included in the energy management process during the sequential optimisation process. This exclusion may compromise the effectiveness of the optimisation methods.

Genetic algorithms have demonstrated success in optimising single-train trajectories for DC traction systems in the context of solving linear optimisation problems [227-233]. In comparison, dynamic programming has exhibited superior performance over genetic and ant colony optimisation algorithms, particularly when the solution space converges during the

process of finding a solution [178]. On the other hand, brute force [234, 235] and direct search optimisation methods [236, 237] have proven to be inefficient, slow, and non-constructive in contrast to metaheuristic techniques. Predominantly, optimisation techniques employ a convex linear cost function. Although convex optimisation is time-efficient and relatively straightforward to implement, it provides a single optimal global solution with the potential uncertainty of a feasible solution to the problem [238-242]. In contrast to convex optimisation, non-convex optimisation functions examine multiple locally optimal solutions in order to explore a viable global solution to the problem. While non-convex optimisation is comparatively slower, it is highly efficient and offers a guaranteed optimal solution [243-247].

In the field of hydrogen & energy reduction for hybrid trains, recent research has explored various methods for co-optimizing train control strategies and onboard energy management simultaneously. In studies [248, 249], Pontryagin's Maximum Principle (PMP) and Dynamic Programming (DP) were integrated to address this issue by using the Hamiltonian as the objective function for DP. However, this approach was inherently limited by the "curse of dimensionality" and boundary-value problems. Peng et al. [250] proposed dynamic programming for co-optimising train driving cycles and energy management in fuel cell trains. They suggested parallelising DP to reduce computation time. Nonetheless, as the dimension of state variables in the dynamic programming model increases, the algorithm's calculation time also rises significantly due to its inherent characteristics. Jibrin et al. [251] tackled the co-optimisation of energy management and speed trajectory by formulating a convex optimisation model, employing convexity relaxation techniques to significantly improve calculation efficiency. However, convex optimisation necessitates that every constraint in the model is convex, which can limit the model's flexibility. In summary, current state-of-the-art studies have utilized Dynamic Programming and convex programming to address co-optimisation ,

highlighting the benefits of applying co-optimisation to hybrid trains. However, these methods still face limitations and challenges that need to be addressed.

In the above-mentioned research, co-optimisation primarily employs dynamic programming [248-250] and convex optimisation [251]. However, this Chapter proposes a new method to address the co-optimisation problem, investigating the energy-saving mechanism of hybrid trains using the co-optimisation model based on Mixed Integer Non-Linear Programming (MINLP). Furthermore, there is a need for further exploration into the energy-saving potential of the regenerative braking process and the enhancement of fuel cell efficiency during application by leveraging the hybridisation of both fuel cells and onboard energy storage devices. Although optimisation algorithms have been successfully applied in the railway industry for conventional railway vehicles, a gap remains in the literature regarding hybrid railway vehicles, whose propulsion systems' complexity and unique characteristics present additional challenges in optimising energy management and train dynamics. Consequently, there is a growing demand for innovative optimisation algorithms tailored to hybrid railway systems.

Existing research predominantly concentrates on optimisation techniques for conventional railway vehicles, leaving a noticeable gap in the application of these methods to hybrid railway systems. Hybrid railway vehicles possess unique propulsion system topologies compared to conventional trains, necessitating the development of advanced optimisation algorithms to effectively address their distinct challenges. These challenges include linear and non-linear constraints associated with hybrid railway vehicles, such as power source sizing, energy management, and train dynamics. To address this research gap, this study proposes a novel approach that utilises non-convex optimisation techniques, allowing for the optimisation of non-linear variables without conditioning while remodelling them as a linear dataset. This

method aims to reduce the noise in the dataset for optimisation caused by conditioning the benchmark dataset, thereby enhancing the results and efficiency of the optimisation process.

The proposed optimisation technique is based on numerical and metaheuristic algorithms to address the optimisation problem in hybrid railway vehicle traction systems by developing a time-based MINLP co-optimisation model. The optimisation method employs a non-linear programming solver to solve the problem, interpreting it through a non-convex, improved Rosenbrock function combined with a highly efficient, improvised "Mayfly Algorithm." The Mayfly Optimisation Algorithm (MOA) has emerged as a promising technique inspired by mayflies' unique behaviour and short lifespan [252]. MOA mimics the swarming and mating behaviours of mayflies, where the algorithm represents each mayfly as a candidate solution searching for the global optimum in the problem's search space. The short lifespan of mayflies encourages rapid exploration and exploitation of the search space, leading to faster convergence and improved results [253, 254]. The Rosenbrock function is a non-linear, non-convex, and continuous function that poses a significant challenge for optimisation algorithms due to its narrow and curved valley containing the global minimum [255]. By employing the MOA to optimise the Rosenbrock function, researchers can assess the algorithm's accuracy, precision, and efficiency in handling complex optimisation problems with intricate landscapes.

Several studies have reported the successful application of the MOA to various optimisation problems, including those involving the Rosenbrock function [256-259]. These studies have demonstrated that MOA can provide accurate and precise solutions for complex optimisation problems. Moreover, the algorithm has proven to be efficient in terms of convergence speed and computational complexity when compared to other metaheuristic algorithms [260, 261]. This study focuses on determining an optimal hybrid train trajectory for a mid-range light hybrid rail vehicle on typical British cross-country and intercity railway routes. The hybrid

train simulator [41] is used for benchmark simulation, and the proposed algorithm can simultaneously optimise multiple hybrid train trajectories.

6.3 Methodology

The hybrid algorithm proposed by the author efficiently solves multi-objective optimisation problems. It considers both global and local search, proving convergence speed and accuracy of optimisation based on improved Rosenbrock performance function and the Mayfly optimisation algorithm. Multiple techniques are implemented to cover the weaknesses of one method with others and achieve an optimal solution. The numerical approach is employed to perform the complex mathematical operation. The evolutionary algorithm mayfly is used along with Rosenbrock non-convex optimisation function to perform non-linear optimisation. The dataset of hybrid railway vehicles used in this study consists of train and route specifications, distance, energy consumption, power demand, traction forces, velocity, acceleration and journey time. The proposed optimisation algorithm was tested and calibrated with various test function variations to achieve the highest level of optimisation capability.

6.3.1 Hybrid Railway Vehicle Modelling

Distance-based mixed-integer linear programming (MILP) models are generally employed to identify the optimal speed trajectory for railway vehicles, where distance represents known parameters and time serves as variable parameters. However, the substantial computational effort is necessary when determining the power from onboard power sources, typically calculated using the formula $P_i = {E_i}/{t_t}$. It is essential to recognise that both energy and time are variables, and the linearisation of the ratio in the MILP model leads to computational complexity due to the significant magnitude difference and non-linear relationship between energy consumption and the corresponding time in the i^{th} distance step.

As an alternative, this study proposes a time-based mixed-integer non-linear programming (MINLP) model to circumvent this non-linear relationship, where time is a known parameter, and distance is a variable parameter. The hybrid train's speed at each time step is determined by the MINLP model, assuming that the train accelerates and decelerates uniformly in each time step. The speed trajectory is divided into n time steps, and the train travels through each step within a fixed time period, the length of which is set to 1 second per step in this case study. The distance travelled in the i^{th} step is denoted by Δd_i.

The vehicle dynamics of the hybrid train were developed by using the Lomonosff Equation based on Newton's second law of motion, as shown in Equation (6.1).

$$M_t(1+\lambda)\frac{d^2s}{dt^2} = TE - \left[C\left(\frac{ds}{dt}\right)^2 + B\left(\frac{ds}{dt}\right) + A\right] - M_t g \sin(\alpha) \tag{6.1}$$

It is assumed that the train maintains a steady rate of acceleration or deceleration in each time interval. As a result, the change in distance Δd_i can be computed by using Equation (6.2).

$$\Delta d_i = (\Delta t \times v_v) \tag{6.2}$$

where v_i is the hybrid train velocity in the i^{th} time step calculated by Equation (6.3).

$$v_i = \frac{1}{2} \times (v_i + v_{i+1}) \tag{6.3}$$

In order to determine the number of steps needed for the simulation, the total running time T and travel distance D are considered. Which allows us to calculate the number of steps by $n = {}^{T}/_{\Delta t}$. As a result, the overall distance covered by the train must adhere to the imposed constraint as given by Equation (6.4).

$$D = \sum_{i=1}^{n} \Delta d_i \tag{6.4}$$

The traction forces exerted on the hybrid train are described by Davis's Equation presented in Equation (6.5).

$$R_i = Cv_i^2 + Bv_i + A \tag{6.5}$$

where A, B & C are empirical constants representing the rolling resistance of a hybrid train, and R_i represents the drag resistance in the i^{th} step.

The acceleration and deceleration values, which are calculated using Equation (6.6), are set to ensure the safe operation of the hybrid train without exceeding their maximum values.

$$A_{acc,max} \geq {(v_{i+1} - v_i)}/{\Delta t} = a_i \geq A_{dec,max} \tag{6.6}$$

where $A_{acc,max}$ is maximum acceleration and $A_{dec,max}$ is the maximum deceleration rate of the hybrid train. The speed limit on the train is imposed by using Equation (6.7).

$$v_i \leq v_{i,lim} \tag{6.7}$$

The traction energy of the hybrid train is calculated by using Equation (6.8).

$$E_{Total} = \frac{1}{2} \times M * (v_{i+1}^2 - v_i^2) + \Delta h_i M g + R_i \Delta d_i \tag{6.8}$$

where M is the total weight of the hybrid train, g is the acceleration due to gravity, Δh_i is the difference between the route's gradient. The traction power of the hybrid train is calculated by using Equation (6.9).

$$P_{Total} = F_t v_i + P_{aux} + P_{loss} \tag{6.9}$$

where F_t are traction forces, v_i is the velocity of the hybrid train, P_{aux} is the auxiliary power used onboard and P_{loss} presents the power losses along the drive train. The state of charge of the hybrid train is calculated by using Equation (6.10).

$$SOC_{Batt} = \frac{E_{initial} + \sum_{j=1}^{i} E_{j,charg} - \sum_{j=1}^{i} E_{j,disch}}{E_{capacity}} \quad (6.10)$$

where $E_{initial}$ is the initial available charge in the battery. $E_{capacity}$ is the total capacity of battery. $E_{j,charg}$ is the charging energy at i^{th} step. $E_{j,disch}$ is the discharging energy at i^{th} step.

The output power of the fuel cell should not exceed the rated power, and the charging and discharging power of the battery should be within the rated charging and discharging power limits. These constraints are established based on the following conditions.

$$\begin{aligned} E_{i,FC} &\leq P_{FC,max}\,\Delta t \\ E_{j,charg} &\leq P_{d,max}\,\Delta t \\ E_{j,disch} &\leq P_{c,max}\,\Delta t \end{aligned} \quad (6.11)$$

where $P_{FC,max}$ is the fuel cell's maximum output power. $P_{d,max}$ is discharging power of the battery and $P_{c,max}$ is charging power of the battery.

6.3.2 Proposed Hybrid Optimisation Model

The author proposes a novel hybrid optimisation algorithm, grounded in sequential hybrid optimisation techniques, to achieve optimised energy consumption for hybrid railway vehicles by focusing on train trajectory and energy efficiency. This hybrid optimisation algorithm is developed in MATLAB, which employs a numerical programming solver, '*fmincon*', to tackle the non-convex optimisation problem and optimise the test function subject to non-convex constraints. The proposed hybrid algorithm follows a sequential optimisation method, considering both global and local search to ensure convergence speed and optimisation accuracy based on Speed Trajectory Optimisation and Energy Management Optimisation. Several techniques are incorporated to compensate for the limitations of one method with others, ultimately achieving an optimal solution. A numerical approach using MINLP &

Piecewise Non-Linearisation (PWNL) is employed to execute complex mathematical operations.

The Speed Trajectory and Energy Management Optimisation functions are subject to non-linear "convex and non-convex" constraints, with the forecast function performing non-convex optimisation. This study's hybrid railway vehicle dataset encompasses train and route specifications, gradient, distance, energy consumption, power demand, traction forces, velocity, and acceleration. The entire optimisation objective is to optimise the energy management of the hybrid train, which depends on speed trajectory and energy efficiency. Consequently, the process is divided into two steps: Speed Trajectory and Energy Management Optimisation. The Speed Trajectory Optimisation utilises the hybrid train's position data from the benchmark dataset, including distance, speed, and acceleration components, generating trajectory points for Energy Management Optimisation. The latter uses the remaining benchmark dataset elements, which include power, energy, and traction forces. The mathematical model of the proposed optimisation algorithm is discussed in the following Section. Figure 18 shows the framework schematic of the hybrid railway vehicle trajectory optimisation using the proposed algorithm.

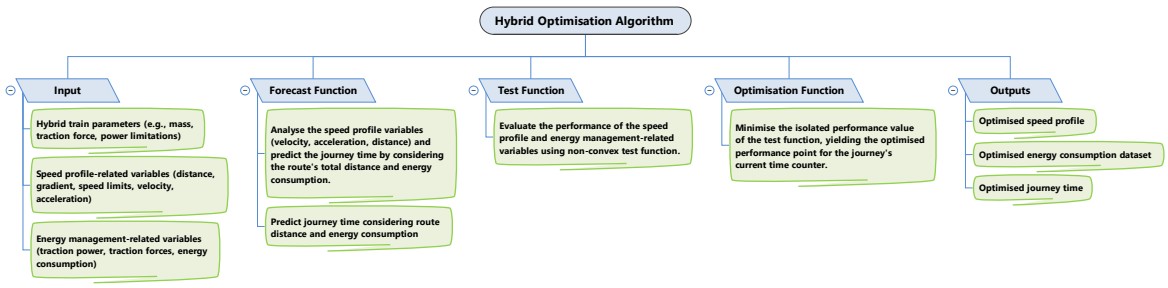

Figure 18: Framework schematic of hybrid railway vehicle trajectory optimisation algorithm

6.3.3 Speed Profile Related Variables

In the Mixed-Integer Non-Linear Programming (MINLP) model, a range of variables associated with speed is incorporated, exhibiting a non-linear relationship between them. To

manage these non-linear relationships, Piecewise Non-Linearisation (PWNL) is employed. PWNL enables the representation of a non-linear function through a series of non-negative variables. Initially, variables such as distance, velocity, and acceleration of the train at the i^{th} step is utilised to indicate the train's position and is expressed by Equations (6.12), (6.13) & (6.14).

$$d_i = \sum_{i=1}^{t} \big(d(x_i)\big) \tag{6.12}$$

$$v_i = \sum_{i=1}^{t} \big(v(x_i)\big) \tag{6.13}$$

$$a_i = \sum_{i=1}^{t} \big(a(x_i)\big) \tag{6.14}$$

where t represents the constraints on speed and acceleration, which are based on the distance, while x_i denotes the variables of a special order set. The hybrid train's inequality constraints for the Speed Trajectory subset, derived from the benchmark dataset, are modelled using Equation (6.15):

$$\begin{aligned} d_{min} < d_x < d_{Inst} \quad & if\ (d_{current} > 0), \\ v_{min} < v_x < v_{Inst} \quad & if\ (d_{current} > 0) \\ a_{min} < a_x < a_{Inst} \quad & if\ (a_{current} > 0) \\ a_{Inst} < a_x < a_{max} \quad & if\ (a_{current} \leq 0) \end{aligned} \tag{6.15}$$

In Equation (6.15), minimum limits for the distance, velocity, and acceleration vectors are represented by d_{min}, v_{min} and a_{min}, respectively. Conversely, d_{max}, v_{max} and a_{max} signify the maximum limits for distance, velocity, and acceleration. The instantaneous rates of the distance, velocity, and acceleration vectors are denoted by d_{Inst}, v_{Inst} and a_{Inst} respectively. The scalar value of the iterative time counter for the distance data from the benchmark

trajectory is equal to $d_{current}$. Furthermore, $d(x_i), v(x_i)$ and $a(x_i)$ represent the instantaneous points at a specific iterative time counter i.

6.3.4 Energy Management Related Variables

In this model, the final energy consumption of the hybrid train is calculated using traction power and tractive forces. The energy consumption rate for a hybrid train is closely associated with its output power and is typically represented in relation to normalised power. Consequently, within this proposed method, the energy consumption rate can be modelled by using Equations (6.16), (6.17) and (6.18).

$$P(x_i') = \sum_{j=1}^{N} \sum_{i=1}^{S} \sum_{x_{i,j}'=1}^{t'} P\,(x_{i,j}') \tag{6.16}$$

$$F(x_i') = \sum_{j=1}^{N} \sum_{i=1}^{S} \sum_{x_{ij}'=1}^{t'} F\,(x_{i,j}') \tag{6.17}$$

$$E(x_i') = \sum_{j=1}^{N} \sum_{i=1}^{S} \sum_{x_{i,j}'=1}^{t'} E\,(x_{i,j}') \tag{6.18}$$

In this model, N denotes the constraints on Power, Energy, and Tractive Forces, while S represents the limits on the number of stations encountered during each route journey. Additionally, t' signifies the constraints on the time required for the route journey in order to consume the total Power and Energy. This approach ensures a comprehensive and structured representation of the various factors influencing the hybrid train's energy consumption. The hybrid train inequality constraints of the energy consumption model are represented by Equation (6.19).

$$P_{min_{i,j}} < P(x_{ij}) < P_{inst_{i,j}} \qquad if\ \left(P_{inst_{i,j}} > 0\right)$$

$$P_{inst_{i,j}} < P(x_{ij}) < P_{max_{i,j}} \qquad if\ \left(P_{inst_{i,j}} \leq 0\right)$$

$$
\begin{aligned}
E_{min_{i,j}} < E(x_{ij}) < E_{inst_{i,j}} \qquad & if \left(E_{inst_{i,j}} > 0\right) \\
E_{inst_{i,j}} < E(x_{ij}) < E_{max_{i,j}} \qquad & if \left(E_{inst_{i,j}} \leq 0\right) \\
F_{min_{i,j}} < F(x_{ij}) < F_{inst_{i,j}} \qquad & if \left(F_{inst_{i,j}} > 0\right) \\
F_{inst_{i,j}} < F(x_{ij}) < F_{max_{i,j}} \qquad & if \left(F_{inst_{i,j}} \leq 0\right)
\end{aligned}
\tag{6.19}
$$

where $P_{min_{i,j}}, P_{inst_{i,j}}$ and $P_{max_{i,j}}$ is the minimum instantaneous and maximum power values of the traction power subset. $E_{min_{i,j}}, E_{inst_{i,j}}$ and $E_{max_{i,j}}$ is the minimum, instantaneous and maximum values of the energy subset. $F_{min_{i,j}}, F_{inst_{i,j}}$ and $F_{max_{i,j}}$ is the traction forces subset's minimum, instantaneous, and maximum power values. $P(x_{i,j}), E(x_{i,j})$ and $F(x_{i,j})$ represents the instantaneous points of power, energy and traction forces at the instantaneous time i, which is an iterative counter.

6.3.5 Forecast Function (Non-Convex Constraints)

The forecast function, incorporated from the Mayfly algorithm, serves as an equality constraint representing the hybrid train's journey time by analysing the route's total distance and energy consumption. Equation (6.20) presents the forecast Equation, which analyses the speed profile variables, including velocity, acceleration, and distance, to determine the journey's duration successfully. This method allows for a thorough evaluation of the hybrid train's performance, ensuring that the optimisation process takes into account all relevant factors.

$$
\begin{aligned}
\overline{G_{best}(x_\iota + 1)} = \sum_{x=1}^{t} G_{best}(x_i) + \sum_{x=t}^{\bar{t}} (2G_{best}(x_i) - d(x_i - 1), \\
if(G(x_i - 1) > G_{best}(x_i - 1))
\end{aligned}
\tag{6.20}
$$

where, $\bar{t}$ denotes the forecasted journey time while $G_{best}(x_i)$ and $2G_{best}(x_i)$represent the instantaneous route gradient rates at the i^{th} iterative time counter from the forecast trajectory. $(G(x_i - 1)$corresponds to the distinct set of gradient values from the starting point of the route

journey. Additionally, $G_{best}(x_i - 1)$ is associated with the forecast value of the starting time for the route journey. Meanwhile, $\overline{G_{best}(x_\iota + 1)}$ signifies the forecast value of the journey time at the next point along the route. This comprehensive approach ensures that all relevant factors are taken into consideration when predicting the hybrid train's performance and journey time.

The forecasted journey consumption of power, traction forces, and energy subsets from the energy management optimisation set are derived from the forecasting executed in Equation (6.21). The forecast Equation serves to estimate the total energy needed to complete the journey time by predicting the energy and power sets of the forecast trajectory. This method enables a comprehensive understanding of fuel requirements, allowing for more accurate and efficient energy management throughout the journey.

$$\overline{G'_{best}(x'_{i,J} + 1)} = \sum_{j=1}^{N}\sum_{i=1}^{S}\left(\sum_{x'=1}^{t'} G'_{best}(x'_{i,j}) + \sum_{x'=t'}^{\bar{t'}} 2G'_{best}(x'_{i,j}) - G'(x'_{i,j} - 1) \right) \quad (6.21)$$

$$if(G'(x'_{i,j} - 1) > G'_{best}(x'_{i,j} - 1))$$

where $\bar{t'}$ denotes the forecasted journey time. $G'_{best}(x'_{i,j})$ and $2G'_{best}(x'_{i,j})$represent the unique instantaneous points of the energy management-related vector at the respective time, station, and vector counters from the forecast trajectory, as evaluated using Equation (6.21). $G'(x'_{i,j} - 1)$ corresponds to the unique point at the first time-step backward journey time counter, originating from the instantaneous time iterative counter of the Energy Management vector within the benchmark trajectory.

Meanwhile, $G'_{best}(x'_{ij} - 1)$ signifies the unique point at the first time-step backward journey time iterative counter from the instantaneous journey time iterative counter of the Energy Consumption vector within the optimised trajectory. Lastly, $\overline{G'_{best}(x'_{iJ} + 1)}$ corresponds to the

unique point at the initial time-step forward journey time iterative counter from the instantaneous time iterative counter of the core vector in the optimised trajectory. The forecast Equation (6.22) evaluates the optimisation process's first iteration to the benchmark trajectory's final time.

$$\overline{G'_{best}(x'_{lJ}+1)} = \sum_{j=1}^{N}\sum_{i=1}^{S}\left(\sum_{x'=1}^{t'} G'_{best}(x'_i) + \sum_{x'=t'}^{\bar{t'}} G'_{best}(x'_{ij}-1) - 2G'_{best}(x'_{ij})\right) \quad (6.22)$$

$$if(G'(x'_{ij}-1) < G'_{best}(x'_{ij}-2))$$

where $G'(x'_{ij}-2)$ corresponds to the unique point of the 2 (seconds) time-step backward journey time counter from the instantaneous time iterative counter of the energy consumption vector of the benchmark trajectory.

6.3.6 Test Function

The evaluation of the speed profile-related variables of the hybrid train from the benchmark trajectory is conducted by using a single non-convex test function. The proposed objective function employed for the benchmark dataset is as follows:

$$f(x_i) = \left[10^{5-m}\sum_{x=1}^{t}(G(x_i+1)-G(x_i)^2)^2 + \left(\frac{1-G(x_i)^2}{10^{15}}\right)\right] \quad (6.23)$$

In the proposed objective function, $G(x_i+1)$ represents the scalar distance value of the distance variable for a one-second time step forward from the instantaneous journey time iterative counter within the benchmark trajectory. The function $f(x_i)$ has a mean of zero and a variance of one. Additionally, m is a design constant with a set value of 3 for the distance vector in the benchmark journey.

Conversely, the performance evaluation of the energy management-related variables subset, which represents the traction power, energy, and traction forces subset model, is assessed

through an alternative approach and presented in Equation (6.24). This method takes into account the unique characteristics and requirements of the energy management subset within the hybrid train trajectory optimisation process.

$$f'(x'_{i,j}) = 10^{5-m'} \sum_{j=1}^{N} \sum_{i=1}^{S} \sum_{x'=1}^{t'} (G'(x'_{i,j}+1) - G'(x'_{i,j})^2)^2 + (1 - G'(x'_{i,j})^2) \qquad (6.24)$$

In the above Equation, $f'(x'_{i,j})$ evaluates the data from the initial to the final time of the iterative station and subset counter while also considering the sum of the differences from the scalar value of the instant journey time, station, and subset iterative counters, respectively. The term $x'_{i,j} + 1$ denotes a one-second time step forward in the journey from the instant iterative time counter of the iterative station and subset counter of the benchmark subset. $G(x_i + 1)$ signifies the unique value of a single subset of the forward journey time iterative counter of the iterative station and subset counter within the benchmark subset.

The test function has a mean of zero and a variance of one, with m' representing the design constant with values ranging from 0 to 24 for the core journey dataset. The design parameters for the cost function were established as follows:

$$m' = \begin{cases} 0 \; to \; 13, & if \; (t' > 2000) \\ 14 \; to \; 24 & if \; (t' < 2000) \end{cases} \qquad (6.25)$$

6.3.7 Optimisation Function (Non-Convex Constraints)

The optimisation function aims to minimise the isolated performance value of the test function and returns the optimised performance point from the core set of the journey's current time counter. Equation (6.26) calculates the optimised speed trajectory for speed profile and position-related variables at the optimised journey time. At each iteration from the initial time to the benchmark journey time, $f(x_i)$ evaluates and returns a scalar performance value, which is then passed to the optimisation function as depicted in Equation (6.26). This optimisation

function minimises the test function's scalar performance value. As a result, it yields the optimised unique performance point and the isolated distance value for the current journey time counter from the optimal trajectory's distance vector, as demonstrated in Equation (6.26).

$$[\, G_{best}(x_i), f_{best}(x_i)] = min_d \sum_{x=1}^{t} f(x_i) \tag{6.26}$$

The instantaneous optimised performance function, denoted as $f_{best}(x_i)$ corresponds to the instant time ranging from 1 second to the benchmark journey time and is subject to the non-linear inequality constraints of the hybrid train, as mentioned in Equation 15. $G_{best}(x_i)$ represents the instantaneous optimised value of the distance and time non-linear dataset for the optimised performance function. The time of the optimised reference journey, $G_{best}(x_i)$ coincides with the benchmark reference journey time, $G(x_i)\ t$. The journey time of the optimised trajectory, $G_{best}(x_i)$, is replaced with the best journey time. By minimising the instantaneous value of the performance function at each iteration from the starting time to the benchmark journey time, the optimised distance vector is determined.

The $f'(x'_{i,j})$ from Equation (6.24) returns the optimised energy management-related variables and passes them to the optimisation function in Equation (6.27). This optimisation function is denoted as $[\, G'_{best}(x'_{ij}), f'_{best}(x'_{ij})]$ minimises the instantaneous performance value at each time and station counter iteration. As a result, the function returns the optimised performance value and the optimised energy consumption dataset for the hybrid train trajectory.

$$[\, G'_{best}(x'_{ij}), f'_{best}(x'_{ij})] = \ min_{d'} \sum_{j=1}^{N} \sum_{i=1}^{S} \sum_{x'=1}^{t'} f'(x'_{ij}) \tag{6.27}$$

where $f'_{best}(x'_{ij})$ represents the instantaneous optimised performance function with respect to the instantaneous time counter iterating from the initial time of the benchmark trajectory and the instantaneous station counter iterating from the initial station to the final station of the

benchmark trajectory. These iterations are subject to the inequality constraints of the hybrid railway vehicle stated in Equation (6.19). $G'_{best}(x'_{ij})$ is the instantaneous value of the energy management-related variables of the optimised performance function. The optimised distance variable is evaluated by minimising the immediate value of the performance function at each iteration of the time, station and vector counter.

6.3.8 Hybrid Optimisation Algorithm Calibration

The hybrid optimisation algorithm underwent a calibration process using various test functions to ensure a robust and efficient cost function. These test functions comprised benchmark data, which was then evaluated by the optimisation and forecast functions. The calibration process employed a combination of typical non-convex and convex objective functions to fine-tune the algorithm's performance. The specific test functions utilised for calibrating the hybrid optimisation algorithm are detailed below:

Table 17: List of test functions used to calibrate the proposed hybrid optimisation algorithm

Function	Equation	Source
Sphere	$f_1(x) = \sum_{i=1}^{t} Gx_{i+1}^2$	[262]
Griewank	$f_2(x) = \frac{1}{4000}\sum_{i=1}^{t} Gx_i^2 - \prod_{i=1}^{t} \cos\left(\frac{x_i}{\sqrt{i}}\right) + 1)$	[263]
Rastrigin	$f_3(x) = \left[(10^t) + \sum_{x=1}^{t} (G(x)^2 - Acos(2\pi x)\right]$	[264]
Schaffer	$f_4(x) = 0.5 + \frac{sin^2\left(\sum_{i=1}^{t} Gx_i^2\right) - 0.5}{\left(1 + 0.001\left(\sum_{i=1}^{t} Gx_i^2\right)\right)^2}$	[265]
Rosenbrock	$f_5(x) = \sum_{i=1}^{t-1} 100\ (Gx_{i+1}^2 - Gx_i)^2 + (Gx_i - 1)^2 \quad \begin{cases} -50 \le x_i \le 50 \\ i = 1,2 \end{cases}$	[266]

Ackley

$$f_6(x) = -20\,exp\left[-0.2\sqrt{\frac{1}{d}\sum_{i=1}^{t} Gx_i^2}\right] - exp\left[\sqrt{\frac{1}{d}\sum_{i=1}^{t}\cos(G2\pi x_i)}\right] + a + \exp(1) \quad [267]$$

In above Equations $G(x)^2$ represents the unique data subset of speed profile and energy management-related variables. The function is evaluated on the hypercube x_i. t represents the dimension of the solution space of each function.

6.3.9 Hybrid Algorithm Performance Validation

6.3.9.1.Parameter settings:

A series of experiments were conducted on the hybrid optimisation algorithm to assess its performance. The non-negative constant, k, was utilised in this study to evaluate the convex and non-convex sets and was initially introduced in the forecast Equation (6.22). The hybrid optimisation algorithm was tested with various values of k, including $k = \{1,2,3,\ldots,8\}$. The dimensions tested within the vector space of the hybrid algorithm were chosen based on the route journey time, t, which was approximately 35 minutes. This selection ensured a comprehensive assessment of the algorithm's effectiveness across different scenarios, ultimately contributing to the development of an optimised trajectory for hybrid railway vehicles.

6.3.9.2.Experimental Results:

The validation results for the Rastrigin, Ackley, Griewank, Schaffer, Rosenbrock, and Sphere functions, as discussed in Section 6.3.9, are presented in Table 18 and Table 19. The parameter k in the hybrid algorithm sets the optimisation parameters by manipulating key aspects of the optimisation function, which subsequently results in the exploration and exploitation of the optimised dataset. As the k value in optimisation iterates from zero to a random value, there is an observed increase in the exploitation and a decrease in the exploration of the hybrid algorithm. The experimental results suggest that the best mean value of the optimised function

initially decreases for each test function optimisation, thereby improving the solution. However, as the value of k increases, the solution deteriorates at specific points in certain cases, two of which are illustrated in Figure 18.

Table 18: Optimisation of Rastrigin, Ackley & Griewank test function by the hybrid algorithm with $k = \{1,2,3, \dots ,8\}$

Test Functions		**Rastrigin (f_1)**	**Ackley (f_2)**	**Griewank (f_3)**
	No. of iterations	**Mean**	**Mean**	**Mean**
k = 1	15	1.86E-06	2.86E-03	1.06E-05
k = 2	10	3.08E-08	1.58E-05	2.98E-07
k = 3	19	2.99E-09	1.49E-06	3.47E-08
k = 4	21	6.59E-10	6.96E-07	7.96E-09
k = 5	17	2.15E-09	1.14E-06	2.84E-08
k = 6	10	7.99E-09	7.58E-06	8.68E-08
k = 7	12	9.59E-08	8.69E-05	7.69E-07
k = 8	14	4.81E-06	2.11E-03	3.19E-05

Table 19: Optimisation of Schaffer, Rosenbrock & Sphere test function by the hybrid algorithm with $k = \{1,2,3, \dots ,8\}$

Test Functions		**Schaffer (f_4)**	**Rosenbrock (f_5)**	**Sphere (f_6)**
	No. of iterations	**Mean**	**Mean**	**Mean**
k = 1	15	2.96E-04	1.88E-08	2.85E-07
k = 2	10	1.99E-06	1.60E-10	2.31E-06
k = 3	19	2.48E-07	1.50E-11	2.99E-09
k = 4	21	5.96E-08	**7.03E-12**	8.97E-05
k = 5	17	2.19E-07	1.15E-11	3.54E-07
k = 6	10	6.88E-07	7.66E-11	8.51E-08
k = 7	12	7.67E-06	8.78E-10	8.69E-07
k = 8	14	3.41E-04	2.13E-08	2.58E-07

It was observed that the performance of the hybrid algorithm employing the Rosenbrock test function with $k = \{4, 5 \,\&\, 6\}$ outperformed all other test functions. The Rastrigin function demonstrated performance levels nearest to the Rosenbrock function; however, for the final implementation, only the Rosenbrock test function was used to perform the case study presented in Section 4. This decision was made based on the superior performance of the

Rosenbrock function in the validation results, which indicated its suitability for effectively optimising hybrid railway vehicle trajectories.

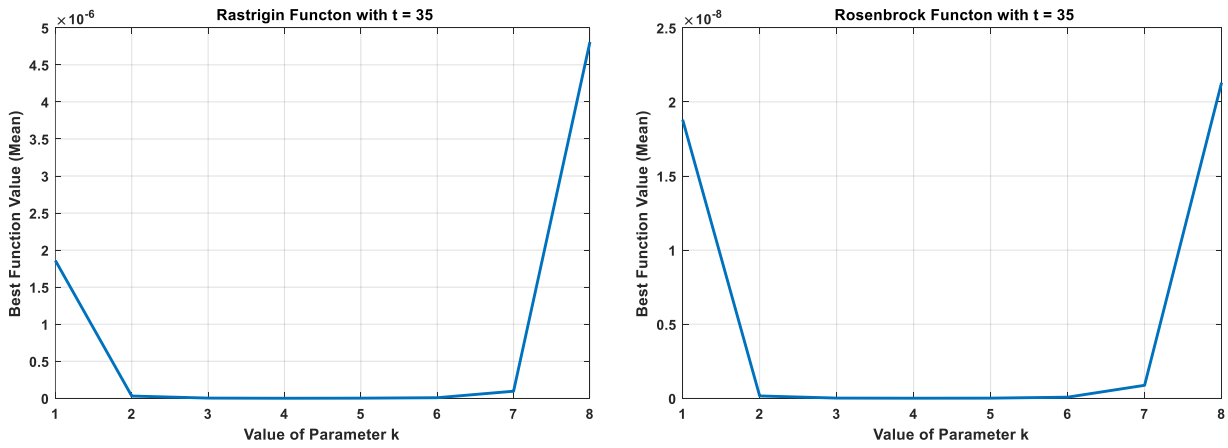

Figure 19: The variations of the best mean value of the Rosenbrock and Rastrigin function concerning k values of the hybrid algorithm

6.4 Case Study

In this research, the case study is conducted by employing a comprehensive simulation of benchmark trajectories for the hybrid railway vehicle, utilising the hybrid train simulator developed by the author in a previous study [41]. The simulation results derived from these benchmark trajectories are subsequently fed into the novel hybrid optimisation algorithm, specifically designed to optimise the single train trajectory of the hybrid railway vehicle.

The case study aims to demonstrate the significant improvements achieved through the application of the proposed hybrid optimisation algorithm, such as a substantial reduction in energy consumption and more efficient utilisation of power sources throughout the journey. Moreover, the study will examine the delicate balance between energy and time trade-offs, which is critical in real-world applications of hybrid railway systems. A detailed block diagram illustrating the various stages and components of the optimisation operation is presented in Figure 20. This graphical representation offers further insights into the intricacies of the

proposed algorithm, thus facilitating a deeper understanding of the underlying optimisation process and its implications for hybrid railway vehicle trajectory optimisation.

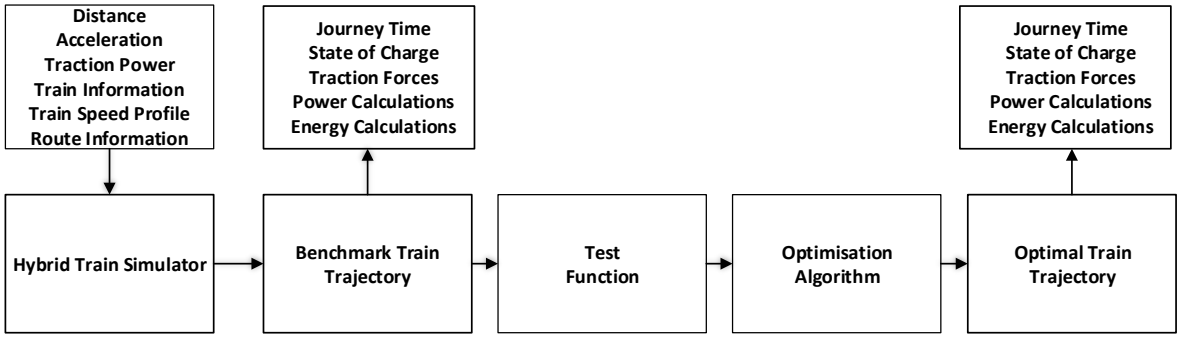

Figure 20: Block diagram of the optimisation process

6.4.1 Route Selection

In this case study, the author has undertaken a detailed analysis of four distinct routes, each chosen for its representation of British cross-country and intercity travel. Spanning a range of distances from 22km to 200km, these routes were carefully selected to provide a comprehensive and representative overview of rail travel within the UK. Each route is subject to a unique speed limit, as mandated by the regulations of Network Rail. While the speed limits of each route were not included in Table 20 due to the complexity of multiple speed limits across longer routes, they were taken into consideration in the analysis.

Table 4 provides an overview of the name and distance of each route, which is instrumental in understanding the scope and scale of this case study. The diverse selection of routes ensures that the findings of this analysis can be applied to a broad range of travel scenarios, thus contributing to the development of more effective and efficient rail travel in the UK.

Table 20: List of the routes utilised in the case study, along with their corresponding distances.

Route No.	Name	Distance
1	Camphill – Birmingham New street	22.40 km
2	Birmingham Moor Street – Strafford-upon-Avon	78.58 km
3	Paddington – Marlow	100 km
4	Gloucester – Westbury	199.37 km

6.4.2 Vehicle Selection

In this case study, a heavily modified British Class 150 rail vehicle equipped with a hybrid propulsion system has been chosen as the subject of analysis. Originally, the British Class 150 diesel train was fitted with a pair of 213 kW Cummins engines, delivering a combined output power of 426 kW. For this investigation, the diesel engine was replaced with a 300 kW hydrogen fuel cell system and a 120.24 kWh battery pack, capable of providing 120 kW of power at a 1C discharge rate. It should be noted that the author's previous research has utilised a different variant of the same vehicle and route [4]. The specifications of the hybrid British Class 150 train under investigation are presented in Table 21.

Table 21: Hybrid train specifications and efficiencies

Parameter	**Value**		**Efficiency**	
Tare mass	74.2 t		Drive train	87%
Starting tractive effort	37.52 kN		Traction motor	95%
Maximum acceleration	0.5 m/s^2		DC-BUS/IGBT	97.5%
Maximum speed	121 km/h		Fuel cell	50%
Davis Equation	$R=1.5+0.006v + 0.0067v^2$	+	Battery	94.5% [268]
Fuel Cell	300 kW			
Battery	120.24 kWh			
Auxiliary power	28 kW			
Available Hydrogen	74 kg			
Energy available in Hydrogen Tanks	2464 kWh			

6.4.3 Trajectories Simulation

Table 22 presents benchmark and optimised trajectories of a hybrid train for four different routes, comparing various power, energy, performance, and range parameters. A detailed technical analysis of the table enables us to derive key insights and assess the consistency of optimised values percentage for essential parameters, such as total energy at wheels, total energy at traction motor, the total energy required for a return journey, journey time, average traction power at wheels, and range.

Total energy at wheels: The optimised trajectories consistently demonstrate a reduction in energy consumption at wheels for all routes. The reduction percentages are 10.91% (Route 1), 12.04% (Route 2), 10.26% (Route 3), and 10.61% (Route 4). This consistency highlights the algorithm's ability to optimise energy consumption for diverse route profiles effectively.

Total energy at traction motor: The optimised trajectories display reduced energy consumption at the traction motor for all routes: 12.07% (Route 1), 12.78% (Route 2), 11.46% (Route 3), and 11.99% (Route 4). These results indicate that the optimisation algorithm consistently improves energy efficiency at the traction motor.

Total energy required for a return journey: A comparison between the benchmark and optimised trajectories reveals a decline in energy consumption for all routes. The reduction percentages are 17.78% (Route 1), 16.29% (Route 2), 16.75% (Route 3), and 16.54% (Route 4). These findings suggest the optimisation algorithm's effectiveness in improving energy efficiency.

Journey time: The optimised trajectories across all routes feature a slight increase in journey time compared to the benchmark values. The differences range from 0.12 minutes (Route 1) to 0.48 minutes (Route 4). This trend suggests that the optimisation algorithm prioritises energy

efficiency over minimising journey duration, which may be an essential consideration for real-world applications.

This increase in journey time can be seen as an energy-time trade-off, where the algorithm accepts slightly longer journey times in exchange for significant reductions in energy consumption. This trade-off is particularly relevant in the context of hybrid railway systems as it balances operational efficiency with environmental and economic concerns. By reducing energy consumption, the hybrid train lowers its operational costs. It contributes to reducing greenhouse gas emissions and overall environmental impact. Therefore, the energy-time trade-off achieved by the optimisation algorithm demonstrates its value in addressing critical aspects of sustainable transportation, making it a viable solution for enhancing the performance and efficiency of hybrid railway vehicles.

Average traction power at wheels: Average traction power at wheels: The optimised trajectories show a reduction in average traction power at wheels across all routes. The reduction percentages are 18.06% (Route 1), 14.36% (Route 2), 14.14% (Route 3), and 14.10% (Route 4). This consistency indicates the algorithm's effectiveness in optimising traction power for improved efficiency.

By reducing stress on traction power, the optimised trajectories not only contribute to energy efficiency but also have the potential to decrease maintenance requirements and increase the life of power sources. Lower average traction power at wheels means reduced wear and tear on mechanical components, such as motors and gearboxes, as well as decreased thermal stress on the electrical systems. As a result, maintenance costs can be lowered, and the service life of critical components can be extended, which ultimately leads to higher overall system reliability and cost-effectiveness.

Range: The range of the train shows improvements in the optimised trajectories for all routes. The increases are 16.00% (Route 1), 16.67% (Route 2), 20.00% (Route 3), and 33.33% (Route 4). This improvement signifies enhanced operational efficiency.

Energy and power distribution: The optimised trajectories showcase the hybrid optimisation algorithm's effectiveness in reducing the fuel cell power at wheels for all routes. This results in a more efficient energy distribution between the fuel cell and battery systems. This translates to decreased hydrogen consumption for one return journey across all routes, with savings varying from 0.42 kg (Route 1) to 2.89 kg (Route 4). The optimisation algorithm thus demonstrates its capability to optimise energy sources for hybrid railway vehicles.

Performance metrics and journey characteristics: The optimised trajectories indicate improvements in several performance metrics. The maximum acceleration reached remains constant between the benchmark and optimised trajectories across all routes, indicating that the optimisation process does not compromise acceleration performance. The total distance travelled remains the same for both benchmark and optimised trajectories, highlighting the algorithm's ability to achieve energy efficiency without altering the route's overall distance.

For brevity, the author focuses solely on Route 1, "Camphill - Birmingham New Street," for a visual presentation in this study. The benchmark trajectory results indicate an energy consumption of 90 kWh, utilising a maximum traction power at wheels of 342 kW. The benchmark trajectory was completed in 34.80 minutes, with an average traction power at wheels of 155 kW.

In this configuration, 28 kW of fuel cell power was allocated exclusively for auxiliary systems, reducing the load stress on the battery. Table 6 reveals that, during the benchmark trajectory simulation, the fuel cell provided 33 kWh of traction energy at the wheels, while the battery pack contributed an additional 22 kWh. The braking system regenerated 35 kWh of energy

stored in the battery pack. The hybrid train consumed 2.85 kg of hydrogen for a return journey, enabling a range of 25 journeys limited by battery charge depletion. Figure 21 shows the benchmark trajectory simulation's traction power and energy consumption profiles.

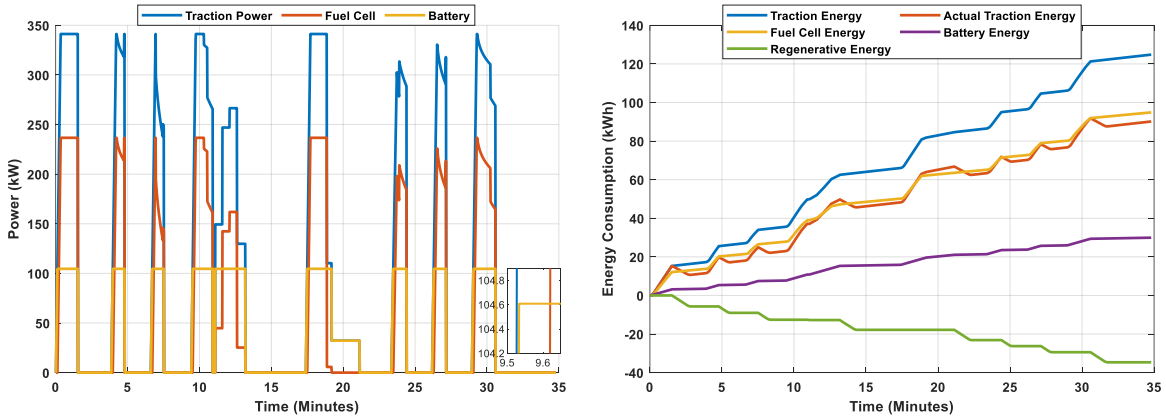

Figure 21: Traction power and energies of benchmark trajectory

In contrast, the optimised trajectory results showcase an energy consumption of 74 kWh, utilising 285 kW of power. The optimised trajectory was completed in 34.92 minutes, with an average traction power at wheels of 127 kW. Similar to the benchmark trajectory simulation, 28 kW of fuel cell power was dedicated exclusively to auxiliary systems in the optimised trajectory, thus reducing the load stress on the battery. As shown in Table 22, the fuel cell supplied 27 kWh of traction energy at the wheels during the optimised trajectory simulation, while the battery pack contributed an additional 22 kWh. The braking system regenerated 38 kWh of energy stored in the battery pack.

The hybrid train consumed 2.43 kg of hydrogen for a return journey, enabling a range of 29 journeys limited by battery charge depletion. Figure 22 illustrates the optimised trajectory simulation's traction power and energy consumption profiles.

Table 22: Benchmark and optimised trajectories of hybrid train simulation results

	Route 1		Route 2		Route 3		Route 4	
Parameter	**Benchmark**	**Optimised**	**Benchmark**	**Optimised**	**Benchmark**	**Optimised**	**Benchmark**	**Optimised**
Power								
Fuel cell power	300 kW	300 kW	300 kW	300 kW	300 kW	300 kW	300 kW	300 kW
Battery power @1-C rating	120 kW	120 kW	120 kW	120 kW	120 kW	120 kW	120 kW	120 kW
Auxiliary power	28 kW	28 kW	28 kW	28 kW	28 kW	28 kW	28 kW	28 kW
Fuel cell power at wheels	237 kW	180 kW	237 kW	180 kW	237 kW	180 kW	237 kW	180 kW
Battery power at wheels	105 kW	105 kW	105 kW	105 kW	105 kW	105 kW	105 kW	105 kW
Average traction power at wheels	155 kW	127 kW	202 kW	173 kW	198 kW	170 kW	234 kW	201 kW
Energy								
Fuel cell energy at wheels	33 kWh	27 kWh	133 kWh	110 kWh	177 kWh	147 kWh	245 kWh	202 kWh
Battery energy at wheels	22 kWh	22 kWh	83 kWh	84 kWh	96 kWh	98 kWh	151 kWh	152 kWh
Total energy at wheels	55 kWh	49 kWh	216 kWh	190 kWh	273 kWh	245 kWh	396 kWh	354 kWh
Total energy at traction motor	58 kWh	51 kWh	227 kWh	198 kWh	288 kWh	255 kWh	417 kWh	367 kWh
Total energy at DC-BUS	59 kWh	52 kWh	233 kWh	204 kWh	295 kWh	265 kWh	428 kWh	373 kWh
Total auxiliary energy	17 kWh	17 kWh	51 kWh	52 kWh	57 kWh	58 kWh	77 kWh	77 kWh
Total output energy for traction & aux	76 kWh	69 kWh	284 kWh	256 kWh	352 kWh	321 kWh	507 kWh	450 kWh
Regenerated energy saved in battery	35 kWh	38 kWh	124 kWh	136 kWh	178 kWh	191 kWh	197 kWh	215 kWh
Total energy required for a return journey	90 kWh	74 kWh	356 kWh	298 kWh	394 kWh	328 kWh	641 kWh	535 kWh
Hydrogen required for one return journey	2.85 kg	2.43 kg	11.50 kg	9.71 kg	12.61 kg	10.92 kg	19 kg	16.11kg
Range of train (return journeys)	25	29	6	7	5	6	3	4
Journey time	34.80 min	34.92 min	106.02 min	106.57 min	119.15 min	119.68 min	164.70 min	165.18 min
Max velocity reached	96.56 km/h	93.00 km/h	96.54 km/h	92.98 km/h	124.83 km/h	121.27 km/h	160.93 km/h	157.37 km/h
Max acceleration reached	0.52 m/s^2	0.52 m/s^2	0.53 m/s^2	0.53 m/s^2	0.48 m/s^2	0.48 m/s^2	0.55 m/s^2	0.55 m/s^2
Total Distance Traveled	22.40 km	22.40 km	78.58 km	78.58 km	100 km	100 km	199.52 km	199.52 km

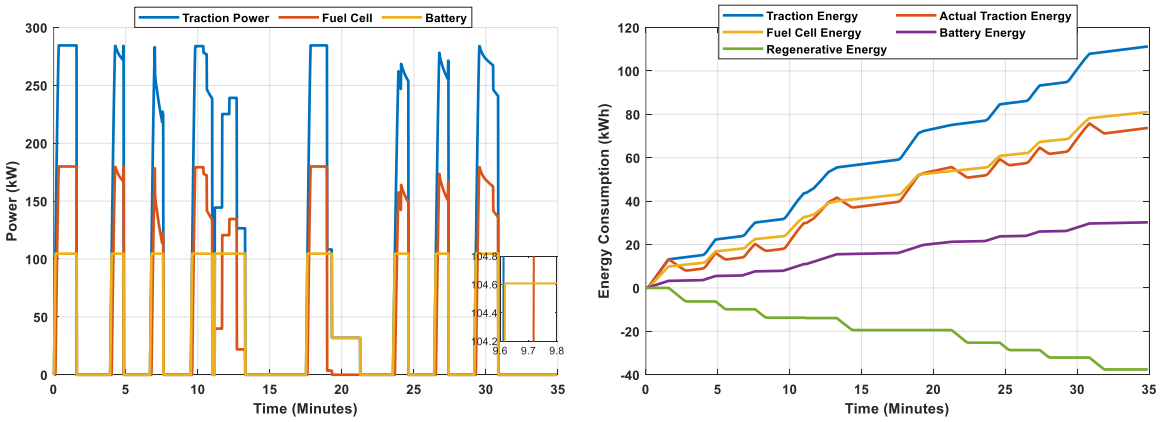

Figure 22: Traction power and energies of optimised trajectory

6.4.4 Analysis of benchmark and optimised results

The hybrid optimisation algorithm developed by the author focuses on the optimal control strategy for hybrid railway vehicles, aiming to improve operational design parameters such as energy consumption, journey time restrictions, and meeting power demand during operation. The case study presented in Section 4 serves as an application for the hybrid optimisation algorithm and focuses on typical UK routes used for cross-country and intercity traffic with varying lengths. This approach ensures the integrity and consistency of the algorithm across diverse scenarios.

Comparative analysis of the benchmark and optimised trajectories demonstrates the algorithm's effectiveness in optimising energy consumption, power source utilisation, and regenerative braking power. The consistency observed in the reduction of average traction power at wheels, the total energy required for a return journey, and hydrogen consumption across all routes indicates the algorithm's efficiency. The optimised trajectories exhibit a minor increase in journey times, indicating that the algorithm prioritises energy efficiency over journey duration minimisation. This optimal energy-time trade-off results in a slight extension of journey times while significantly reducing energy consumption. This trade-off showcases the algorithm's capacity to focus on energy efficiency, a critical aspect of sustainable transportation systems. Despite the initial perception of increased journey times as a drawback, the considerable

reduction in energy consumption compensates for the minimal time increase. This balance promotes both economic and environmental sustainability for hybrid railway vehicles while achieving the most effective energy-time trade-off possible through the algorithm.

The case study results reveal that the hybrid train is equipped with a sufficiently sized battery pack and fuel cell. Due to multiple stops on each route, the hybrid train generates ample regenerative energy, which is utilised to recharge the batteries during the journey. The battery pack is depleted consistently in benchmark and optimised trajectory simulations for all routes, contributing to a more extensive range of journeys in the optimised trajectories. The optimal use of power sources directly impacts the economic life of fuel cells and batteries, as they experience less stress during the journey. This reduction in stress on traction power sources results in decreased maintenance requirements and increased life expectancy for the power sources.

Additionally, a graphical comparison of benchmark and optimised trajectories is presented in Figure 23 and Figure 24. It is evident from Figure 23 that the benchmark trajectory utilised a maximum traction power of 342 kW, whereas the optimised trajectory utilised a maximum power of 285 kW for the hybrid train. Additionally, the benchmark trajectory consumed 90 kWh of energy, whereas the optimised trajectory consumed only 74 kWh of energy. Figure 24 depicts the disparity between the speed profile and state of charge of the battery for the hybrid trains in both benchmark and optimised trajectories of route 1.

Prior research on railway vehicle optimisation [41, 178, 234] has indicated that there is often a significant trade-off between energy consumption and journey time during the optimisation process. Nevertheless, the author's proposed hybrid optimisation algorithm for hybrid railway vehicles effectively minimises the utilisation of power sources without compromising journey time constraints. The optimised trajectories reveal an average decrease of 15.18% in traction power at wheels, signifying the algorithm's proficiency in enhancing traction power efficiency

across all routes. Furthermore, the optimised trajectories display an average reduction of 16.85% in total energy consumption, emphasising the algorithm's ability to decrease energy consumption under diverse route lengths and conditions. With an average increase in journey times of only 0.40%, the optimised trajectories showcase the algorithm's capacity to achieve a well-balanced energy-time trade-off, prioritising energy efficiency without significantly compromising journey duration. This seamless integration of priorities underscores the effectiveness of the algorithm and its potential to contribute substantially to the development of more sustainable and efficient railway transportation systems.

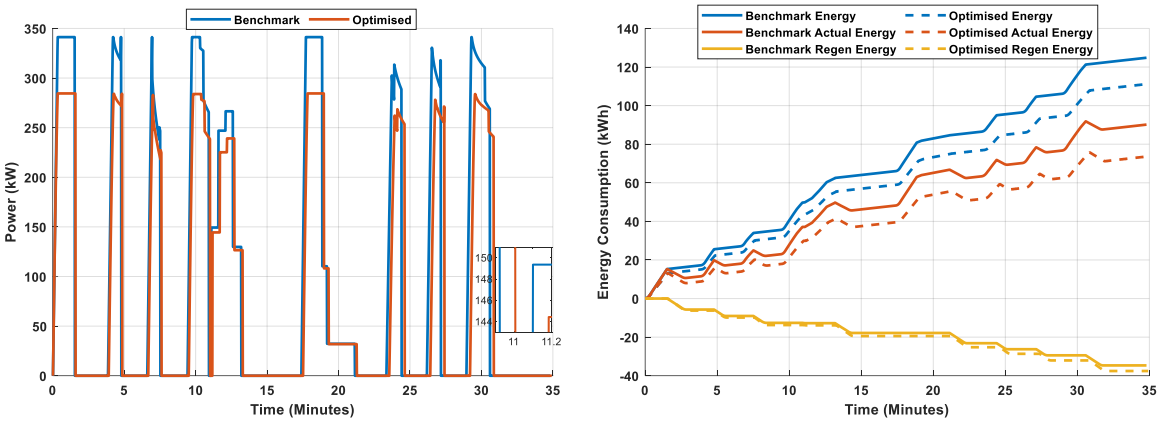

Figure 23: Traction power and energies of benchmark & optimised trajectories

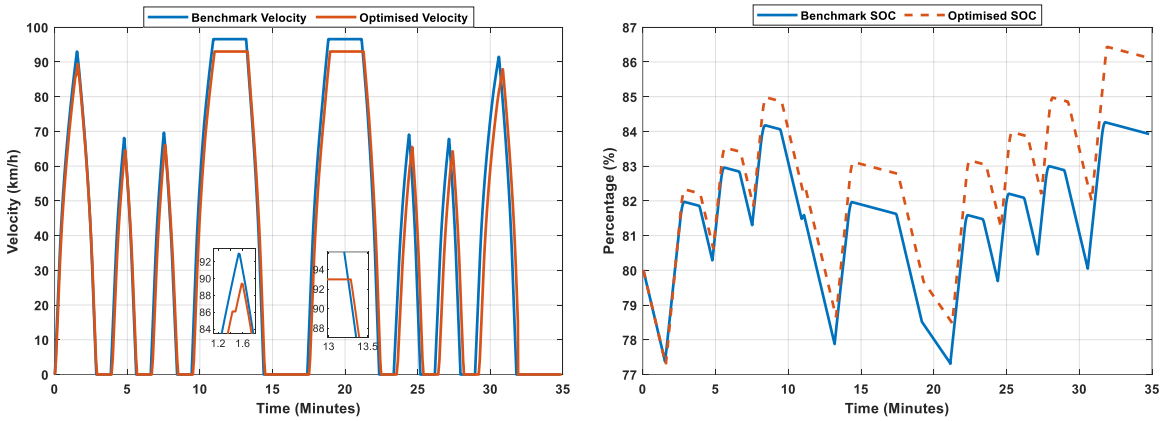

Figure 24: Comparison of velocity and state of charge of benchmark and optimised trajectories

6.4.5 Main Findings & Contributions

The research has led to several key findings, which have contributed to the development of a more comprehensive and robust framework for optimising the energy consumption and operational performance of hybrid railway vehicles.

6.4.5.1.Theoretical Contributions:

Development of a novel optimisation algorithm: This Chapter introduces a new hybrid optimisation algorithm that combines a non-linear programming solver with the highly efficient "Mayfly Algorithm" to address the complex optimisation problem associated with hybrid railway vehicles.

Adaptability to hybrid railway vehicles: The proposed algorithm is specifically designed to adapt to the unique characteristics of hybrid railway vehicles, leveraging their hybrid powertrain capabilities for efficient energy management.

Optimal energy-time trade-off: The algorithm effectively balances energy efficiency and journey time across various routes and conditions, demonstrating its ability to optimise the energy consumption profile throughout the journey.

6.4.5.2.Practical Contributions

Improved energy efficiency: The optimised trajectories display an average reduction of 16.85% in total energy consumption and a 15.18% reduction in traction power, emphasising the algorithm's potential for lowering energy % power consumption in real-world scenarios.

Minimised journey time impact: With an average increase in journey times of only 0.40%, the algorithm achieves a well-balanced energy-time trade-off, prioritising energy efficiency without significantly compromising journey duration.

Enhanced sustainability and operational performance: The proposed hybrid optimisation algorithm has the potential to contribute substantially to the development of more sustainable

and efficient railway transportation systems by optimising the energy consumption and operational performance of hybrid railway vehicles.

6.4.5.3.Developed Framework

Following the research and analysis of the data, a developed framework has been created, which combines the theoretical and practical contributions. This framework emphasises the importance of optimising energy consumption and operational performance in hybrid railway vehicles while maintaining a balance between energy efficiency and journey time. The framework also highlights the need for adaptive algorithms to address hybrid railway vehicles' unique characteristics, ensuring effective energy management and sustainable transportation systems.

6.5 Summary

This Chapter presents the development of a novel optimisation algorithm for hybrid railway vehicles by utilisation of MILNP & PWNL models. The objective is to generate efficient trajectories that enable effective power distribution, optimal energy consumption, and economical use of multiple onboard power sources, leading to reduced maintenance costs, time, and extended operational life of these sources.

The algorithm's superior performance is attributed to its adaptability to the unique characteristics of hybrid railway vehicles, leveraging their hybrid powertrain capabilities for efficient energy management. It considers various operational parameters, such as traction power. speed profile, route’s gradient, journey time, traction forces, regenerative braking, and auxiliary power requirements, to optimise the energy consumption profile throughout the journey.

The optimised trajectories exhibit an average reduction of 16.85% in total energy consumption, with an average increase in journey times of only 0.40% and a 15.18% reduction in traction

power. The algorithm achieves a well-balanced energy-time trade-off, prioritising energy efficiency without significantly compromising journey duration. This balance is crucial in sustainable transportation systems, where reducing energy consumption and emissions is vital without severely impacting service quality and travel times.

In conclusion, the proposed hybrid optimisation algorithm demonstrates an exceptional ability to optimise energy consumption and operational performance of hybrid railway vehicles, contributing significantly to the ongoing efforts towards more sustainable and efficient railway transportation systems. This study's contributions advance the hybrid railway vehicle optimisation field and provide valuable insights for future research and practical applications in developing sustainable and efficient railway transportation systems.

The current study provides a solid foundation for further research in the hybrid railway vehicle optimisation field. Future works could explore the following directions:

Integration of machine learning techniques: Developing advanced algorithms incorporating machine learning techniques, such as deep learning or reinforcement learning, to enhance the adaptability and performance of the optimisation algorithm.

Real-time optimisation: Investigating the feasibility of implementing the proposed optimisation algorithm in real-time, enabling dynamic trajectory adjustments based on real-time data, such as traffic conditions, weather, or system malfunctions.

Multi-objective optimisation: Expanding the optimisation framework to consider multiple objectives simultaneously, such as energy efficiency, journey time, passenger comfort, and system reliability, to achieve a more comprehensive optimisation solution.

Large-scale applications: Evaluating the proposed algorithm's performance on large-scale railway networks, assessing its scalability and efficiency in more complex and interconnected transportation systems.

By addressing these potential future works, researchers can continue to refine and expand upon the current study, contributing to the advancement of sustainable and efficient railway transportation systems.

7 OPTIMAL HYBRID TRAIN TRAJECTORY PREDICTION BASED ON ANN

7.1 Introduction

There are several approaches to developing an optimal control strategy for energy and power distribution in hybrid railway vehicles, including linear and dynamic programming [31]. However, these techniques do not provide an online solution as they assume the algorithm knows the entire future trajectory [10]. As a result, these algorithms can only be used for benchmarking performance for online energy and power control strategies [32]. Despite the limitations, using numerical and metaheuristic optimisation techniques to optimise the operational parameters of individual components in the system can still be beneficial when the current state of the hybrid vehicle is known [33]. Rule-based strategies for hybrid energy management systems translate the driver input and determine the energy distribution between power sources [34]. On the other hand, energy management strategies based on optimisation algorithms use stochastic driving profiles to minimise energy consumption and can convert battery energy into fuel consumption equivalent using an electronic collaborative manufacturing approach [35, 36]. The use of Machine Learning can offer a promising solution to the energy management strategies of hybrid railway vehicles. Machine Learning is defined as a set of attributes learned from large amounts of input data, with each data set having linked sub-attributes [269]. It effectively solves complex and non-linear dynamic systems when precise and accurate system modelling is difficult or impossible [270]. By integrating fuzzy logic controllers with Machine Learning, a robust approach can be developed to tackle hybrid railway vehicles' power and energy management strategy challenges [271]. This approach operates by observing the environment state and then taking action based on the observed state.

The system then receives a reward for the action taken and uses it to derive a strategy by learning from previous actions [270, 272].

The railway industry has seen widespread adoption of machine learning techniques in recent times. These techniques have been applied in various areas, such as predicting attributes of railway passengers affected by accidents detecting defects in railway vehicle wheels, monitoring fatigue of steel bridges caused by railway vehicles, identifying joints on the railway tracks and assessing the condition of the railway track for carriage body vibrations. A decision tree classifier was used to predict the attributes of passengers affected by accidents [18], a convolutional neural network algorithm was used to detect defects in railway vehicle wheels [273], proper orthogonal decomposition in conjunction with an artificial neural network was used to detect fatigue in steel bridges [274], and a deep learning algorithm based on end-to-end time series classification was employed to detect joints on the railway track [21] and monitor its condition for carriage body vibrations [275].

The research [276] suggests that adopting machine learning into conventional scheduling algorithms increases the probability of finding achievable solutions while reducing non-useful calculations. Artificial neural networks (ANNs) are a common type of Machine Learning that is frequently used for classification, clustering, pattern recognition and prediction in various data analysis fields [277]. ANNs classification methods for an application are holistic and can be evaluated based on data analysis characteristics such as precision, execution, convergence, fault lenience and scalability [278, 279]. Compared to conventional machine learning classifiers, ANNs classification modelling benefits from the high-speed analysis given in a large-scale implementation, making ANNs a suitable candidate for processing a large data set from the railway industry [280]. Although the adaptation of machine learning is becoming a norm in the railway industry, there is a lack of studies that present the optimised predicted traction powers for hybrid railway vehicles.

The growth of the hybrid railway sector has resulted in the availability of a large volume of data for analysis. The conventional multi-classification models often struggle to process such large data sets and tend to be less efficient and accurate. Machine learning classifiers can be used to analyse data and make predictions, such as classifying a data set into high, medium or low classes. The use of data classification technology in the railway industry is widespread, covering various areas such as maintenance, operation, and safety [281]. The author also uses large datasets from previous research [41] and is aimed to develop a new and improved custom algorithm for hybrid railway vehicles, as the conventional models may not be suitable for processing the large data sets from these vehicles. The author chose to utilise Artificial Neural Networks (ANNs) for this purpose due to their efficiency in handling large data sets, ability to self-learn, adaptivity, nonlinearity, and advanced input/output mapping [282].

The use of machine learning, particularly artificial neural networks (ANNs), for energy management strategies and estimation of hybrid railway vehicle trajectories is a promising solution that is still in the early stages of research. While previous research has focused on mathematical models or static data to develop energy management strategies, machine learning can offer a more effective solution for non-linear dynamic systems. However, there is a lack of studies that present the optimised predicted traction powers for hybrid railway vehicles using ANNs. The trajectory of a hybrid railway vehicle refers to the path or route that the train follows. It is the representation of the driver's input into the train or the input provided by the automatic driver operation of the train. The hybrid train trajectory includes parameters including hydrogen consumption, carbon dioxide emissions, traction energy, traction power, train velocity, acceleration and journey time.

This Chapter focuses on addressing the gaps in existing methodologies for estimating the states of hybrid trains by employing a neural network. Neural networks allow for learning non-linear relationships between input and output parameters, which is a significant advantage over

physical models that rely on linear relationships and struggle to capture real-world complexities. The proposed approach also automates the decision-making process, reduces computation time, and minimises human errors in large datasets. By utilising neural networks to identify hidden patterns and make intelligent decisions, this Chapter aims to present an innovative and efficient solution for estimating the states of electrified trains.

This Chapter aims to develop two artificial neural networks (ANN) models to comprehend and predict the essential features of hybrid railway vehicles and their optimal trajectories. Based on the literature and the research gaps identified in Chapter 2, 3, 6 and 7, this study objectives are as follows:

• To design a system capable of effectively processing and comprehending the large dataset of hybrid railway vehicles.

• To create two fundamental architectures based on time and power to serve as the basis for the ANN predictive models.

• To implement a grading point system that filters out irrelevant and inadequate data from the hybrid railway dataset.

• To develop two ANN models that can accurately predict the hybrid railway vehicle's parameters and optimal trajectories

This Chapter is an expanded version of the studies that resulted in the paper *" Prediction of the Optimal Hybrid Train Trajectory by Using Artificial Neural Network Models*," submitted to be published in IEEE Transactions on Intelligent Transportation Systems, for which the author was the primary contributor and the lead author.

Both techniques are tested and validated in the case study presented in this Chapter. The developed methods will help predict an optimal hybrid train trajectory and eliminate

computational speed, excessive processing time, resources and inaccuracy of conventional optimisation techniques.

7.2 Artificial Neural Network

This study aimed to develop two artificial neural network (ANN) models to predict the critical output parameters of the hybrid railway vehicle trajectory. The ANN models were designed using the feed-forward and cascade-forward neural network topologies. The hybrid train was configured by adjusting its operational characteristics by altering various parameters such as Davis parameters, inertial and total mass, rotatory allowance, tractive effort, maximum acceleration & speed limit, traction forces, and traction & braking power, as shown in Table 2.

The ANN model was designed to predict the optimal trajectory for a specific route by considering five different hybrid trains and their respective featured parameters. For each hybrid train, 2000 simulated trajectories were generated on the same route with different rated power configurations to train both ANN models.

The ANN models were developed using a two-layer neural network structure with multiple hidden layers consisting of small nodal neurons and a hyperbolic tangent sigmoid transfer function. The output layer was designed with a linear transfer function. The decision to use a two-layer structured neural network was based on extensive research and analysis [283-285], which showed that it is an effective design for solving non-linear function fitting regression problems and has been shown to outperform other models in terms of performance consistently. Both neural network models are composed of an input layer, hidden layer, and output layer that work together to predict each parameter individually. This is achieved through the optimisation of the neurons in the hidden layer using the tan sigmoid transfer function, followed by the

inputs. The hybrid train simulator was used as the primary data source for training the ANN models.

The proposed artificial neural network (ANN) models operate in three main stages. Firstly, the models undergo a training phase where they are fed with simulated trajectories of multiple hybrid trains. These trajectories train both the feed-forward neural network (FFNN) and the cascade-forward neural network (CFNN) models aligned with their power or time-based architectures. Secondly, the trained models are fed with new route information and desired power or time-based architectures in the predictivity phase. The models then predict the hybrid train profile and relevant optimal trajectory. Finally, the predicted hybrid train profile is fed into a hybrid train simulator to produce a benchmark trajectory in the validation phase. This is then compared with the predicted trajectories from both models.

These stages demonstrate the effectiveness and accuracy of the proposed ANN models in predicting the critical parameters of a hybrid train profile, enabling efficient and optimised train

operations. Figure 25 provides an overview of both proposed ANN models for predicting a hybrid train trajectory.

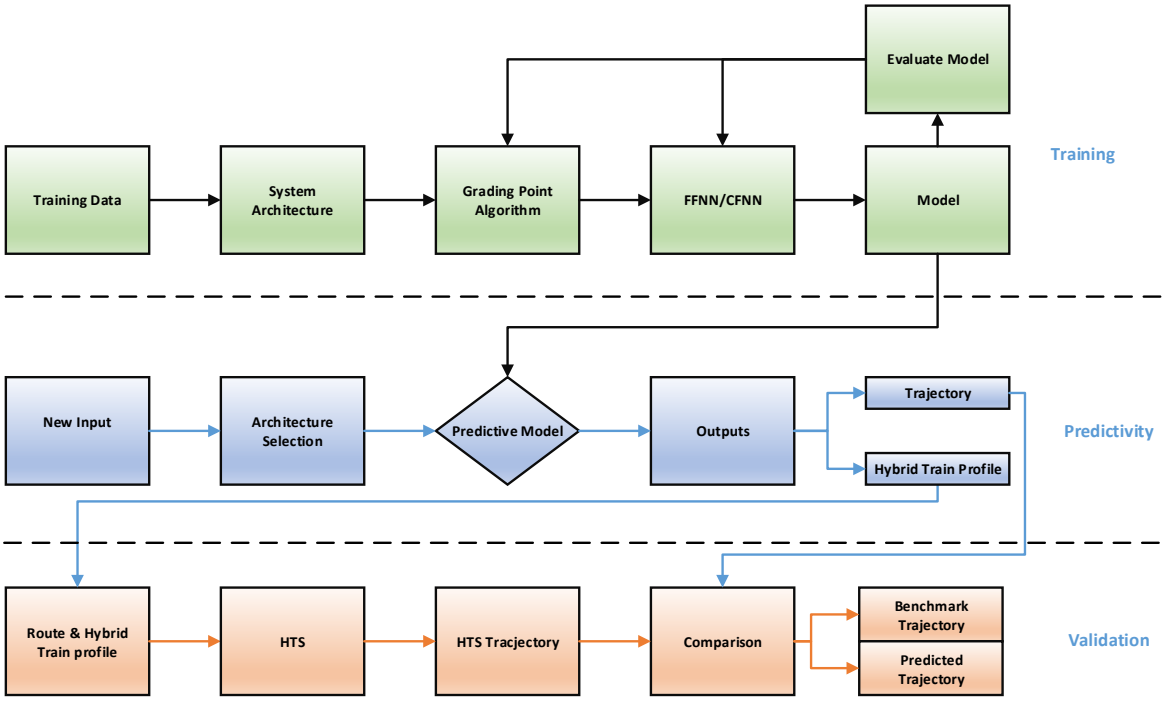

Figure 25: An overview of the proposed artificial neural network structure for hybrid railway vehicle

The following Sections will provide an overview of the methodology used to develop both models, including introductions to feed-forward and cascade-forward neural network topologies, the generation of data for training the ANN models, the development of a grading point system to condition the training data, the training stage, the selection of the backpropagation algorithm, and testing and validation of the ANN models to predict the best trajectory for a hybrid railway vehicle on a specific route.

7.2.1 Generation of Training Data

To carry out the study outlined in this Chapter, the author generated simulated trajectories from five different hybrid trains that were simulated on the same route using a hybrid train simulator [41]. Each hybrid train generated 200 trajectories, with different rated power values causing variation in the trajectory data. These datasets were then fed into both ANN models to train the

network. The output parameters of HTS served as input variables for both artificial neural network models, which were categorised into static, dynamic, and target parameters. The static variables remained constant throughout the simulation, dynamic parameters varied according to the hybrid train's power demand, and the target variable was set as the output of the ANN. Table 23 illustrates the static, dynamic, and target variables used in the ANN algorithms.

Table 23: Input parameters classification for artificial neural network

Dynamic Parameters	Static Parameters	Target Parameters
Power Supply	Track Distance	Hydrogen Consumption
Energy Demand	Track Gradient	Carbon Dioxide Emissions
Regenerative Energy	Station Position	Traction Energy
Traction Forces	Track Speed Limits	Traction Power
Train Velocity	Davis Parameters	Journey Time
Train Acceleration	Rotary Allowance	
Journey Time	Tractive Effort	
	Inertial Mass	
	Total Mass of Train	

The route information for all the hybrid trains remained constant in the training data generation process. The "Power Supply" parameter of the hybrid trains was specifically designed for each trajectory to determine the most efficient power configuration by applying the ANN algorithms proposed in this study. For example, the initial trajectory was set with the minimum feasible power supply of 150 kW (combining both battery and fuel cell power). Subsequently, the power supply was incrementally increased by 1% for each subsequent trajectory, resulting in the final 200th trajectory having a traction power at the wheels of 1086 kW.

7.2.1.1. Input Training Data

The training data for the proposed Artificial Neural Network (ANN) model is divided into two sets. One set contains information about the hybrid train's physical characteristics, while the other set includes trajectory data corresponding to the train's movement.

The hybrid train training data consists of several parameters, such as the inertial mass (I_1), the total mass of the train (I_2), Davis parameters (I_3), rotary allowance (I_4), tractive effort of the

train (I_5), maximum acceleration (I_6), the maximum speed of the train (I_7), and rated power supply (I_8). On the other hand, the trajectory data set comprises the hybrid train speed profile (I_9), acceleration (I_{10}), traction forces (I_{11}), traction power (I_{12}), traction energy (I_{13}), hydrogen consumption (I_{14}), and journey completion time (I_{15}). These parameters serve as input values for the proposed ANN models, which predict the desired outputs.

To ensure that the proposed ANN models are accurately trained, the input and output parameters have been analyzed systematically from the Hybrid Train Simulator by determining the ranges of nominal values of hybrid trains. The input parameters of the hybrid train are carefully analysed to ensure that the proposed ANN models produce results that are within the practical range and are realistically achievable. Table 24 presents the key input parameters of hybrid trains used in training both artificial neural network models. It is important to note that some of the hybrid train inputs, namely (I_1) to (I_5), cannot be precisely controlled, as these parameters can only be roughly transformed by changing the type of hybrid train used on the route.

Table 24: Journey time and energy consumption key input parameter of hybrid trains used for the training both artificial neural network models

Input Parameters	**Train 1**	**Train 2**	**Train 3**	**Train 4**	**Train 5**
I_1: Inertial mass (tonnes)	70	90.20	110.20	130.20	150.20
I_2: Total Mass (tonnes)	74.37	97.64	119.29	140.94	162.59
I_3: Davis Parameters	1.743	1.8430	1.943	1.9943	1.843
	0.0212	0.1512	0.1821	0.1921	0.221
	0.0047	0.0074	0.0074	0.0094	0.009
I_4: Rotary Allowance	0.0625	0.0825	0.0825	0.0825	0.0825
I_5: Traction Effort (kN)	34.335	44.2431	54.0531	63.8631	73.6731
I_6: Max Acceleration (m/s^2)	0.4905	0.4905	0.4905	0.4905	0.4905
I_7: Max Velocity (m/s)	10.23369	9.677525	9.546606	9.381794	9.347271
I_8: Rated Power Supply (kWh)	150...,*n*	150...,*n*	150...,*n*	150...,*n*	150...,*n*

In conclusion, the training data for the proposed ANN model includes the hybrid train's physical characteristics and trajectory data. The systematic analysis of the input and output parameters ensures that the proposed ANN models produce realistic and practical results. The ANN models' ability to predict the power and journey time of the hybrid train makes them crucial in determining the train's trajectory.

7.2.1.2. Target Data / Decision Parameters

The decision parameters for the proposed Artificial Neural Network (ANN) model were based on critical factors such as hydrogen consumption (O_2), carbon dioxide emissions (O_2), energy consumption(O_2), power demand (O_2), and journey time (O_2). These parameters are a basis for the ANN models to predict the optimal hybrid train trajectory and its respective hybrid train configuration on the desired route.

Various types of trains exist, each with its unique set of parameters and energy consumption patterns, depending on their quality, track conditions, and environment. However, our region of interest lies in predicting the parameters mentioned above covered by each train individually, which serve as the essential key output parameters of hybrid railway vehicle trajectory and assist in determining the desired outputs for hybrid trains.

Our primary objective is to design the ANN models so that, by tuning its decision parameters, it can predict an optimal trajectory and hybrid train profile after being trained by a multitude of trajectories. This predicted trajectory estimation would help us determine the best and most efficient route track system with its corresponding predicted output parameters (O) for power, energy, time, CO_2, and H_2 over other trains

7.2.2 Data Processing

Data processing is a crucial aspect of modern technological systems, and its importance cannot be overstated. In this study, we will explore two sub-Sections that shed light on different approaches to data processing: time and power-based architectures and grading point systems.

The time- and power-based architectures are designed to address the challenges associated with hybrid train systems' time and power constraints. These architectures offer a holistic method of predicting hybrid railway vehicle performance on specific routes by providing insights into the various input parameters that influence these systems' trajectories. On the other hand, the grading point system serves as a filter during the training stage of the proposed artificial neural network (ANN) models, which helps to identify and eliminate irrelevant trajectories. This system enhances the efficiency of the ANN models and provides an optimal power configuration for training the models. Together, these data processing approaches demonstrate the flexibility and adaptability of modern data processing systems and their potential to improve the performance of complex systems.

7.2.2.1 Time & Power based Architecture

The proposed Artificial Neural Network (ANN) models can perform calculations in both the time and power domains. The models are designed as time and power-based architectures, considering hybrid trains' power and time constraints, regardless of their configurations. The time constraint directly affects the train's fuel and energy consumption and limits the duration of the train journey. In order to manage energy consumption and consider economic factors, the time-based architecture features a set of input parameters with the train's journey time as the primary source of interest in the output. On the other hand, power-based modelling features a set of input parameters with the traction power as the primary source of interest at the output. It is important to note that the variation in these input parameters can significantly affect the trajectory of the hybrid train. By creating both time and power-based models that consider the constraints of both time and power, this study offers a holistic method to predict the trajectory of a hybrid railway vehicle on a specific route.

The time-based architecture is designed to output a set of parameters that focus on time, including CO_2 emissions, H_2 consumption, traction energy consumption, and traction power.

The time-based architecture model uses the training trajectories with time as the output data set. The train's journey time is optimised using a sigmoid transfer function. Assuming Input dataset: $X = x_1, x_2 \ldots, x_n$ where x_1 represents a set of input parameters such as speed, distance, and track characteristics and the output dataset: $Y = y_1, y_2 \ldots, y_n$ where y_1 represents the journey time of the train. The sigmoid transfer function can be represented as follows:

$$f(x) = \frac{1}{1 + e^{-x}} \tag{7.1}$$

The optimisation can be performed by utilising the $\min(f(Y))$

On the other hand, the power-based architecture is designed to output a set of parameters that focus on power, including CO_2 emissions, H_2 consumption, traction energy consumption, and journey. The power-based architecture model also uses the training trajectories, with power as the output data set, and optimizes the traction power of the hybrid train using the neural network cost function. Assuming the Input dataset: $X = x_1, x_2 \ldots, x_n$ where x_1 represents a set of input parameters such as speed, distance, and track characteristics and the output dataset: $Y = y_1, y_2 \ldots, y_n$ where y_1 represents the traction power of the hybrid train. The neural network cost function is represented as follows:

$$C(W) = \frac{1}{2n} * \sum_{i} 1^n \|y_i - f(x_i; W)\|^2 \tag{7.2}$$

where W represents the weights and biases of the neural network, and $f(x_i; W)$ represents the predicted output. The optimisation can be performed by utilising the $\min(C(W))$.

By utilising these two different architectures, the models can provide insights into how the different parameters affect each other and allow for more accurate predictions of the system's performance being analysed. It is important to note that these models can be further customized based on the system's specific requirements and can be adjusted to incorporate additional parameters as needed. Overall, the flexibility and adaptability of these models make them

valuable tools for understanding and improving the performance of complex systems. During the training stage, both artificial neural network (ANN) models are specifically configured to ensure that the prediction process can be completed through either architecture in separate or parallel sequences without compromising the performance of either model.

7.2.2.2 Grading Point System

During the training process of the proposed ANN, which is based on controlled simulated data and involves approximately 10,000 trajectories with varying traction power configurations, the efficiency of the network may decline. To overcome this challenge, a supervised grading point system has been developed to monitor and select the most suitable trajectory with an optimal power configuration, which is then fed into the training stage. Figure 26 provides a visual representation of the grading point system structure. By implementing this system, the efficiency of the proposed ANN models can be improved.

Figure 26: Grading point system structure for ANN training data

The grading point system is used during the training stage to accurately recognize relevant hybrid train trajectories and eliminate any abnormal fluctuations in the data. This system efficiently arranges the data sets for training the ANN models by assigning points to each input and output parameter based on predicted performance values. Based on the architecture of the ANN model, the author has selected the desired target parameter, either the traction power or journey time value. The user's choice of the desired output parameter will establish boundary limits with a maximum deviation of ±8% to prevent unnecessary computation time due to irrelevant trajectories.

The grading points system acts as a filter between the training stage and the proposed ANN models, using a trial and error technique to select a relevant data set from any given amount of hybrid train trajectories. A lookup table is generated to scale down the data set to a user-specified limit, and irrelevant trajectories are filtered out until the boundary limitations established by the user's desired output value are met. The filtration process is achieved by finding trajectories with lower carbon dioxide emissions, hydrogen and energy consumption, and minimum traction power or time. The data is then sampled and fed into both ANN models for training.

7.2.3 Feedforward artificial neural network

The Feed-forward Neural Network (FFNN) is a widely used topology of artificial neural networks due to its ability to predict non-linear structures between input and output [286]. The FFNN comprises several hidden layers, each with a number of computing nodes, also known as neurons, which are responsible for identifying the relationship between input and output. As the computation moves from one hidden layer to another, the neurons in each layer calculate the output and pass it on to the next layer. The hidden layers are designed to interpret the relationship between input and output, while the output layer maps the final computation to the desired output values using a linear transfer function. The number of neurons in each hidden layer can be adjusted during the training phase, which helps the FFNN better fit the target values. The neurons in each layer are connected by distinguished assembly lines and are assigned weights based on the tan-sigmoid and linear transfer functions. Figure 27 illustrates the FFNN structure and its mapping of weights to desired target values.

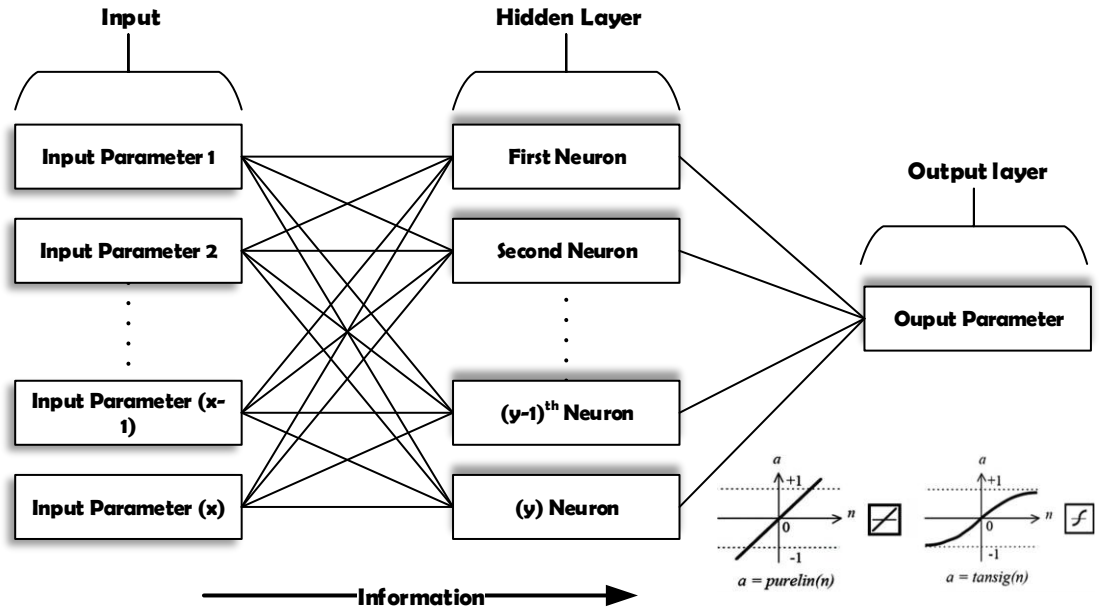

Figure 27: General overview of the typical feed-forward neural network model

In order to maintain the proper operation of the ANN model, accurate regulation of the weights and biases associated with the neurons in each layer is crucial. This ensures that the network is able to accurately predict the target outputs based on a set of predetermined input parameters. The regulation of weights and biases is usually achieved through supervised training, where the network is fed a sequence of input parameters and their corresponding target values. This study uses Equations (7.3) and (7.4) in weight balancing of FFNN topology.

$$H_{neuron}(x) = f\left[\sum_{x=0}^{s}(I(x) \times W(x,j)) + b(x)\right] \tag{7.3}$$

where $H_{neuron}(x)$ presents the hidden neurons and $I(x)$ presents the input parameters. $W(x,j)$ illustrates the vector of weights associated with the neuron, and $b(x)$ is the bias weight associated with the neuron. f presents the activation function of the artificial neural network.

$$O_{FFNN}(y) = f\left[\sum_{y=0}^{d}(H_{neuron}(j) \times W(j,y)) + b(y)\right] \tag{7.4}$$

where $O_{FFN}(y)$ presents the output of neurons.

7.2.4 Cascade forward artificial neural network

The CFNN is designed with additional connections from the input to each hidden layer and from the hidden layer to the output layer, making it ideal for understanding both linear and non-linear relationships between input and output [287]. This topology is particularly suitable for time series predictions due to its direct connection between input and output. The use of a single hidden layer in the CFNN can closely estimate continuous functions that map real number intervals to output intervals of real numbers. This is why the CFNN topology is used in this study, as the research focuses on time and power-based architecture. Figure 28 shows a general illustration of the cascade forward neural network topology.

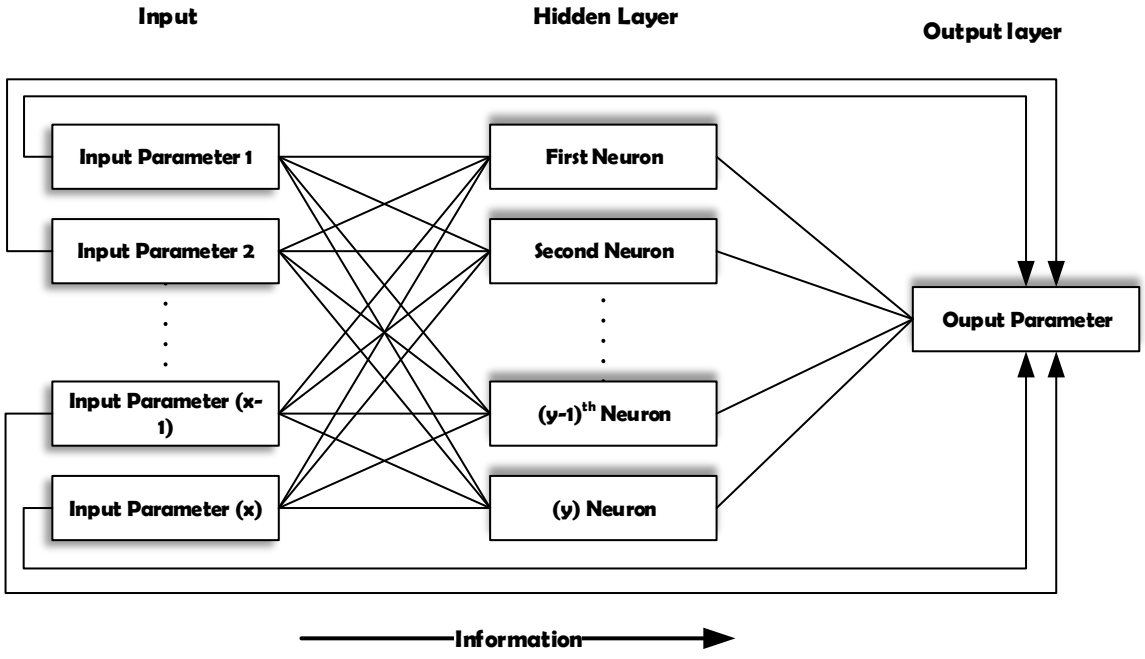

Figure 28: General overview of typical cascade forward neural network model

It is necessary to adjust the weights and biases of the neurons within the network. This is similar to the process in a feed-forward neural network. The vector of weights and biases associated with a neuron is adjusted using Equation (7.5) for CFNN topology.

$$O_{CFNN}(z) = f\left[\sum_{z=0}^{d}\left(H_{neuron}(j) \times W_j(j,z) + I(x) \times W_x(x,z)\right) + b(z)\right] \quad (7.5)$$

where $O_{CFNN}(z)$ presents the output neuron, $W_x(x,z)$ is the vector of weight, and $b(z)$ is the biases weight associated with neurons in the proposed ANNs. This Equation calculates the updated weight and bias values based on the previous values, the learning rate, and the gradient of the error function with respect to the weight and bias values. Adjusting the weights and biases is repeated multiple times during the training phase to minimize the error function and improve the accuracy of the neural network's predictions.

7.2.5 Selection of Backpropagation Algorithm

During the learning phase of ANN, the main challenge is overfitting, which limits the learning abilities of the network by simply memorizing the data and not being able to identify the relationships between input and output. To reduce errors between the network and training layers and adjust its weights and biases, the backpropagation algorithm, also known as the BP method, plays a critical role in developing the ANN models. Therefore, selecting a suitable backpropagation algorithm is crucial in addressing the overfitting issue. In the case of hybrid train parameters, the author aims to predict the best possible train trajectory with the optimal configurations of both ANN models by utilising the best backpropagation algorithm. This will keep the ANN model efficient and capable of handling the hybrid railway vehicle system.

In this study, the proposed ANN models were trained using four different backpropagation algorithms to select the most suitable method while addressing the overfitting issue and minimizing the errors. For the sake of brevity, this Chapter does not include a detailed discussion of each backpropagation algorithm considered in this study. However, further information on these algorithms can be found in the literature cited in the references [288-291]. Table 25 and Table 26 present the results of training the neural network with each backpropagation algorithm. All the algorithms were configured with a single hidden layer

layout containing ten neurons to predict the best hybrid train output parameters as a function of input variables.

Table 25 and Table 26 compare the performance of four different backpropagation algorithms, including Gradient Descent with Momentum, BFGS Quasi-Newton, One-step Secant, and Bayesian Regularization, in training the ANN models. While the first three algorithms required fewer training iterations and less time to complete the training, their error magnitudes and correlation coefficient values were not as good as the Bayesian Regularization algorithm. The Gradient Descent with Momentum algorithm had the lowest number of training iterations, resulting in a high error magnitude and poor performance. On the other hand, the Bayesian Regularization algorithm took more time to train. However, it resulted in higher accuracy, lower error magnitude, and better R values compared to the other algorithms. The results demonstrate that the Bayesian algorithm outperforms the others and is the most suitable backpropagation algorithm for the proposed ANN models.

Table 25: Comparison of backpropagation algorithms for both time and power-based architectures for artificial neural networks based on FFNN topology

Time-Based Architecture	**FFNN Topology**		
Output Parameter	**R values**	**Mean Squared Error**	**Iteration Number**
Gradient descent with momentum	0.979	4.7312	144
One-step secant BP	0.998	0.2599	156
BFGS Quasi-Newton	0.995	0.1988	169
Bayesian regularisation	0.999	0.1212	1000
Power-Based Architecture			
Gradient descent with momentum	0.981	0.9574	112
One-step secant BP	0.996	0.2184	436
BFGS Quasi-Newton	0.992	0.1927	204
Bayesian regularisation	0.999	0.1891	1000

Table 26: Comparison of backpropagation algorithms for both time and power-based architecture for artificial neural network based on CFNN topology

Time-Based Architecture	**CFNN Topology**		
Output Parameter	**R values**	**Mean Squared Error**	**Iteration Number**
Gradient descent with momentum	0.983	0.6531	101
One-step secant BP	0.995	0.1921	152
BFGS Quasi-Newton	0.993	0.2976	115
Bayesian regularisation	0.999	0.172	862
Power-Based Architecture			
Gradient descent with momentum	0.985	30.9025	69
One-step secant BP	0.997	2.701	140
BFGS Quasi-Newton	0.996	1.0613	276
Bayesian regularisation	0.999	0.1911	968

Figure 29 presents the progression of mean square training and validation errors for both ANN models in each epoch while employing the Bayesian regularisation algorithm as the primary BP algorithm and linear regression analysis between the output values predicted by both ANN models and the corresponding data for the output targets. Despite the non-linear relationship between the input and output parameters, the analysis suggests that both ANN models can accurately predict the target output values for hybrid train trajectories. This finding indicates that the proposed ANN models can be relied upon for predicting the best possible train trajectory with the best configurations of hybrid train input variables.

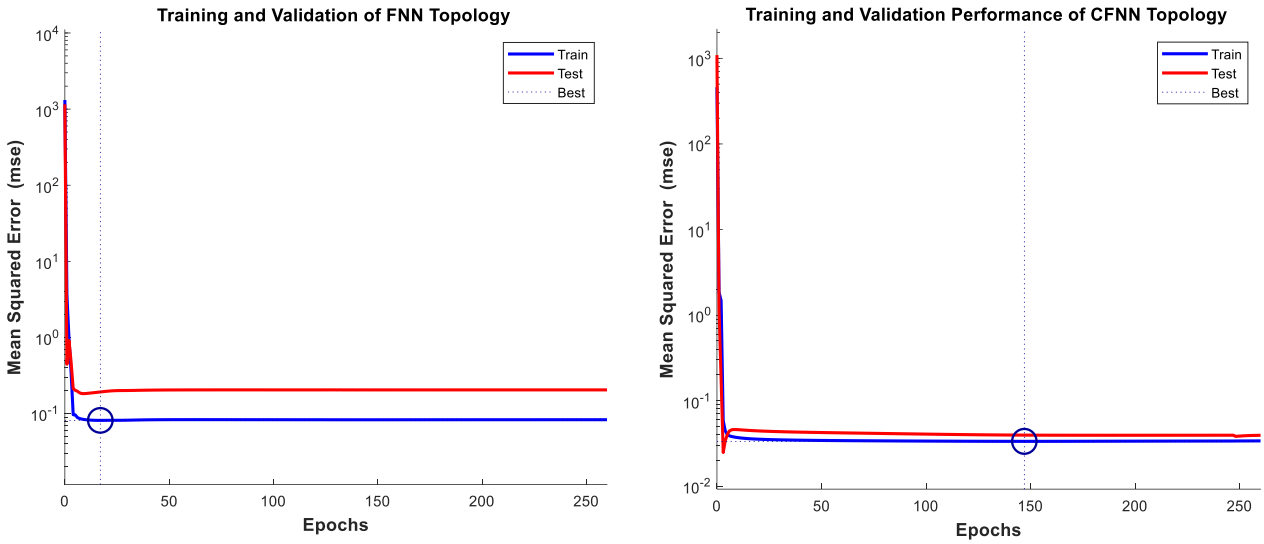

Figure 29: Mean square error produced during the training and validation of both ANN models by using the BP algorithm

Additionally, Table 5 shows that both ANN models have similar network training errors during the training and validation stage. The training and validation outcomes shown in Figure 29 indicate a high degree of association between the predicted and observed hybrid train output values for both ANN models. The magnitude of the error in both proposed ANN models is computed using Equation (7.6).

$$Mean\_Squared_{error} = \sqrt{\frac{1}{n}\sum_{i=1}^{n}(x_{i-}x_i^{\diamond})^2} \tag{7.6}$$

where x_i and $x_i^{\diamond}$ are observed and predicted hybrid train output parameters based on the proposed ANN models, and n presents the number of samples.

Figue 30 shows the regression plots for the simulated training and testing datasets of both feed-forward and cascade-forward neural networks. These plots indicate that the correlation coefficient values for both ANN models are quite similar. It was observed that the feed-forward neural network had an R-value range of 0.9751 to 0.9994, while the cascade-forward neural network had an R-value range of 0.9832 to 0.9992.

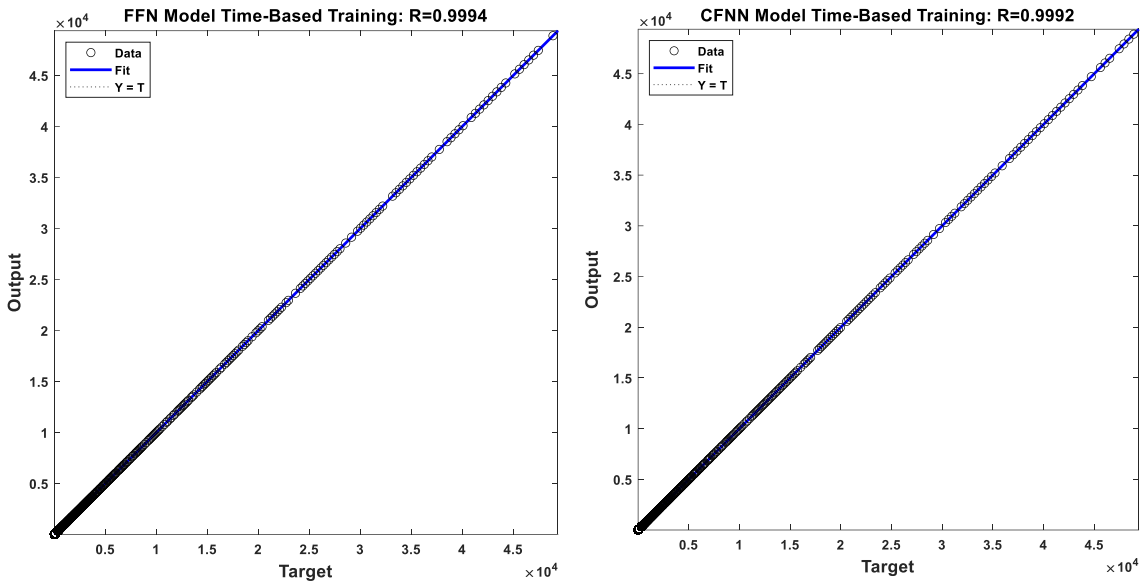

Figue 30: Regression of actual output values against target output values for FNN and CFNN topology

7.2.6 Neural Network Structure

This Section aims to optimise both ANN models to predict the best possible trajectories by configuring the number of neurons in the hidden layer. The proposed artificial neural network design consists of a single hidden layer with ten neurons. The Bayesian regularisation algorithm was chosen as the backpropagation algorithm for both ANN models to minimise the mean squared error and R values (correlation coefficient) to obtain an optimal hybrid train trajectory with reduced error magnitude. Feed-forward and cascade-forward neural network topologies were used to optimise the mean square validation error in predicting the trajectory. The optimal number of neurons in the hidden layer was determined by incrementing the number of neurons and monitoring the error magnitude and R values. The process was repeated until both FFNN and CFNN topologies could predict the trajectory with a minimum network validation error and a significant testing error. The maximum mean square errors between the training and test sets should be close to avoid overfitting, as indicated in Table 27. The training dataset was divided into three subsets (70% for training, 15% for validation, and 15% for testing), which were randomly chosen to avoid overfitting.

Table 27: Number of neurons in the hidden layer, testing & validation errors produced by time and power-based architecture ffnn topology

Output Parameters	Neuron No.	MSE		MAE	
		Training	Validation	Training	Validation
Time-Based FFNN Topology	10	0.2313	0.2403	0.2842	0.2615
Time-Based CFNN Topology	10	0.0457	0.0498	0.0840	0.0811
Power-Based FFNN Topology	10	1.6860	1.5781	0.0067	0.0059
Power-Based CFNN Topology	10	0.0257	0.0262	0.0616	0.0598
Time-Based FFNN Topology	8	0.3251	0.6043	0.0012	0.2323
Time-Based CFNN Topology	8	0.0598	0.0756	0.1102	0.0958
Power-Based FFNN Topology	8	1.8964	1.601	0.0121	0.0687
Power-Based CFNN Topology	8	0.0435	0.0566	0.0854	0.0935
Time-Based FFNN Topology	6	0.2313	0.5477	0.0027	0.2143
Time-Based CFNN Topology	6	0.0965	0.0784	0.0489	0.0714
Power-Based FFNN Topology	6	1.9831	1.4069	0.0101	0.3242
Power-Based CFNN Topology	6	0.0393	0.0244	0.0518	0.0583

Figure 31 presents the FFNN topology used in proposed ANN models signifying the ANN optimal sub-networks with a hidden layer consisting of neurons carrying the tan sigmoid transfer function weights associated with neurons and the output layer having linear transfer function weights associated with neurons. In feedforward neural network topology, there is no direct relationship between the input and output layers for hybrid train parameters, as shown in Figure 31. However, in cascade forward topology, there is a direct relationship between input and output layers for hybrid train parameters.

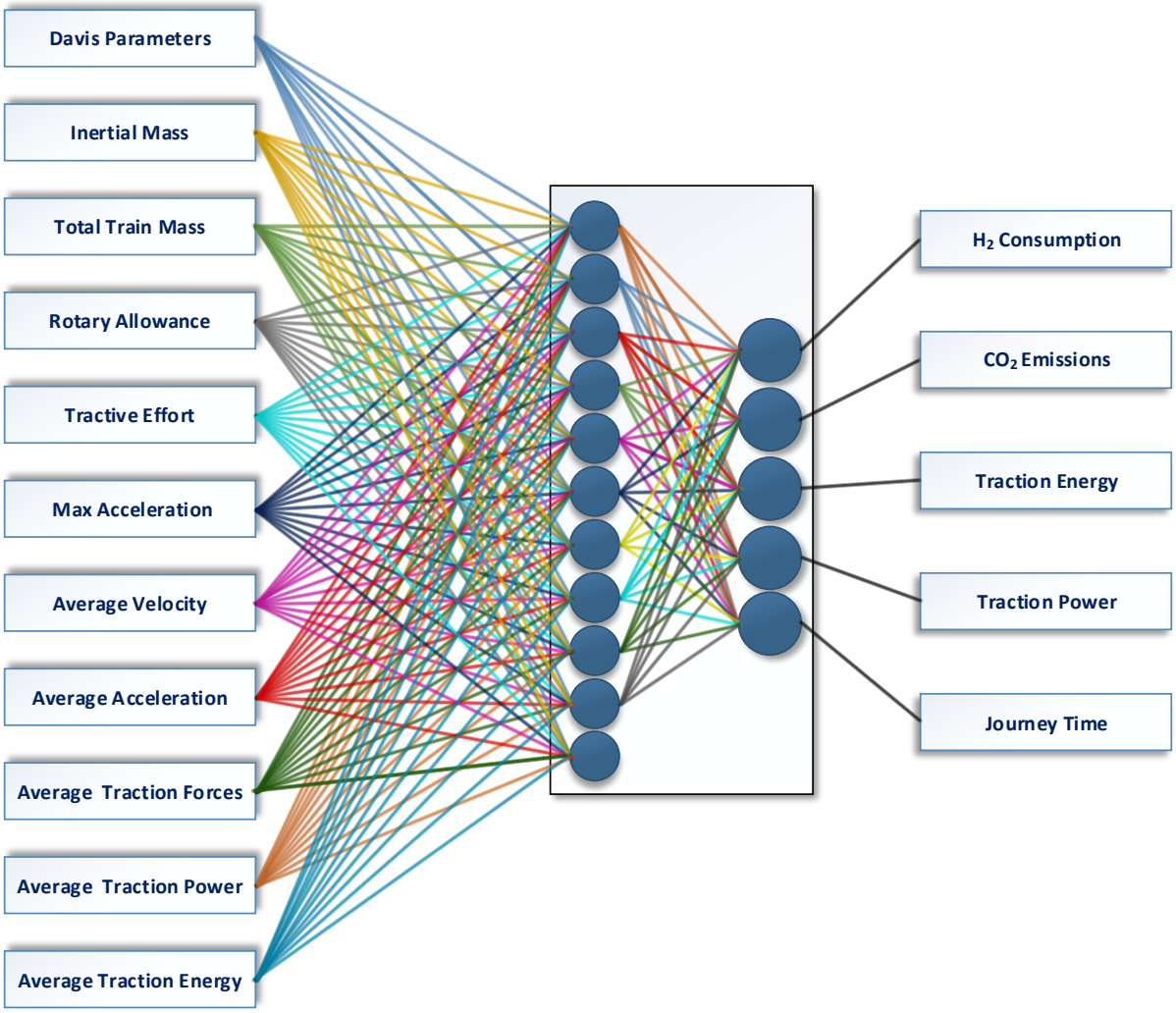

Figure 31: The optimised Artificial Neural Network model for the hybrid train based on FFNN Topology

7.3 Case Studies

7.3.1 Model Validation

The proposed artificial neural network models were rigorously tested and validated through a detailed case study. The performance of both models was evaluated by computing the mean square normalization error and mean absolute performance error. Furthermore, the authenticity of the output produced by predictive ANN models was verified using a hybrid train simulator. The predictive model was fed with new route information, along with desired power and expected journey time, to perform the validation, corresponding to the power-based and time-

based architectures. The predictive model considered the static parameters of the route and, based on its intelligence, predicted a hybrid train profile that consisted of several critical parameters, such as the inertial mass (I_1), the total mass of the train (I_2), Davis parameters (I_3), rotary allowance (I_4), tractive effort of the train (I_5), maximum acceleration (I_6), the maximum speed of the train (I_7), and rated power supply (I_8). In addition, an optimal predicted trajectory was also predicted consisting of parameters such as the hybrid train speed profile (I_9), acceleration (I_{10}), traction forces (I_{11}), traction power (I_{12}), traction energy (I_{13}), hydrogen consumption (I_{14}), and journey completion time (I_{15}).

The hybrid train profile was then fed into the hybrid train simulator (HTS) to simulate the predicted train on the same route and produce the trajectory. This trajectory is referred to as the benchmark trajectory and was compared with the predicted trajectories produced by ANN models to perform a comparative analysis. The results of this study demonstrate the effectiveness and accuracy of the proposed ANN models in predicting the critical parameters of a hybrid train profile, thereby enabling efficient and optimised train operations.

Table 28: Hybrid train profile predicted by FFNN topology in power-based architecture

Input Parameters	Time-Based Train	MSE	Mean Error	Max Error
I_1: Inertial mass (tonnes)	70	0.11917	0.2084%	1.9988%
I_2: Total Mass (tonnes)	74.37	0.12485	0.2157%	2.0108%
I_3: Davis Parameters	1.743 0.0212 0.0047	0.11603	0.2004%	1.9904%
I_4: Rotary Allowance	0.0625	0.11602	0.1996%	1.9855%
I_5: Traction Effort (kN)	34.335	0.11742	0.2002%	1.9817%
I_6: Max Acceleration (m/s^2)	0.4905	0.12005	0.2082%	1.9989%
I_7: Max Velocity (m/s)	10.233	0.12388	0.2153%	2.0100%
I_8: Rated Power Supply (kWh)	150...,*n*	0.11588	0.1998%	1.9825%

Table 30 and Table 29 present the hybrid train profile inputs predicted by both ANN models, which were subsequently fed into the hybrid train simulator (HTS) for generating the benchmark trajectory. It is worth noting that the Davis parameters of each hybrid train used in

author simulations were obtained from the original train manufacturers (OEM) and were initially determined based on the aerodynamics of the train. These parameters were typically calculated analytically and verified through wind tunnel tests by OEM.

Table 29: Hybrid Train Profile Predicted By CFNN Topology In Time-Based Architecture

Input Parameters	Time-Based Train	MSE	Mean Error	Max Error
I_1: Inertial mass (tonnes)	72	0.11937	0.2065%	1.9856%
I_2: Total Mass (tonnes)	76.45	0.12554	0.2163%	1.9968%
I_3: Davis Parameters	1.753 0.0235 0.0087	0.11608	0.2004%	1.9809%
I_4: Rotary Allowance	0.0629	0.11595	0.1998%	1.9827%
I_5: Traction Effort (kN)	35.414	0.1175	0.2022%	1.9796%
I_6: Max Acceleration (m/s2)	0.4913	0.12007	0.2076%	1.9883%
I_7: Max Velocity (m/s)	11.0452	0.12479	0.2165%	1.9972%
I_8: Rated Power Supply (kWh)	150...,n	0.11656	0.2009%	1.9821%

However, the ANN models proposed in this study utilised a combination of the hybrid train weight, velocity, and air resistance to predict the correct parameters for achieving an optimal trajectory. This approach enabled the models to accurately determine the optimal hybrid train profile inputs required for the efficient and effective operation of the train. The results of the study demonstrate the ability of the proposed ANN models to predict the complex parameters of a hybrid train profile, thus providing significant benefits for the transportation industry.

Comparing the predicted hybrid train profiles, we can see that both topologies and architectures have similar performance in terms of mean squared error (MSE) and maximum error. However, the CFNN topology in the time-based architecture shows a slightly lower MSE and maximum error than the FFNN topology in the power-based architecture. Specifically, the MSE for the CFNN topology in the time-based architecture ranges from 0.11595 to 0.12554, while the MSE for the FFNN topology in the power-based architecture ranges from 0.11588 to 0.12485.

The maximum error for the CFNN topology in the time-based architecture ranges from 1.9796% to 1.9972%, while the maximum error for the FFNN topology in the power-based

architecture ranges from 1.9855% to 2.0108%. In terms of mean error, both topologies and architectures have similar performance, with mean errors ranging from 0.1996% to 0.2157% for the FFNN topology in the power-based architecture and from 0.2009% to 0.2163% for the CFNN topology in the time-based architecture.

Overall, the CFNN topology-based predictive model in the time-based architecture shows slightly better performance than the FFNN topology in the power-based architecture, as it has a lower MSE and maximum error. However, the differences in performance between the two topologies and architectures are relatively small, so both may be viable options depending on the specific requirements of the application.

Table 30 and Table 31 represent the results for identifying the optimal structure of both ANN models. The time-based architecture results suggest that the Power Consumption (O_4) has a lower mean squared error in FFN topology and Carbon Dioxide Emission (O_2) has a lower mean squared error in the CFNN topology. On the contrary, the power-based architecture results indicate that Carbon Dioxide Emissions (O_2) has a lower mean squared error in FFN topology, while Power Consumption (O_4) has a lower mean squared error in CFN topology compared to others. Overall the FFNN topology has the lowest average mean square error in time-based architecture, while the CFNN topology has the lowest average mean square in power-based architecture.

The differences in the ratios of output parameters are attributed to the complex calibration of the values' scale during configuration and alteration. Furthermore, the upper limit of variation in percentage error between the trained ANN models' actual output and the desired output obtained by the hybrid train simulator for testing and validation during the training operation is significantly lower.

Table 30: Mean squared, mean & maximum errors attained for all five outputs parameters over 50 input configurations by CFNN model based on time and power-based architecture

Time-Based Architecture CFNN Topology			
Output Parameter	**MSE**	**Mean Error**	**Max Error**
O_1: H_2 Consumption (kg)	0.11989	0.2072%	1.9876%
O_2: CO_2 Emissions (kg)	0.124995	0.2171%	1.9975%
O_3: Energy Consumption (kWh)	0.116092	0.1999%	1.9803%
O_4: Power Consumption kW)	0.115864	0.1998%	1.9832%
O_5: Journey Time (Minutes)	0.117782	0.2028%	1.9802%
Power-Based Architecture CFNN Topology			
Output Parameter	**MSE**	**Mean Error**	**Max Error**
O_1: H_2 Consumption (kg)	0.20214	0.2137%	1.9941%
O_2: CO_2 Emissions (kg)	0.170389	0.1768%	1.9572%
O_3: Energy Consumption (kWh)	0.190575	0.2001%	1.9805%
O_4: Power Consumption kW)	0.190328	0.1998%	1.9801%
O_5: Journey Time (Minutes)	0.191782	0.2015%	1.9818%

Table 31: Mean squared, mean & maximum errors obtained for all five outputs parameters over 50 input configurations by FFNN model based on time and power-based architecture

Time-Based Architecture FFNN Topology			
Output Parameter	**MSE**	**Mean Error**	**Max Error**
O_1: H_2 Consumption (kg)	0.24391	0.1323%	1.9127%
O_2: CO_2 Emissions (kg)	0.151429	0.0799%	1.8606%
O_3: Energy Consumption (kWh)	0.515879	0.3051%	2.0855%
O_4: Power Consumption kW)	1.416153	1.1948%	2.9751%
O_5: Journey Time (Minutes)	0.262495	0.1432%	1.9237%
Power-Based Architecture FFFN Topology			
Output Parameter	**MSE**	**Mean Error**	**Max Error**
O_1: H_2 Consumption (kg)	0.018663	0.2995%	2.9527%
O_2: CO_2 Emissions (kg)	0.018500	0.1976%	1.9652%
O_3: Energy Consumption (kWh)	0.013055	0.2237%	3.1527%
O_4: Power Consumption kW)	0.012636	0.2449%	3.5658%
O_5: Journey Time (Minutes)	0.017493	0.1862%	1.9584%

The results suggest that the optimal structure of ANN models is influenced by the architecture type, whether time-based or power-based. Additionally, the choice of topology also plays a

significant role in determining the lowest average MSE. Finally, the case study confirms that the upper limit of variation in percentage error between actual and desired output obtained by predictive models is comparatively low, highlighting the effectiveness of this approach for model training and validation.

7.3.2 Optimal Trajectory Analysis and Comparison

Figure 32 presents a comparison of the benchmark trajectory and the predicted trajectories by both topologies in each architecture. The benchmark trajectory was produced by a hybrid train simulator by using the predicted. hybrid train information, and the predicted trajectories were obtained during the validation process.

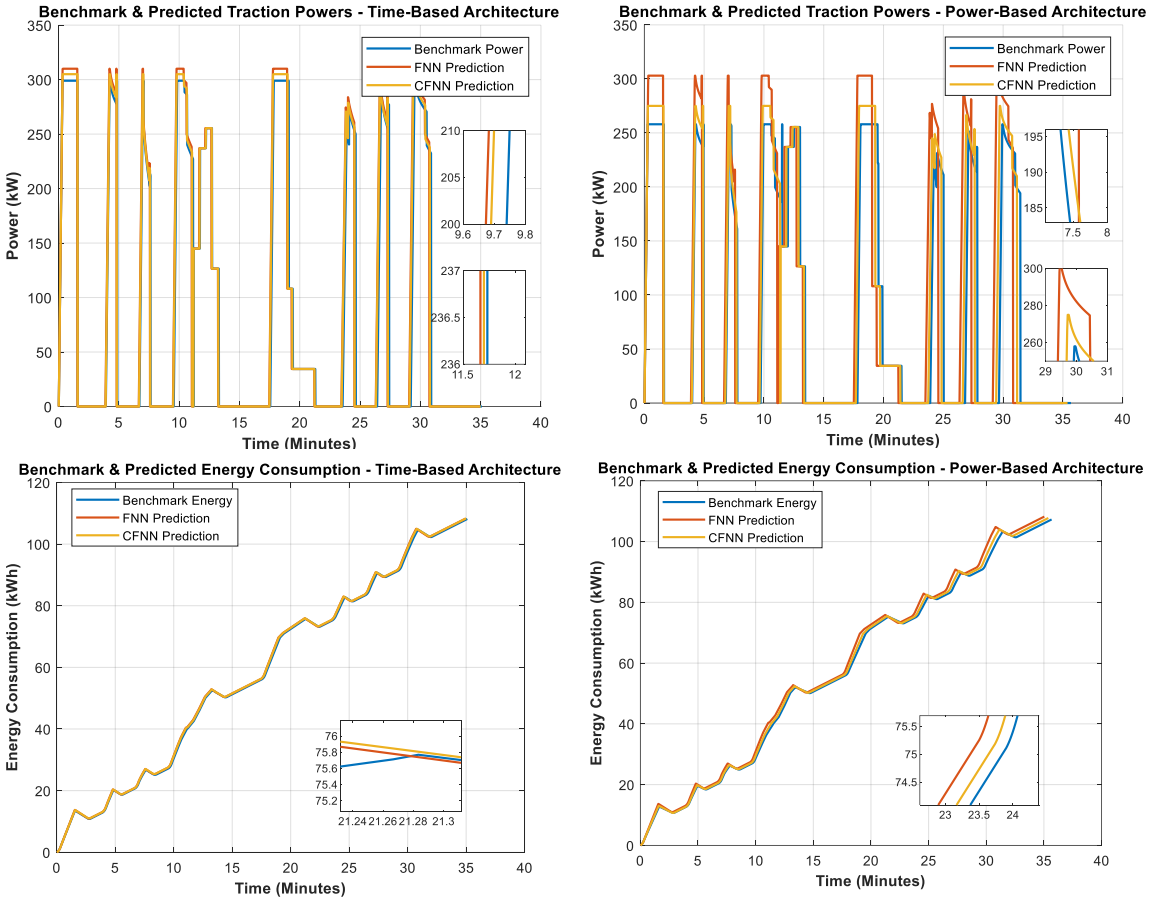

Figure 32: Comparison of time-based and power-based architecture ANN models for a specific route

In the time-based architecture, the FFNN model predicted a 3.6% increase in traction power, 0.11% increase in energy consumption, and 0.03% increase in journey time compared to the benchmark trajectory. On the other hand, the CFNN model predicted a 2.10% increase in traction power, a 0.18% increase in energy consumption, and a 4.78% decrease in journey time compared to the benchmark trajectory.

In the power-based architecture, the FFNN model predicted a 16% increase in traction power, a 0.9% increase in energy consumption, and a 1.75% decrease in journey time compared to the benchmark trajectory. In comparison, the CFNN model predicted a 6.4% increase in traction power, a 0.44% increase in energy consumption, and a 0.03% increase in journey time compared to the benchmark trajectory.

The average percentage difference between benchmark and FFNN for time-based architecture is 0.85%, and for power-based architecture is 0.92%, and the average percentage difference between benchmark and CNFN for time-based architecture is 0.18%, and for power-based architecture is 0.46%.

Overall, the CFNN topology performed better than the FFNN topology in both architectures, as evidenced by the lower mean squared error (MSE) and percentage difference in predicted parameters compared to the benchmark trajectory. The results of this study suggest that the proposed CFNN topology can be used to predict hybrid train performance in both time and power-based architectures with good accuracy and low computation time and expense. Table 32 presents the detailed output values obtained from the benchmark and the values predicted by both ANN models.

Table 32: Benchmark and predicted output values for both ANN models

	Time-Based Architecture			Power-based Architecture		
Outputs	**Benchmark**	**FNN**	**CFN**	**Benchmark**	**FNN**	**CFN**
O_1: H_2 Consumption (kg)	2.5327	2.5325	2.5326	2.54	2.53	2.54
O_2: CO_2 Emissions (kg)	20.515	20.513	20.514	20.63	20.5	20.63
O_3: Energy Consump (kWh)	108.15	108.27	108.35	107.28	108.22	107.76
O_4: Power Consumption l	299	310	305	258	303	275
O_5: Journey Time (Minut	35.83	35.84	34.12	35.66	35.04	35.67

Figure 33 illustrates the patterns of hydrogen consumption and carbon dioxide emissions predicted by artificial neural network models and the actual carbon dioxide emissions. The results show that the predictive model based on CFNN topology accurately predicted the hydrogen consumption pattern, which closely resembled the benchmark consumption in both architectures. Moreover, the time-based architecture model predicted lower levels of carbon dioxide emissions.

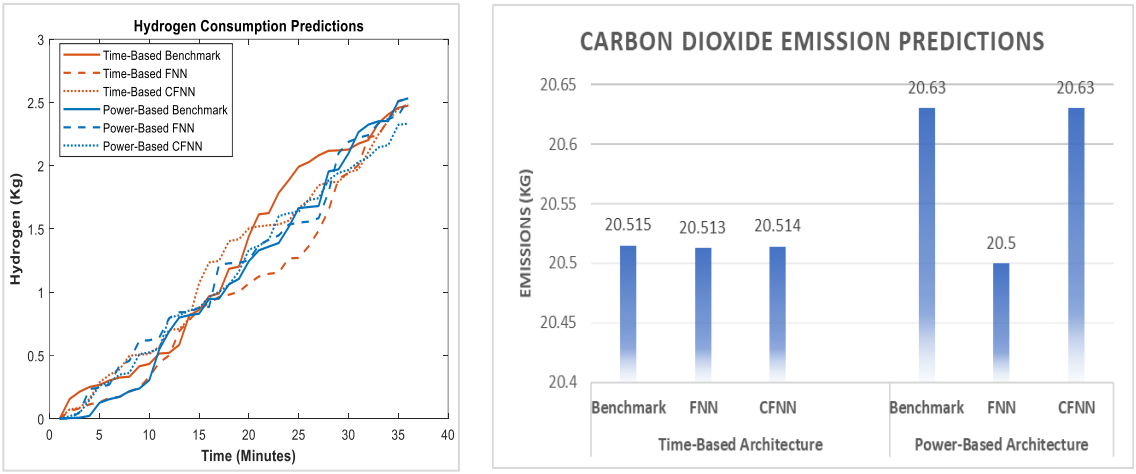

Figure 33: Comparison of time-based and power-based architecture ANN models hydrogen and carbon dioxide emissions for a specific route

The results demonstrate that the cascade forward topology is more accurate and efficient in predicting hydrogen consumption and carbon dioxide emissions. These findings have

important implications for improving the efficiency and sustainability of hydrogen production processes, which are crucial for achieving a more environmentally-friendly energy system.

7.4 Summary

This Section proposes two artificial neural networks (ANN) models, based on time and power-based architectures, for predicting the critical parameters of a hybrid train profile and its relevant optimal trajectory. The performance of both models was evaluated by computing the mean square normalization error and mean absolute performance error. The authenticity of the output was verified using a hybrid train simulator. The results of this study demonstrate the effectiveness and accuracy of the proposed ANN models in predicting the critical parameters of a hybrid train profile, thereby enabling efficient and optimised train operations.

The proposed ANN models were able to accurately determine the optimal hybrid train profile inputs required for the efficient and effective operation of the train. Specifically, the study's results demonstrate the models' ability to predict the complex parameters of a hybrid train profile, thus providing significant benefits for the transportation industry. The predictive models have the potential to be used in real-life scenarios to optimise train operations and reduce energy consumption.

Comparing the performance of the two models, we can see that both topologies and architectures have similar performance in terms of mean squared error (MSE) and maximum error. However, the CFNN topology in the time-based architecture shows a slightly lower MSE and maximum error than the FFNN topology in the power-based architecture. Both architectures and topologies performed similarly, with mean errors ranging from 0.19% to 0.21%. The average percentage difference between the benchmark and FFNN/CNFN trajectories was also reported, with the time-based architecture having lower differences (0.18% and 0.85%) than the power-based architecture (0.46% and 0.92%).

In conclusion, utilising neural networks offers significant benefits in estimating the states of hybrid trains. By accurately capturing complex, non-linear relationships between input and output parameters, neural networks outperform traditional models, which may be limited in their ability to represent real-world scenarios. Furthermore, neural networks provide a more efficient and scalable approach for predicting trajectories, making them well-suited for large datasets and real-time applications. Implementing neural networks leads to improved accuracy, efficiency, and adaptability, which are essential for the evolving challenges in the railway industry. Future improvements may include incorporating more complex parameters to improve accuracy and expanding the study to include more diverse routes and trains. Overall, this study provides valuable insights into using ANN models to predict critical parameters of a hybrid train profile and optimise train operations.

8 CONCLUSION AND FUTURE WORK

8.1 General Summary

This thesis is divided into two parts, covering the literature review, and the application of proposed optimisation techniques for hybrid railway vehicles.

The first part comprises three chapters, where Chapter 1 delves into hybrid railway vehicle traction energy and energy management systems. Chapter 2 reviews conventional and modern railway traction systems, including drives, power sources, and energy storage systems. Chapter 3 discusses conventional and contemporary optimisation techniques, with a focus on numerical, metaheuristics, and the modern evolutionary algorithm, Mayfly. The importance of dynamic programming in optimisation techniques is also highlighted.

The second part of this thesis demonstrates the application of optimisation techniques in hybrid railway vehicles. Chapter 4 presents the development of a hybrid train simulator, which is integrated with energy evaluation, optimisation algorithms, and neural network models in Chapters 5, 6 and 7, respectively. Chapter 4 also introduces an automatic smart switching technique, which yields a 6% reduction in energy consumption compared to conventional hybrid trains and a 65% reduction compared to diesel trains.

Chapter 6 develops a customised non-convex optimisation algorithm for hybrid railway vehicles, achieving an average reduction of 16.85% in total energy consumption, a 0.40% increase in journey times, and a 15.18% reduction in traction power. Chapter 7 presents two artificial neural network models for predicting optimal train trajectories. Both architectures and topologies perform similarly, with mean errors ranging from 0.19% to 0.21%.

The case studies in Chapters 5, 6 and 7 validate the hypothesis that hybrid railway vehicles' traction power and energy can be optimised through a system-level execution of optimisation operations.

8.2 Main Contributions

8.2.1 Hybrid Train Simulator Development

A bespoke hybrid train simulator has been developed in MATLAB to fulfil the research objectives outlined in this thesis. This simulator is capable of analysing train movements on diverse railway routes, incorporating traction performance, customised speed limits, and multiple power sources. It adjusts various power sources based on journey requirements and real-time energy demands. The hybrid train simulator was validated against a well-established single train simulator from the University of Birmingham, with an accuracy range of ±5. Throughout this thesis, the hybrid train simulator is employed in implementing automatic smart switching, applying a hybrid optimisation algorithm, and deploying artificial neural network models.

8.2.2 Automatic Smart Switching Control

The objective of minimising excessive power source usage and utilising the appropriate power source according to the power demand and track terrain is accomplished through an energy evaluation study of hybrid trains incorporating smart switching. The implementation of the smart switching technique aims to assess the impact of power demand on power sources. The hybrid train simulator employs the route's gradient as a reference for switching between power sources. Depending on whether the track is level, uphill, or downhill, the train utilises power from the pre-designated power sources, as programmed by the driver for that specific route.

8.2.3 Hybrid Optimisation Algorithm

A hybrid optimisation algorithm has been developed specifically for hybrid railway vehicle trajectory optimisation. The proposed hybrid algorithm employs an integrated optimisation approach to attain an efficient hybrid train trajectory while minimising energy consumption. Most previous research in this area tends to overlook linear and non-linear datasets for hybrid railway vehicles, which are crucial for establishing an accurate baseline for optimisation techniques. The hybrid optimisation method utilises a non-linear programming solver to address the optimisation problem, interpreted through a non-convex enhanced Rosenbrock function, combined with a highly efficient, improvised "Mayfly algorithm". Ultimately, the hybrid optimisation algorithm integrates various numerical and metaheuristic algorithms, encompassing every aspect of optimising hybrid trains within a reasonable computation time. The energy-saving performance showcased in this thesis is based on simulations of an actual route.

8.2.4 Artificial Neural Network Models

The challenges associated with handling large datasets from the railway industry and the underutilisation of artificial neural networks (ANNs) for such issues are addressed. ANNs are introduced as an alternative method for determining the optimal train trajectory for hybrid railway vehicles. The developed ANN models exhibit efficient self-learning, adaptivity, nonlinearity, and advanced input-output mapping capabilities for large hybrid train datasets. Both models effectively predicted optimal trajectories for an actual route within a reasonable computation time. This demonstrates that the optimal trajectory for a hybrid train can also be achieved using machine learning techniques, as opposed to conventional optimisation methods alone.

8.3 Future Work

8.3.1 Validation and Verification

All the studies presented in this thesis rely on theoretical computer simulations, offering valuable insights into the development of energy efficiency in hybrid railway traction engineering. However, the validation and verification of the proposed study context remain areas for future work. The research in this thesis proposes novel energy-saving techniques for hybrid railway vehicles, which can inspire further advancements in the energy efficiency of hybrid railway traction systems.

8.3.2 Validation of Optimisation Algorithm & ANN models

railway simulation. The results of the study present the theoretical performance of traction energy reduction. Field tests should be conducted to validate the study's findings. Similarly, ANN models predict optimal trajectories using simulated datasets. Actual datasets of various hybrid trains can be used to validate the real-time application of artificial neural networks for hybrid trains.

8.3.3 Further Research work Extensions

For future work as an extension to the research presented in this thesis following topics are suggested:

- The hybrid train simulator is designed for single-train movement simulation. In future work, it can be improved and extended for use in multiple train movement simulations equipped with signalling and system features for hybrid trains.
- The automatic smart switching technique is based on three decision factors: level, uphill, and downhill. More elaborate decision factors can be designed in future work, such as decision parameters classification based on gradient percentage.

- The simulation performed in this thesis focuses on a hydrogen hybrid train. These techniques can be applied to different hybrid configurations as well. Future work can explore these configurations in parallel.
- Although the data generated for this research is as realistic as possible, some unrealistic trajectories may appear due to the simplicity of the train operating pattern. Therefore, it may be worthwhile to search for an efficient train trajectory using quick numerical searching methods for cross-validation.
- The optimisation of multiple hybrid train trajectories within a network can also be a valuable future work extension. This would be beneficial for designing an optimal signalling system for hybrid trains.
- In future work, further development in artificial neural network models based on compression approaches can bring potential improvements in predicting the optimal trajectories of hybrid trains.

APPENDIX A FLOWCHART OF MAYFLY OPTIMISATION ALGORITHM

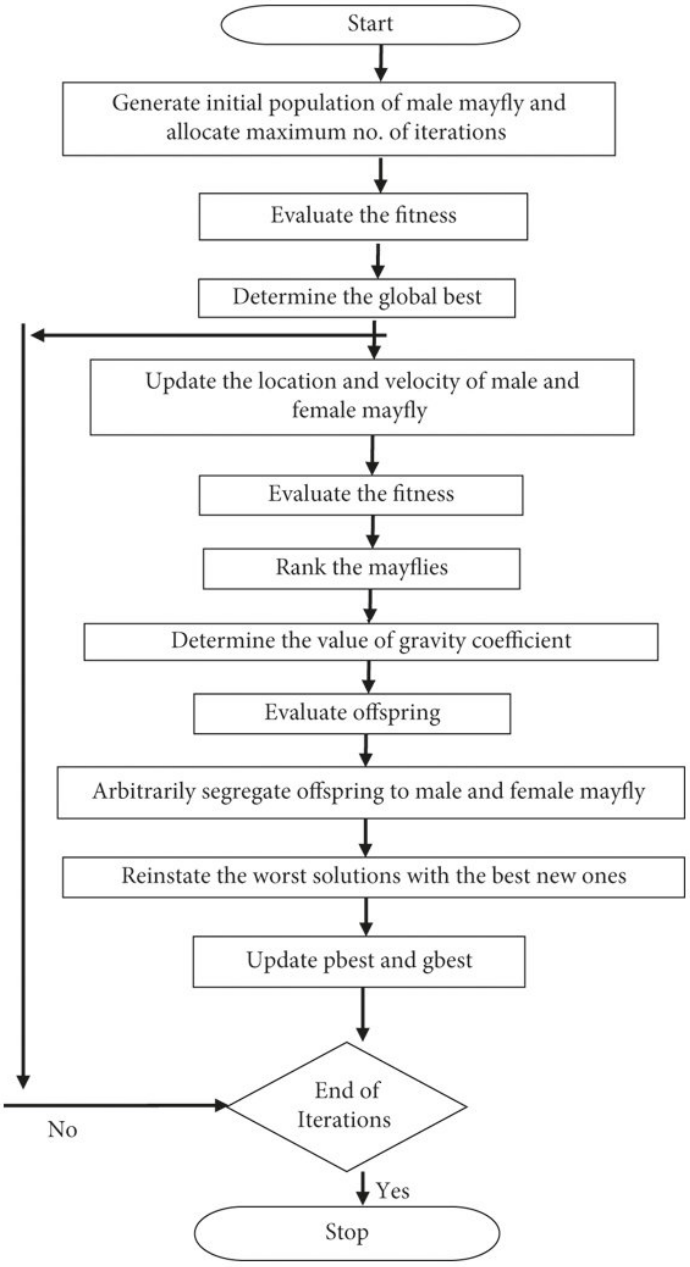

Figure 34: Flowchart of the proposed mayfly optimisation algorithm

APPENDIX B TEST FUNCTIONS USED TO CALIBRATE HYBRID OPTIMISATION ALGORITHM

The hybrid optimisation algorithm was calibrated via various test functions to achieve a robust and efficient non-convex cost function. Each test function was fed with benchmark data to be evaluated by optimisation and forecast function. The test functions were derived from typical non-convex and convex objective functions to perform a calibration process. Each test function used to calibrate the hybrid optimisation algorithm is given as follows:

B.1. Rastrigin Function

Rastrigin function is a non-linear test function that is generally used to test genetic algorithms. It has various local minima and is highly multimodal; however, the minimum location is frequently distributed [264]. The Rastrigin function is mathematically expressed as:

$$f_1(x) = \left[(10^t) + \sum_{x=1}^{t} (G(x)^2 - Acos(2\pi x)\right] \tag{B.1}$$

where is $G(x)^2$ represents the unique data subset of the distance, velocity and acceleration. The function is evaluated on the hypercube x_i ranges between $[-5.12, 5.12]$. A is equal to 10, and t represent the dimension of the solution space of the Rastrigin function.

B.2. Ackley Function

Ackley is a well-known non-convex optimisation function used to test the performance of optimisation algorithms. The Ackley test function generally performs in two dimension mode and is characterised by a nearly flat outer region and a large hole at the centre [267]. The Ackley function is mathematically expressed as:

$$f_2(x) = -20\, exp\left[-0.2\sqrt{\frac{1}{d}\sum_{i=1}^{t} Gx_i^2}\right] - exp\left[\sqrt{\frac{1}{d}\sum_{i=1}^{t} \cos(G2\pi x_i)}\right] + a + \exp(1) \tag{B.2}$$

where $G(x)$ represents the unique data subset of the distance, velocity and acceleration. The hypercube x_i ranges between $[-32.768, 32.768]$. t represents the dimension of the solution space of Ackley's function.

B.3. Griewank Function

The hybrid optimisation algorithm was also tested with the griewank function with many widespread local minima distributed regularly by using Equation (B.3) [263]:

$$f_3(x) = \frac{1}{4000}\sum_{i=1}^{t} Gx_i^2 - \prod_{i=1}^{t} \cos\left(\frac{x_i}{\sqrt{i}}\right) + 1) \tag{B.3}$$

where $G(x_i)$ represents the unique data subset of the distance, velocity and acceleration. The hypercube x_i ranges between $[-600, 600]$. t represents the input domain of the Griewank function.

B.4. Schaffer Function

The sphere function is a continuous and two-dimensional test function with a smaller input domain and is mathematically expressed as [265]:

$$f_4(x) = 0.5 + \frac{sin^2(\sum_{i=1}^{t} Gx_i^2) - 0.5}{\left(1 + 0.001\,(\sum_{i=1}^{t} Gx_i^2)\right)^2} \tag{B.4}$$

where $G(x_i)$ represents the unique data subset of the distance, velocity and acceleration. The hypercube x_i ranges between $[-100, 000]$. t represents the dimension of the solution space. The minimum value of the Schaffer function of $f_4(x)$ is equal to zero.

B.6. Rosenbrock Function

The Rosenbrock function is a classic test function widely used for numerical non-linear optimisation problems [266]. It is a two-dimensional unimodal parabolic function with a global

minimum in a curved shaped valley. The Rosenbrock function implemented in the hybrid optimisation algorithm is presented in Equation (B.5):

$$f_5(x) = \sum_{i=1}^{t-1} 100\ (Gx_{i+1}^2 - Gx_i)^2 + (Gx_i - 1)^2 \quad \begin{cases} -50 \leq x_i \leq 50 \\ i = 1,2 \end{cases} \tag{B.5}$$

where $G(x_i)$ represents the unique data subset of the distance, velocity and acceleration. The hypercube x_i ranges between $[-50, 50]$. The global minima of the Rosenbrock function can be located at $(x, y) = (1,1)$ with the value of the function $f_5(x, y) = 0$.

B.6. Sphere Function

The sphere function is a unimodal continuous and convex test function with a t local minima except for the global one [262]. The sphere function used in the hybrid algorithm is presented as:

$$f_6(x) = \sum_{i=1}^{t} Gx_{i+1}^2 \tag{B.6}$$

where $G(x_i)$ represents the unique data subset of the distance, velocity and acceleration. The hypercube x_i ranges between $[-100, 100]$. t represents the dimension of the solution space. The minimum value of the Schaffer function of $f_6(x)$ is equal to zero.

REFERENCES

[1] V. V. k. Turlapati, "Modeling and Optimization of a Plug-in hybrid electric vehicle," Master of Science (MS), Mechanical Engineering, Clemson University, All Theses. 917, 2010. [Online]. Available: https://tigerprints.clemson.edu/all_theses/917

[2] R. D. Sharma, D. Sharma, K. Awasthi, and N. A. Shamsi, "Power Management and Energy Optimization in Hybrid Electric Vehicle—A Review," Singapore, 2019: Springer Singapore, in Advances in Fluid and Thermal Engineering, pp. 585-594.

[3] A. Fathy, H. Rezk, and A. M. Nassef, "Robust hydrogen-consumption-minimization strategy based salp swarm algorithm for energy management of fuel cell/supercapacitor/batteries in highly fluctuated load condition," *Renewable Energy*, vol. 139, pp. 147-160, 2019/08/01/ 2019, doi: https://doi.org/10.1016/j.renene.2019.02.076.

[4] J. J. Mwambeleko and T. Kulworawanichpong, "Battery electric multiple units to replace diesel commuter trains serving short and idle routes," *Journal of Energy Storage*, vol. 11, pp. 7-15, 2017/06/01/ 2017, doi: https://doi.org/10.1016/j.est.2017.01.004.

[5] S. Xie, X. Hu, T. Liu, S. Qi, K. Lang, and H. Li, "Predictive vehicle-following power management for plug-in hybrid electric vehicles," *Energy*, vol. 166, pp. 701-714, 2019/01/01/ 2019, doi: https://doi.org/10.1016/j.energy.2018.10.129.

[6] C. Ghenai and M. Bettayeb, "Modelling and performance analysis of a stand-alone hybrid solar PV/Fuel Cell/Diesel Generator power system for university building," *Energy*, vol. 171, pp. 180-189, 2019/03/15/ 2019, doi: https://doi.org/10.1016/j.energy.2019.01.019.

[7] M. Cipek, D. Pavković, Z. Kljaić, and T. J. Mlinarić, "Assessment of battery-hybrid diesel-electric locomotive fuel savings and emission reduction potentials based on a realistic mountainous rail route," *Energy*, vol. 173, pp. 1154-1171, 2019/04/15/ 2019, doi: https://doi.org/10.1016/j.energy.2019.02.144.

[8] H. Ritchie and M. Roser. CO_2 and Greenhouse Gas Emissions [Online] Available: https://ourworldindata.org/co2-and-other-greenhouse-gas-emissions

[9] A. P. Roskilly, R. Palacin, and J. Yan, "Novel technologies and strategies for clean transport systems," *Applied Energy*, vol. 157, pp. 563-566, 2015/11/01/ 2015, doi: https://doi.org/10.1016/j.apenergy.2015.09.051.

[10] T. Din and S. Hillmansen, "Energy consumption and carbon dioxide emissions analysis for a concept design of a hydrogen hybrid railway vehicle," *IET Electrical Systems in Transportation*, vol. 8, no. 2, pp. 112-121. [Online]. Available: https://digital-library.theiet.org/content/journals/10.1049/iet-est.2017.0049

[11] Z. Tian, N. Zhao, S. Hillmansen, C. Roberts, T. Dowens, and C. Kerr, "SmartDrive: Traction Energy Optimization and Applications in Rail Systems," *IEEE Transactions on Intelligent Transportation Systems*, vol. 20, no. 7, pp. 2764-2773, 2019, doi: 10.1109/TITS.2019.2897279.

[12] P. Fragiacomo and F. Piraino, "Numerical modelling of a PEFC powertrain system controlled by a hybrid strategy for rail urban transport," *Journal of Energy Storage*, vol. 17, pp. 474-484, 2018/06/01/ 2018, doi: https://doi.org/10.1016/j.est.2018.04.011.

[13] A. Hoffrichter, A. R. Miller, S. Hillmansen, and C. Roberts, "Well-to-wheel analysis for electric, diesel and hydrogen traction for railways," *Transportation Research Part D: Transport and Environment*, vol. 17, no. 1, pp. 28-34, 2012/01/01/ 2012, doi: https://doi.org/10.1016/j.trd.2011.09.002.

[14] D. Meegahawatte, S. Hillmansen, C. Roberts, M. Falco, A. McGordon, and P. Jennings, "Analysis of a fuel cell hybrid commuter railway vehicle," *Journal of Power Sources,* vol. 195, no. 23, pp. 7829-7837, 2010/12/01/ 2010, doi: https://doi.org/10.1016/j.jpowsour.2010.02.025.

[15] C. Wu, W. Zhang, S. Lu, Z. Tan, F. Xue, and J. Yang, "Train Speed Trajectory Optimization With On-Board Energy Storage Device," *IEEE Transactions on Intelligent Transportation Systems,* pp. 1-11, 2018, doi: 10.1109/TITS.2018.2881156.

[16] N. Bizon, "Real-time optimization strategies of Fuel Cell Hybrid Power Systems based on Load-following control: A new strategy, and a comparative study of topologies and fuel economy obtained," *Applied Energy,* vol. 241, pp. 444-460, 2019/05/01/ 2019, doi: https://doi.org/10.1016/j.apenergy.2019.03.026.

[17] N. M. T. Nicu Bizon, Frede Blaabjerg, Erol Kurt, *Energy Harvesting and Energy Efficiency,* 1 ed. (Technology, Methods, and Applications). Springer International Publishing, 2017, p. 661.

[18] V. Das, S. Padmanaban, K. Venkitusamy, R. Selvamuthukumaran, F. Blaabjerg, and P. Siano, "Recent advances and challenges of fuel cell based power system architectures and control – A review," *Renewable and Sustainable Energy Reviews,* vol. 73, pp. 10-18, 2017/06/01/ 2017, doi: https://doi.org/10.1016/j.rser.2017.01.148.

[19] H. S. Nicu Bizon, Naser Mahdavi Tabatabaei, *Analysis, Control and Optimal Operations in Hybrid Power Systems*, 1 ed. (Green Energy and Technology). London: Springer, London, 2013.

[20] N. Bizon and E. Kurt, "Performance analysis of the tracking of the global extreme on multimodal patterns using the Asymptotic Perturbed Extremum Seeking Control scheme," *International Journal of Hydrogen Energy,* vol. 42, no. 28, pp. 17645-17654, 2017/07/13/ 2017, doi: https://doi.org/10.1016/j.ijhydene.2016.11.173.

[21] T. Keulen, M. Steinbuch, J. Kessels, and D. L. Foster, "Energy management in hybrid electric vehicles: Benefit of prediction," *IFAC Proceedings Volumes (IFAC-PapersOnline),* 01/01 2010, doi: 10.3182/20100712-3-DE-2013.00027.

[22] J. T B A Kessels, M. W T Koot, P. P. J. van den Bosch, and D. Kok, "Online Energy Management for Hybrid Electric Vehicles," *Vehicular Technology, IEEE Transactions on,* vol. 57, pp. 3428-3440, 12/01 2008, doi: 10.1109/TVT.2008.919988.

[23] A. Albrecht, P. Howlett, P. Pudney, X. Vu, and P. Zhou, "The key principles of optimal train control—Part 1: Formulation of the model, strategies of optimal type, evolutionary lines, location of optimal switching points," *Transportation Research Part B: Methodological,* vol. 94, pp. 482-508, 2016/12/01/ 2016, doi: https://doi.org/10.1016/j.trb.2015.07.023.

[24] A. Albrecht, P. Howlett, P. Pudney, X. Vu, and P. Zhou, "The key principles of optimal train control—Part 2: Existence of an optimal strategy, the local energy minimization principle, uniqueness, computational techniques," *Transportation Research Part B: Methodological,* vol. 94, pp. 509-538, 2016/12/01/ 2016, doi: https://doi.org/10.1016/j.trb.2015.07.024.

[25] P. Fragiacomo and P. Francesco, "Energy performance of a Fuel Cell hybrid system for rail vehicle propulsion," *Energy Procedia,* vol. 126, pp. 1051-1058, 2017/09/01/ 2017, doi: https://doi.org/10.1016/j.egypro.2017.08.312.

[26] N. Zhao, L. Chen, Z. Tian, C. Roberts, S. Hillmansen, and J. Lv, "Field test of train trajectory optimisation on a metro line," *IET Intelligent Transport Systems,* vol. 11, no. 5, pp. 273-281, 2017, doi: 10.1049/iet-its.2016.0214.

[27] RSSB. "GB Operational Concept Standalone Driver Advisory System (S-DAS)." https://www.rssb.co.uk/Library/groups-and-committees/2013-standalone-das-operational-concept.pdf (accessed 10-10, 2019).

[28] Z. Hainan, S. Xubin, C. Lei, G. Shigen, and D. Hairong, "Analysis and design of Driver Advisory System (DAS) for energy-efficient train operation with real-time information," in *2016 IEEE International Conference on Intelligent Rail Transportation (ICIRT)*, 23-25 Aug. 2016 2016, pp. 99-104, doi: 10.1109/ICIRT.2016.7588717.
[29] A. Ivan, G. Marco, P. Cesare, R. Gianfranco, and S. Marco, "Optimization of Supervisory Control Strategy for Parallel Hybrid Vehicle with Provisional Load Estimate," 2004.
[30] C.-C. Lin, H. Peng, J. W. Grizzle, and J. Kang, "Power management strategy for a parallel hybrid electric truck," *IEEE Trans. Control. Syst. Technol.*, vol. 11, pp. 839-849, 2003.
[31] E. D. Tate and S. P. Boyd, "Finding Ultimate Limits of Performance for Hybrid Electric Vehicles," *SAE transactions*, vol. 109, pp. 2437-2448, 2000.
[32] S. Delprat, J. Lauber, T.-M. Guerra, and J. Rimaux, "Control of a parallel hybrid powertrain: optimal control," *IEEE Transactions on Vehicular Technology*, vol. 53, pp. 872-881, 2004.
[33] T. Hofman and v. R. R. Druten, "Energy analysis of hybrid vehicle powertrains," 2004.
[34] J. Park *et al.*, "Intelligent Vehicle Power Control Based on Machine Learning of Optimal Control Parameters and Prediction of Road Type and Traffic Congestion," *IEEE Transactions on Vehicular Technology*, vol. 58, pp. 4741-4756, 2009.
[35] V. H. Johnson, K. Wipke, and D. Rausen, "HEV Control Strategy for Real-Time Optimization of Fuel Economy and Emissions," *SAE transactions*, vol. 109, pp. 1677-1690, 2000.
[36] A. Sciarretta, L. Guzzella, and M. Back, "A Real-Time Optimal Control Strategy for Parallel Hybrid Vehicles with On-Board Estimation of the Control Parameters," *IFAC Proceedings Volumes*, vol. 37, pp. 489-494, 2004.
[37] L. Guzzella and A. Sciarretta, "Electric and Hybrid-Electric Propulsion Systems," in *Vehicle Propulsion Systems: Introduction to Modeling and Optimization*. Berlin, Heidelberg: Springer Berlin Heidelberg, 2013, pp. 67-162.
[38] Y.-J. Han, K.-H. Kim, S.-I. Seo, C.-S. Park, S.-H. Han, and Y.-M. Kim, "Traction system characteristics of railway vehicle," *제어로봇시스템학회 학술대회논문집*, pp. 1351-1354, 2005.
[39] L. Buhrkall, "Traction system case study," in *The 9th Institution of Engineering and Technology Professional Development Course on Electric Traction Systems*, 2006: IET, pp. 53-71.
[40] R. J. Hill, "Electric railway traction. Part 3. Traction power supplies," *Power Engineering Journal*, vol. 8, no. 6, pp. 275-286, 1994, doi: 10.1049/pe:19940604.
[41] T. Din, Z. Tian, K. Li, S. Hillmansen, and C. Roberts, "Operation and energy evaluation of diesel and hybrid trains with smart switching controls," *Control Engineering Practice*, vol. 116, p. 104935, 2021/11/01/ 2021, doi: https://doi.org/10.1016/j.conengprac.2021.104935.
[42] N. Srisakda, P. Sumitsawan, A. Fukuda, T. Ishizaka, and C. Sangsrichan, "Reduction of vehicle fuel consumption from adjustment of cycle length at a signalized intersection and promotional use of environmentally friendly vehicles," *Engineering and Applied Science Research*, Article vol. 49, no. 1, pp. 18-28, 2022, doi: 10.14456/easr.2022.2.
[43] A. Hoffrichter, "Hydrogen as an energy carrier for railway traction," 2013.
[44] R. Hill, "Electric railway traction. II. Traction drives with three-phase induction motors," *Power Engineering Journal*, vol. 8, pp. 143-152, 1994.
[45] R. Hill, "Electric railway traction. I. Electric traction and DC traction motor drives," *Power Engineering Journal*, vol. 8, pp. 47-56, 1994.

[46] P. Pozzobon, "Transient and steady-state short-circuit currents in rectifiers for DC traction supply," *IEEE Transactions on Vehicular Technology*, vol. 47, no. 4, pp. 1390-1404, 1998, doi: 10.1109/25.728534.
[47] Z. Tian, "System energy optimisation strategies for DC railway traction power networks," 2017.
[48] A. J. Wharton, "CHAPTER 1 - Engine Types," in *Diesel Engines (Third Edition)*, A. J. Wharton Ed. Oxford: Butterworth-Heinemann, 1991, pp. 1-18.
[49] G. Thompson, "THE AMERICAN PASSENGER TRAIN IN THE MOTOR AGE: ARCHIVAL AND ECONOMETRIC ANALYSES OF EXPLANATIONS FOR THE DECLINE IN CALIFORNIA, 1910-1941," 1987.
[50] M. C. Duffy and I. o. E. Engineers, *Electric Railways: 1880-1990*. Institution of Engineering and Technology, 2003.
[51] J. Welsh, *Union Pacific's streamliners*. Minneapolis, MN: Voyageur Press (in English), 2008.
[52] J. Martins, F. Brito, D. Pedrosa, V. Monteiro, and J. L. Afonso, "Real-Life Comparison between Diesel and Electric Car Energy Consumption," 2013.
[53] H. I. Andrews, "Railway Traction: The Principles of Mechanical and Electrical Railway Traction," 1986.
[54] h. cArcinogens, p. hAbIts, and I. Monographs, "DIESEL AND GASOLINE ENGINE EXHAUSTS AND SOME NITROARENES. IARC MONOGRAPHS ON THE EVALUATION OF CARCINOGENIC RISKS TO HUMANS," *IARC monographs on the evaluation of carcinogenic risks to humans*, vol. 105, pp. 9-699, 2014.
[55] N. Statistics, "Rail Infrastructure and Assets," *Office of Rail Road*, no. 1, p. 16, 2020, doi: https://dataportal.orr.gov.uk/media/1842/rail-infrastructure-assets-2019-20.pdf.
[56] S. Lu, S. Hillmansen, and C. Roberts, "A Power-Management Strategy for Multiple-Unit Railroad Vehicles," *IEEE Transactions on Vehicular Technology*, vol. 60, pp. 406-420, 2011.
[57] V. Shamardina, M. V. Anishchenko, S. M. Lemeshko, and R. V. Kanunnikov, "Functional efficiency enhancement of diesel-electric locomotive traction system," *2017 International Conference on Modern Electrical and Energy Systems (MEES)*, pp. 20-23, 2017.
[58] A. R. Miller, J. Peters, B. Smith, and O. Velev, "Analysis of fuel cell hybrid locomotives," *Journal of Power Sources*, vol. 157, pp. 855-861, 2006.
[59] A. R. Miller, K. Hess, D. Barnes, and T. L. Erickson, "System design of a large fuel cell hybrid locomotive," *Journal of Power Sources*, vol. 173, pp. 935-942, 2007.
[60] F. J. D. Libao and R. O. Dizon, "Rule-Based Energy Management Strategy for Hybrid Electric Road Train," in *2018 IEEE 10th International Conference on Humanoid, Nanotechnology, Information Technology,Communication and Control, Environment and Management (HNICEM)*, 29 Nov.-2 Dec. 2018 2018, pp. 1-4, doi: 10.1109/HNICEM.2018.8666390.
[61] K. Ogawa, T. Yamamoto, H. Hasegawa, and T. Furuya, "Development of the fuel-cell/battery hybrid railway vehicle," in *2009 IEEE Vehicle Power and Propulsion Conference*, 7-10 Sept. 2009 2009, pp. 1730-1735, doi: 10.1109/VPPC.2009.5289693.
[62] K. Valeriy, S. Viktor, H. Petro, S. Myamlin, K. Yevhen, and L. Vitalij, "Hybrid railway traction power supply system," in *2020 IEEE 4th International Conference on Intelligent Energy and Power Systems (IEPS)*, 7-11 Sept. 2020 2020, pp. 208-211, doi: 10.1109/IEPS51250.2020.9263194.
[63] S. Hillmansen, "Sustainable traction drives," in *2009 4th IET professional Development Course on Railway Electrification Infrastructure and Systems*, 1-5 June 2009 2009, pp. 255-265, doi: 10.1049/ic.2009.0023.

[64] F. Schmid and C. J. Goodman, "Electric railway systems in common use," *IET Conference Proceedings*, pp. 1-1. [Online]. Available: https://digital-library.theiet.org/content/conferences/10.1049/ic_20050618

[65] C. Goodman, "Overview of electric railway systems and the calculation of train performance," 2006.

[66] M. Mermet-Guyennet, "New power technologies for traction drives," in *SPEEDAM 2010*, 14-16 June 2010 2010, pp. 719-723, doi: 10.1109/SPEEDAM.2010.5542097.

[67] M. Halwas, L. Hausmann, F. Wirth, J. Fleischer, B. Jux, and M. Doppelbauer, "Influences of Design and Manufacturing on the Performance of Electric Traction Drives," in *2020 International Conference on Electrical Machines (ICEM)*, 23-26 Aug. 2020 2020, vol. 1, pp. 488-494, doi: 10.1109/ICEM49940.2020.9270899.

[68] M. K. Mahapatra and P. Singh, "Chapter 24 - Fuel Cells: Energy Conversion Technology," in *Future Energy (Second Edition)*, T. M. Letcher Ed. Boston: Elsevier, 2014, pp. 511-547.

[69] A. Coralli, B. J. M. Sarruf, P. E. V. de Miranda, O. Luigi, S. Specchia, and N. Q. Minh, "Chapter 2 - Fuel Cells," in *Science and Engineering of Hydrogen-Based Energy Technologies*, P. E. V. de Miranda Ed.: Academic Press, 2019, pp. 39-122.

[70] M. El-Shafie, S. Kambara, and Y. Hayakawa, "Hydrogen Production Technologies Overview," *Journal of Power and Energy Engineering*, vol. 07, pp. 107-154, 2019.

[71] A. Ursua, L. M. Gandia, and P. Sanchis, "Hydrogen Production From Water Electrolysis: Current Status and Future Trends," *Proceedings of the IEEE*, vol. 100, no. 2, pp. 410-426, 2012, doi: 10.1109/JPROC.2011.2156750.

[72] R. A. Rozendal, H. V. M. Hamelers, G. J. W. Euverink, S. J. Metz, and C. J. N. Buisman, "Principle and perspectives of hydrogen production through biocatalyzed electrolysis," *International Journal of Hydrogen Energy*, vol. 31, no. 12, pp. 1632-1640, 2006/09/01/ 2006, doi: https://doi.org/10.1016/j.ijhydene.2005.12.006.

[73] E-Conversion. "Fuel cell principle." https://www.e-conversion.de/fuel-cell-principle/ (accessed 21, 2022).

[74] T. Din and S. Hillmansen, "Energy consumption and carbon dioxide emissions analysis for a concept design of a hydrogen hybrid railway vehicle," *IET Electrical Systems in Transportation*, vol. 8, no. 2, pp. 112-121, 2018, doi: https://doi.org/10.1049/iet-est.2017.0049.

[75] S. Tao *et al.*, "Energy management strategy based on dynamic programming with durability extension for fuel cell hybrid tramway," *Railway Engineering Science*, 2021/09/09 2021, doi: 10.1007/s40534-021-00247-w.

[76] Alstom. "Coradia iLint™ – the world's 1st hydrogen powered train." (accessed.

[77] S. Lu, D. H. Meegahawatte, S. Guo, S. Hillmansen, C. Roberts, and C. J. Goodman, "Analysis of energy storage devices in hybrid railway vehicles," in *2008 International Conference on Railway Engineering - Challenges for Railway Transportation in Information Age*, 25-28 March 2008 2008, pp. 1-6.

[78] S. Hillmansen and R. Ellis, "Electric railway traction systems and techniques for energy saving," in *IET 13th Professional Development Course on Electric Traction Systems*, 3-6 Nov. 2014 2014, pp. 1-6, doi: 10.1049/cp.2014.1432.

[79] F. Torabi and P. Ahmadi, "Chapter 6 - Lead–acid batteries," in *Simulation of Battery Systems*, F. Torabi and P. Ahmadi Eds.: Academic Press, 2020, pp. 149-215.

[80] H. Chen, T. N. Cong, W. Yang, C. Tan, Y. Li, and Y. Ding, "Progress in electrical energy storage system: A critical review," *Progress in Natural Science*, vol. 19, no. 3, pp. 291-312, 2009/03/10/ 2009, doi: https://doi.org/10.1016/j.pnsc.2008.07.014.

[81] J. Lach, K. Wro bel, J. Wróbel, P. Podsadni, and A. Czerwinski, "Applications of carbon in lead-acid batteries: a review," *Journal of Solid State Electrochemistry*, vol. 23, pp. 693-705, 2019.
[82] N. Omar *et al.*, "Analysis of Nickel-Based Battery Technologies for Hybrid and Electric Vehicles," in *Reference Module in Chemistry, Molecular Sciences and Chemical Engineering*: Elsevier, 2014.
[83] K. Pourabdollah, "Development of electrolyte inhibitors in nickel cadmium batteries," *Chemical Engineering Science*, vol. 160, pp. 304-312, 2017/03/16/ 2017, doi: https://doi.org/10.1016/j.ces.2016.11.038.
[84] G. Karkera, M. A. Reddy, and M. Fichtner, "Recent developments and future perspectives of anionic batteries," *Journal of Power Sources*, vol. 481, p. 228877, 2021/01/01/ 2021, doi: https://doi.org/10.1016/j.jpowsour.2020.228877.
[85] F. Torabi and P. Ahmadi, "Chapter 1 - Battery technologies," in *Simulation of Battery Systems*, F. Torabi and P. Ahmadi Eds.: Academic Press, 2020, pp. 1-54.
[86] T. Müller and B. Friedrich, "Development of a recycling process for nickel-metal hydride batteries," *Journal of Power Sources*, vol. 158, no. 2, pp. 1498-1509, 2006/08/25/ 2006, doi: https://doi.org/10.1016/j.jpowsour.2005.10.046.
[87] D. Choi *et al.*, "Li-ion battery technology for grid application," *Journal of Power Sources*, vol. 511, p. 230419, 2021/11/01/ 2021, doi: https://doi.org/10.1016/j.jpowsour.2021.230419.
[88] A. F. Burke, "Batteries and Ultracapacitors for Electric, Hybrid, and Fuel Cell Vehicles," *Proceedings of the IEEE*, vol. 95, no. 4, pp. 806-820, 2007, doi: 10.1109/JPROC.2007.892490.
[89] T. Yi and L. ZhiMei, "Study on modeling and application of ultracapacitor," in *2014 IEEE Workshop on Advanced Research and Technology in Industry Applications (WARTIA)*, 29-30 Sept. 2014 2014, pp. 999-1002, doi: 10.1109/WARTIA.2014.6976443.
[90] H.-q. Li, Y. Zou, and Y.-y. Xia, "A study of nitroxide polyradical/activated carbon composite as the positive electrode material for electrochemical hybrid capacitor," *Electrochimica Acta*, vol. 52, no. 5, pp. 2153-2157, 2007/01/01/ 2007, doi: https://doi.org/10.1016/j.electacta.2006.08.031.
[91] G. G. Amatucci, F. Badway, J. Shelburne, A. G. I. Plitz, A. DuPasquier, and S. Menocal, (Electrochemical Society Proceedings Series). Pennington, N.J.: Electrochemical Society (in 英語), 2002.
[92] A. Burke and M. Miller, "Performance characteristics of lithium-ion batteries of various chemistries for plug-in hybrid vehicles," 2009.
[93] J. Schindall, "The Charge of the Ultracapacitors," *IEEE Spectrum*, vol. 44, no. 11, pp. 42-46, 2007, doi: 10.1109/MSPEC.2007.4378458.
[94] N. L. Hinov, D. N. Penev, and G. I. Vacheva, "Ultra capacitors charging by regenerative braking in electric vehicles," in *2016 XXV International Scientific Conference Electronics (ET)*, 12-14 Sept. 2016 2016, pp. 1-4, doi: 10.1109/ET.2016.7753484.
[95] P. Radcliffe, J. S. Wallace, and L. H. Shu, "Stationary applications of energy storage technologies for transit systems," in *2010 IEEE Electrical Power & Energy Conference*, 25-27 Aug. 2010 2010, pp. 1-7, doi: 10.1109/EPEC.2010.5697222.
[96] J. Li, D. Xin, H. Wang, and C. Liu, "Application of Energy Storage System in Rail Transit: A Review," in *2022 International Conference on Power Energy Systems and Applications (ICoPESA)*, 25-27 Feb. 2022 2022, pp. 539-552, doi: 10.1109/ICoPESA54515.2022.9754481.

[97] M. Hannan, M. A. Al Mamun, A. Hussain, H. Basri, and R. A. Begum, "A review on technologies and their usage in solid waste monitoring and management systems: Issues and challenges," *Waste Management,* vol. 43, pp. 509-523, 2015.
[98] M. Hedlund, J. Lundin, J. De Santiago, J. Abrahamsson, and H. Bernhoff, "Flywheel energy storage for automotive applications," *Energies,* vol. 8, no. 10, pp. 10636-10663, 2015.
[99] V. Lappas, D. Richie, C. Hall, J. Fausz, and B. Wilson, "Survey of technology developments in flywheel attitude control and energy storage systems," *Journal of guidance, control, and dynamics,* vol. 32, no. 2, pp. 354-365, 2009.
[100] Z. ZhAng, W. Gao, and Y. Zhou, "Reliability modeling and maintenance optimization of the diesel system in locomotives," *Eksploatacja i Niezawodność,* vol. 14, pp. 302-311, 2012.
[101] C. Myung, H. Lee, K. Choi, Y. Lee, and S. Park, "Effects of gasoline, diesel, LPG, and low-carbon fuels and various certification modes on nanoparticle emission characteristics in light-duty vehicles," *International Journal of Automotive Technology,* vol. 10, pp. 537-544, 2009.
[102] T. B. Reddy, *Linden's handbook of batteries*. McGraw-Hill Education, 2011.
[103] P. Pei and H. Chen, "Main factors affecting the lifetime of Proton Exchange Membrane fuel cells in vehicle applications: A review," *Applied Energy,* vol. 125, pp. 60-75, 2014.
[104] B. Belvedere, M. Bianchi, A. Borghetti, A. De Pascale, M. Paolone, and R. Vecci, "Experimental analysis of a PEM fuel cell performance at variable load with anodic exhaust management optimization," *international journal of hydrogen energy,* vol. 38, no. 1, pp. 385-393, 2013.
[105] K. Zhang, J. Yang, C. Liu, J. Wang, and D. Yao, "Dynamic Characteristics of a Traction Drive System in High-Speed Train Based on Electromechanical Coupling Modeling under Variable Conditions," *Energies,* vol. 15, no. 3, p. 1202, 2022.
[106] B. Gou, X. Ge, S. Wang, X. Feng, J. B. Kuo, and T. G. Habetler, "An open-switch fault diagnosis method for single-phase PWM rectifier using a model-based approach in high-speed railway electrical traction drive system," *IEEE Transactions on Power Electronics,* vol. 31, no. 5, pp. 3816-3826, 2015.
[107] S. Yang, A. Bryant, P. Mawby, D. Xiang, L. Ran, and P. Tavner, "An industry-based survey of reliability in power electronic converters," *IEEE transactions on Industry Applications,* vol. 47, no. 3, pp. 1441-1451, 2011.
[108] Z. Ismail, "Microprocessor control of electro-mechanical actuators," Loughborough University, 1986.
[109] F. Ciancetta, A. Ometto, G. D'Ovidio, and C. Masciovecchio, "Modeling, Analysis and Implementation of an Urban Electric Light-Rail Train Hydrogen Powered," *International Review of Electrical Engineering (IREE),* vol. 14, p. 237, 08/31 2019, doi: 10.15866/iree.v14i4.17629.
[110] A. Khosravi, R. N. N. Koury, L. Machado, and J. J. G. Pabon, "Energy, exergy and economic analysis of a hybrid renewable energy with hydrogen storage system," *Energy,* vol. 148, pp. 1087-1102, 2018/04/01/ 2018, doi: https://doi.org/10.1016/j.energy.2018.02.008.
[111] D. Murray-Smith, *Design Options for Hybrid Trains Powered by Hydrogen Fuel Cells and Batteries for Routes in the Highlands of Scotland: Results for the case of a three-coach multiple- unit train.* A Report for the Scottish Association for Public Transport, 2020.
[112] S. Kent, D. Gunawardana, T. Chicken, and R. Ellis, "FCEMU Project - Phase 1 Report-Issue 1," in "Future Railway Powertrain Challenge; Fuel Cell Electric Multiple Unit (FCEMU) Project," University of Birmingham, Hitachi Rail, Fuel Cell Systems

Limited., 2016, vol. 2021. [Online]. Available: https://www.birmingham.ac.uk/Documents/college-eps/railway/1-Class-156-Fuel-Cell-Electric-Multiple-Unit-Feasibility-Study-Issue-1.pdf
[113] A. Hoffrichter, S. Hillmansen, and C. Roberts, "Conceptual propulsion system design for a hydrogen-powered regional train," *IET Electrical Systems in Transportation*, vol. 6, no. 2, pp. 56-66. [Online]. Available: https://digital-library.theiet.org/content/journals/10.1049/iet-est.2014.0049
[114] M. Haji Akhoundzadeh *et al.*, "A Conceptualized Hydrail Powertrain: A Case Study of the Union Pearson Express Route," *World Electric Vehicle Journal*, vol. 10, no. 2, p. 32, 2019. [Online]. Available: https://www.mdpi.com/2032-6653/10/2/32.
[115] F. Zhang, P. Zhao, M. Niu, and J. Maddy, "The survey of key technologies in hydrogen energy storage," *International Journal of Hydrogen Energy*, vol. 41, no. 33, pp. 14535-14552, 2016/09/07/ 2016, doi: https://doi.org/10.1016/j.ijhydene.2016.05.293.
[116] U. Mukherjee, M. Elsholkami, S. Walker, M. Fowler, A. Elkamel, and A. Hajimiragha, "Optimal sizing of an electrolytic hydrogen production system using an existing natural gas infrastructure," *International Journal of Hydrogen Energy*, vol. 40, no. 31, pp. 9760-9772, 2015/08/17/ 2015, doi: https://doi.org/10.1016/j.ijhydene.2015.05.102.
[117] B. Nastasi and G. Lo Basso, "Hydrogen to link heat and electricity in the transition towards future Smart Energy Systems," *Energy*, vol. 110, pp. 5-22, 2016/09/01/ 2016, doi: https://doi.org/10.1016/j.energy.2016.03.097.
[118] E. Haghi, M. Fowler, and K. Raahemifar, "Co-benefit analysis of incentives for energy generation and storage systems; a multi-stakeholder perspective," *International Journal of Hydrogen Energy*, vol. 44, no. 19, pp. 9643-9671, 2019/04/12/ 2019, doi: https://doi.org/10.1016/j.ijhydene.2018.08.150.
[119] J. Nocedal, "Wright St. Numerical optimization," ed: New York, Springer, 2006.
[120] C. A. Frangopoulos, *Exergy, Energy System Analysis, and Optimization* (EXERGY, ENERGY SYSTEM ANALYSIS AND OPTIMIZATION). National Technical University of Athens (NTUA), Greece 2009.
[121] M. W. Jeter, *Mathematical programming: an introduction to optimization*. Routledge, 2018.
[122] Y. Eren, İ. B. Küçükdemiral, and İ. Üstoğlu, "Chapter 2 - Introduction to Optimization," in *Optimization in Renewable Energy Systems*, O. Erdinç Ed. Boston: Butterworth-Heinemann, 2017, pp. 27-74.
[123] P. Pezzini, O. Gomis-Bellmunt, and A. Sudrià-Andreu, "Optimization techniques to improve energy efficiency in power systems," *Renewable and Sustainable Energy Reviews*, vol. 15, no. 4, pp. 2028-2041, 2011/05/01/ 2011, doi: https://doi.org/10.1016/j.rser.2011.01.009.
[124] Q. Tao, X. Liu, and M. Xue, "A dynamic genetic algorithm based on continuous neural networks for a kind of non-convex optimization problems," *Applied Mathematics and Computation*, vol. 150, no. 3, pp. 811-820, 2004/03/17/ 2004, doi: https://doi.org/10.1016/S0096-3003(03)00309-6.
[125] J. Nocedal and S. Wright, *Numerical Optimization*. Springer New York, 2006.
[126] X.-S. Yang, "3 - Optimization algorithms," in *Introduction to Algorithms for Data Mining and Machine Learning*, X.-S. Yang Ed.: Academic Press, 2019, pp. 45-65.
[127] N. M. Temme, *Asymptotic Methods for Integrals* (Asymptotic Methods for Integrals).
[128] J. S. Arora, "Additional Topics on Optimum Design," in *Introduction to Optimum Design*, 3 ed. Boston: Academic Press, 2012, pp. 841-850.
[129] M. Mahdi and M. Shiker, "Three-term of new conjugate gradient projection approach under Wolfe condition to solve unconstrained optimization problems,“in press”,

accepted paper for publication," *Jour of Adv Research in Dynamical & Control Systems*, vol. 12, no. 7, 2020.
[130] J.-F. Bonnans, J. C. Gilbert, C. Lemarechal, and C. A. Sagastizábal, *Numerical Optimization*, 2 ed. (Theoretical and Practical Aspects). Springer-Verlag Berlin Heidelberg, 2006, p. 494.
[131] J. D. Knowles, R. A. Watson, and D. W. Corne, "Reducing Local Optima in Single-Objective Problems by Multi-objectivization," Berlin, Heidelberg, 2001: Springer Berlin Heidelberg, in Evolutionary Multi-Criterion Optimization, pp. 269-283.
[132] F. Glover, "Future paths for integer programming and links to artificial intelligence," *Computers & Operations Research*, vol. 13, no. 5, pp. 533-549, 1986/01/01/ 1986, doi: https://doi.org/10.1016/0305-0548(86)90048-1.
[133] Z. C. Tian, W. Q. Chen, P. Tang, J. G. Wang, and X. Shi, "Building Energy Optimization Tools and Their Applicability in Architectural Conceptual Design Stage," *Energy Procedia*, vol. 78, pp. 2572-2577, 2015/11/01/ 2015, doi: https://doi.org/10.1016/j.egypro.2015.11.288.
[134] M. Gendreau and J.-Y. Potvin, *Handbook of Metaheuristics*, 3 ed. (International Series in Operations Research & Management Science). Springer, Cham, p. 604.
[135] Y. Gao and D. Song, "A New Improved Genetic Algorithms and its Property Analysis," in *2009 Third International Conference on Genetic and Evolutionary Computing*, 14-17 Oct. 2009 2009, pp. 73-76, doi: 10.1109/WGEC.2009.150.
[136] D. Whitley, "A genetic algorithm tutorial," *Statistics and Computing*, vol. 4, no. 2, pp. 65-85, 1994/06/01 1994, doi: 10.1007/BF00175354.
[137] P. J. M. van Laarhoven and E. H. L. Aarts, "Simulated annealing," in *Simulated Annealing: Theory and Applications*, P. J. M. van Laarhoven and E. H. L. Aarts Eds. Dordrecht: Springer Netherlands, 1987, pp. 7-15.
[138] C. Voudouris and E. P. K. Tsang, "Guided Local Search," in *Handbook of Metaheuristics*, F. Glover and G. A. Kochenberger Eds. Boston, MA: Springer US, 2003, pp. 185-218.
[139] P. Beullens, L. Muyldermans, D. Cattrysse, and D. Van Oudheusden, "A guided local search heuristic for the capacitated arc routing problem," *European Journal of Operational Research*, vol. 147, no. 3, pp. 629-643, 2003/06/16/ 2003, doi: https://doi.org/10.1016/S0377-2217(02)00334-X.
[140] M. Pluciński, "Application of the Ant Colony Algorithm for the Path Planning," in *Enhanced Methods in Computer Security, Biometric and Artificial Intelligence Systems*, Boston, MA, J. Pejaś and A. Piegat, Eds., 2005// 2005: Springer US, pp. 345-352.
[141] L. Shi, L. Li, W. Zhao, and B. Qu, "A Delay-Constrained Multicast Routing Algorithm Based on the Ant Colony Algorithm," in *Proceedings of the International Conference on Information Engineering and Applications (IEA) 2012*, London, Z. Zhong, Ed., 2013// 2013: Springer London, pp. 875-882.
[142] F. Glover, M. Laguna, and R. Marti, "Scatter Search," in *Advances in Evolutionary Computing: Theory and Applications*, A. Ghosh and S. Tsutsui Eds. Berlin, Heidelberg: Springer Berlin Heidelberg, 2003, pp. 519-537.
[143] K. Price, R. M. Storn, and J. A. Lampinen, *Differential Evolution*, 1 ed. (Natural Computing Series, A Practical Approach to Global Optimization). Springer, Berlin, Heidelberg, 2005, p. 539.
[144] K. V. Price, "Differential Evolution," in *Handbook of Optimization: From Classical to Modern Approach*, I. Zelinka, V. Snášel, and A. Abraham Eds. Berlin, Heidelberg: Springer Berlin Heidelberg, 2013, pp. 187-214.

[145] M. Birattari, L. Paquete, T. Stützle, and K. Varrentrapp, "Classification of metaheuristics and design of experiments for the analysis of components," *Teknik Rapor, AIDA-01-05*, 2001.
[146] D. E. Goldberg and J. H. Holland, "Genetic Algorithms and Machine Learning," *Machine Learning*, vol. 3, no. 2, pp. 95-99, 1988/10/01 1988, doi: 10.1023/A:1022602019183.
[147] S. Mirjalili, "Genetic Algorithm," in *Evolutionary Algorithms and Neural Networks: Theory and Applications*. Cham: Springer International Publishing, 2019, pp. 43-55.
[148] Z. Michalewicz, "Genetic algorithms + data structures = evolution programs (2nd, extended ed.)," 1994.
[149] X.-S. Yang, *Biology-Derived Algorithms in Engineering Optimization*. Taylor & Francis Group, LLC, 2006, 2006, pp. 1-12.
[150] M. Dorigo, M. Birattari, and T. Stutzle, "Ant colony optimization," *IEEE Computational Intelligence Magazine*, vol. 1, no. 4, pp. 28-39, 2006, doi: 10.1109/MCI.2006.329691.
[151] C. Cotta and R. Schaefer, "Bioinspired algorithms and complex systems," *Journal of Computational Science*, vol. 23, pp. 192-194, 2017/11/01/ 2017, doi: https://doi.org/10.1016/j.jocs.2017.11.010.
[152] S. I. Gass and M. C. Fu, "Ant Colony Optimization," in *Encyclopedia of Operations Research and Management Science*. Boston, MA: Springer US, 2013, pp. 72-72.
[153] M. Dorigo, "Optimization, learning and natural algorithms," Ph. D. Thesis, Politecnico di Milano, Italy, 1992.
[154] A. M. Bagirov, N. Karmitsa, and S. Taheri, "Metaheuristic Clustering Algorithms," in *Partitional Clustering via Nonsmooth Optimization: Clustering via Optimization*. Cham: Springer International Publishing, 2020, pp. 165-183.
[155] V. Maniezzo, L. M. Gambardella, and F. de Luigi, "Ant Colony Optimization," in *New Optimization Techniques in Engineering*. Berlin, Heidelberg: Springer Berlin Heidelberg, 2004, pp. 101-121.
[156] S. Mirjalili, "Ant Colony Optimisation," in *Evolutionary Algorithms and Neural Networks: Theory and Applications*, S. Mirjalili Ed. Cham: Springer International Publishing, 2019, pp. 33-42.
[157] U. Setzmann and W. Wagner, "A new method for optimizing the structure of thermodynamic correlation equations," *International Journal of Thermophysics*, vol. 10, no. 6, pp. 1103-1126, 1989.
[158] D. Lichtblau, "Differential evolution in discrete optimization," *International Journal of Swarm Intelligence and Evolutionary Computation*, vol. 1, no. 2012, pp. 1-10, 2012.
[159] Z. Zeng, M. Zhang, T. Chen, and Z. Hong, "A new selection operator for differential evolution algorithm," *Knowledge-Based Systems*, vol. 226, p. 107150, 2021/08/17/ 2021, doi: https://doi.org/10.1016/j.knosys.2021.107150.
[160] K. Zervoudakis and S. Tsafarakis, "A mayfly optimization algorithm," *Computers & Industrial Engineering*, vol. 145, p. 106559, 2020/07/01/ 2020, doi: https://doi.org/10.1016/j.cie.2020.106559.
[161] X. Guo, X. Yan, and K. Jermsittiparsert, "Using the modified mayfly algorithm for optimizing the component size and operation strategy of a high temperature PEMFC-powered CCHP," *Energy Reports*, vol. 7, pp. 1234-1245, 2021/11/01/ 2021, doi: https://doi.org/10.1016/j.egyr.2021.02.042.
[162] M. Li, H. Chen, X. Shi, S. Liu, M. Zhang, and S. Lu, "A multi-information fusion “triple variables with iteration” inertia weight PSO algorithm and its application," *Applied Soft Computing*, vol. 84, p. 105677, 2019.

[163] T. Bhattacharyya, B. Chatterjee, P. K. Singh, J. H. Yoon, Z. W. Geem, and R. Sarkar, "Mayfly in harmony: A new hybrid meta-heuristic feature selection algorithm," *IEEE Access*, vol. 8, pp. 195929-195945, 2020.
[164] R. Bellman, *The theory of dynamic programming*. Bulletin of the American Mathematical Society, 1954, pp. 503-515.
[165] S. Dreyfus, "Richard Bellman on the Birth of Dynamic Programming," *Operations Research*, vol. 50, no. 1, pp. 48-51, 2002, doi: 10.1287/opre.50.1.48.17791.
[166] A. Lew and H. Mauch, "Dynamic Programming: A Computational Tool (Studies in Computational Intelligence)," 2006.
[167] "Introduction to Markov Decision Processes," in *Approximate Dynamic Programming*, 2011, pp. 57-109.
[168] T. H. Cormen, C. E. Leiserson, R. L. Rivest, and C. Stein, *Introduction to Algorithms, Third Edition*. The MIT Press, 2009.
[169] P. Norvig, "Techniques for automatic memoization with applications to context-free parsing," *Comput. Linguist.*, vol. 17, no. 1, pp. 91–98, 1991.
[170] P. Bradley, "The history of simulation in medical education and possible future directions," *Medical education*, vol. 40, no. 3, pp. 254-262, 2006.
[171] E. Petersen and A. Taylor, "A structured model for rail line simulation and optimization," *Transportation Science*, vol. 16, no. 2, pp. 192-206, 1982.
[172] M. M. Dessouky and R. C. Leachman, "A simulation modeling methodology for analyzing large complex rail networks," *Simulation*, vol. 65, no. 2, pp. 131-142, 1995.
[173] N. Zhao, "Railway Traffic Flow Optimisation With Different Control Systems," PhD, Electronic, Electrical and System Engineering, University of Birmingham, Bimingham, 2013.
[174] Z. Li, L. Chen, C. Roberts, and N. Zhao, "Dynamic trajectory optimization design for railway driver advisory system," *IEEE Intelligent Transportation Systems Magazine*, vol. 10, no. 1, pp. 121-132, 2018.
[175] W. ShangGuan, X.-H. Yan, B.-G. Cai, and J. Wang, "Multiobjective optimization for train speed trajectory in CTCS high-speed railway with hybrid evolutionary algorithm," *IEEE Transactions on Intelligent Transportation Systems*, vol. 16, no. 4, pp. 2215-2225, 2015.
[176] Z. Tian *et al.*, "Modeling and simulation of DC rail traction systems for energy saving," in *17th International IEEE Conference on Intelligent Transportation Systems (ITSC)*, 2014: IEEE, pp. 2354-2359.
[177] M.-H. Kang, "A GA-based algorithm for creating an energy-optimum train speed trajectory," *Journal of International Council on Electrical Engineering*, vol. 1, no. 2, pp. 123-128, 2011.
[178] S. Lu, S. Hillmansen, T. K. Ho, and C. Roberts, "Single-train trajectory optimization," *IEEE Transactions on Intelligent Transportation Systems*, vol. 14, no. 2, pp. 743-750, 2013.
[179] H. Douglas, P. Weston, D. Kirkwood, S. Hillmansen, and C. Roberts, "Method for validating the train motion equations used for passenger rail vehicle simulation," *Proceedings of the Institution of Mechanical Engineers, Part F: Journal of Rail and Rapid Transit*, vol. 231, 02/15 2016, doi: 10.1177/0954409716631784.
[180] B. Allotta, R. Conti, E. Meli, and A. Ridolfi, "Modeling and Control of a Full-Scale Roller-Rig for the Analysis of Railway Braking Under Degraded Adhesion Conditions," *IEEE Transactions on Control Systems Technology*, vol. 23, no. 1, pp. 186-196, 2015, doi: 10.1109/TCST.2014.2320672.
[181] W. J. Wang, P. Shen, J. H. Song, J. Guo, Q. Y. Liu, and X. S. Jin, "Experimental study on adhesion behavior of wheel/rail under dry and water conditions," *Wear*, vol. 271,

no. 9, pp. 2699-2705, 2011/07/29/ 2011, doi: https://doi.org/10.1016/j.wear.2011.01.070.
[182] W. Zhang, J. Chen, X. Wu, and X. Jin, "Wheel/rail adhesion and analysis by using full scale roller rig," *Wear*, vol. 253, no. 1, pp. 82-88, 2002/07/01/ 2002, doi: https://doi.org/10.1016/S0043-1648(02)00086-8.
[183] Y. Kimura, M. Sekizawa, and A. Nitanai, "Wear and fatigue in rolling contact," *Wear*, vol. 253, no. 1, pp. 9-16, 2002/07/01/ 2002, doi: https://doi.org/10.1016/S0043-1648(02)00077-7.
[184] H. Hu, A. Batou, and H. Ouyang, "Coefficient of friction random field modelling and analysis in planar sliding," *Journal of Sound and Vibration*, vol. 508, p. 116197, 2021/09/15/ 2021, doi: https://doi.org/10.1016/j.jsv.2021.116197.
[185] A. Baron, M. Mossi, and S. Sibilla, "The alleviation of the aerodynamic drag and wave effects of high-speed trains in very long tunnels," *Journal of Wind Engineering and Industrial Aerodynamics*, vol. 89, no. 5, pp. 365-401, 2001/04/01/ 2001, doi: https://doi.org/10.1016/S0167-6105(00)00071-4.
[186] P. Gkortzas, "Study on optimal train movement for minimum energy consumption," Independent thesis Advanced level (degree of Master (Two Years)) Student thesis, 2013. [Online]. Available: http://urn.kb.se/resolve?urn=urn:nbn:se:mdh:diva-21234
[187] B. P. Rochard and F. Schmid, "A review of methods to measure and calculate train resistances," *Proceedings of the Institution of Mechanical Engineers, Part F: Journal of Rail and Rapid Transit*, vol. 214, no. 4, pp. 185-199, 2000, doi: 10.1243/0954409001531306.
[188] P. Fajri, R. Ahmadi, and M. Ferdowsi, "Test bench for emulating electric-drive vehicle systems using equivalent vehicle rotational inertia," in *2013 IEEE Power and Energy Conference at Illinois (PECI)*, 22-23 Feb. 2013 2013, pp. 83-87, doi: 10.1109/PECI.2013.6506039.
[189] K. Kim and S. I.-J. Chien, "Optimal train operation for minimum energy consumption considering track alignment, speed limit, and schedule adherence," *Journal of Transportation Engineering*, vol. 137, no. 9, pp. 665-674, 2011.
[190] T. Albrecht, C. Gassel, A. Binder, and J. van Luipen, "Dealing with operational constraints in energy efficient driving," in *IET Conference on Railway Traction Systems (RTS 2010)*, 2010: IET, pp. 1-7.
[191] G. H. dos Santos and N. Mendes, "Analysis of numerical methods and simulation time step effects on the prediction of building thermal performance," *Applied Thermal Engineering*, vol. 24, no. 8, pp. 1129-1142, 2004/06/01/ 2004, doi: https://doi.org/10.1016/j.applthermaleng.2003.11.029.
[192] K. Liu, T. Yamamoto, and T. Morikawa, "Impact of road gradient on energy consumption of electric vehicles," *Transportation Research Part D: Transport and Environment*, vol. 54, pp. 74-81, 2017/07/01/ 2017, doi: https://doi.org/10.1016/j.trd.2017.05.005.
[193] P. Suttakul, T. Fongsamootr, W. Wongsapai, Y. Mona, and K. Poolsawat, "Energy consumptions and CO2 emissions of different powertrains under real-world driving with various route characteristics," *Energy Reports*, vol. 8, pp. 554-561, 2022/11/01/ 2022, doi: https://doi.org/10.1016/j.egyr.2022.05.216.
[194] D. S. D. Purba, E. Kontou, and C. Vogiatzis, "Evacuation route planning for alternative fuel vehicles," *Transportation Research Part C: Emerging Technologies*, vol. 143, p. 103837, 2022/10/01/ 2022, doi: https://doi.org/10.1016/j.trc.2022.103837.
[195] G. Jacobs, "Railway Track Diagrams," vol. 2019, 2 ed. Bradford: Trackmaps, 2005.
[196] R. Moeini, P. Weston, P. Tricoli, T. Dinh, A. McGordon, and D. Hughes, "Enhancement of Reliability in Condition Monitoring Techniques in Wind Turbines,"

in *2019 23rd International Conference on Mechatronics Technology (ICMT)*, 23-26 Oct. 2019 2019, pp. 1-6, doi: 10.1109/ICMECT.2019.8932141.

[197] P. Bubna, D. Brunner, J. J. Gangloff, S. G. Advani, and A. K. Prasad, "Analysis, operation and maintenance of a fuel cell/battery series-hybrid bus for urban transit applications," *Journal of Power Sources,* vol. 195, no. 12, pp. 3939-3949, 2010/06/15/ 2010, doi: https://doi.org/10.1016/j.jpowsour.2009.12.080.

[198] O. V. Arriaza, D.-W. Kim, D. Y. Lee, and M. A. Suhaimi, "Trade-off analysis between machining time and energy consumption in impeller NC machining," *Robotics and Computer-Integrated Manufacturing,* vol. 43, pp. 164-170, 2017.

[199] I. Bisaga, P. Parikh, J. Tomei, and L. S. To, "Mapping synergies and trade-offs between energy and the sustainable development goals: A case study of off-grid solar energy in Rwanda," *Energy Policy,* vol. 149, p. 112028, 2021.

[200] D. Gao, Z. Jin, and Q. Lu, "Energy management strategy based on fuzzy logic for a fuel cell hybrid bus," *Journal of Power Sources,* vol. 185, no. 1, pp. 311-317, 2008.

[201] P. Pisu and G. Rizzoni, "A comparative study of supervisory control strategies for hybrid electric vehicles," *IEEE transactions on control systems technology,* vol. 15, no. 3, pp. 506-518, 2007.

[202] A. Sciarretta and L. Guzzella, "Control of hybrid electric vehicles," *IEEE control systems magazine,* vol. 27, no. 2, pp. 60-70, 2007.

[203] H. Li, A. Ravey, A. N'Diaye, and A. Djerdir, "Online adaptive equivalent consumption minimization strategy for fuel cell hybrid electric vehicle considering power sources degradation," *Energy Conversion and Management,* vol. 192, pp. 133-149, 2019/07/15/ 2019, doi: https://doi.org/10.1016/j.enconman.2019.03.090.

[204] Z. Zhang, C. Guan, and Z. Liu, "Real-Time Optimization Energy Management Strategy for Fuel Cell Hybrid Ships Considering Power Sources Degradation," *IEEE Access,* vol. 8, pp. 87046-87059, 2020, doi: 10.1109/ACCESS.2020.2991519.

[205] J. Cao and A. Emadi, "A new battery/ultracapacitor hybrid energy storage system for electric, hybrid, and plug-in hybrid electric vehicles," *IEEE Transactions on power electronics,* vol. 27, no. 1, pp. 122-132, 2011.

[206] D. Wang, Q. Miao, and M. Pecht, "Prognostics of lithium-ion batteries based on relevance vectors and a conditional three-parameter capacity degradation model," *Journal of Power Sources,* vol. 239, pp. 253-264, 2013.

[207] K. M. Almatar, "Transit-Oriented Development in Saudi Arabia: Riyadh as a Case Study," *Sustainability,* vol. 14, no. 23, p. 16129, 2022. [Online]. Available: https://www.mdpi.com/2071-1050/14/23/16129.

[208] K. Mohammed Almatar, "Traffic congestion patterns in the urban road network: (Dammam metropolitan area)," *Ain Shams Engineering Journal,* vol. 14, no. 3, p. 101886, 2023/04/01/ 2023, doi: https://doi.org/10.1016/j.asej.2022.101886.

[209] M. W. Jeter, "Mathematical Programming: An Introduction to Optimization," 1986.

[210] K. Deng *et al.*, "Deep reinforcement learning based energy management strategy of fuel cell hybrid railway vehicles considering fuel cell aging," *Energy Conversion and Management,* vol. 251, p. 115030, 2022/01/01/ 2022, doi: https://doi.org/10.1016/j.enconman.2021.115030.

[211] H. Peng, J. Li, L. Löwenstein, and K. Hameyer, "A scalable, causal, adaptive energy management strategy based on optimal control theory for a fuel cell hybrid railway vehicle," *Applied Energy,* vol. 267, p. 114987, 2020/06/01/ 2020, doi: https://doi.org/10.1016/j.apenergy.2020.114987.

[212] P. Shao, W. Guo, Q. Lei, and C. Zeng, "Adaptive compound control for the real-time hybrid simulation of high-speed railway train–bridge coupling vibration," *Structural*

Control and Health Monitoring, vol. 28, no. 11, p. e2816, 2021, doi: https://doi.org/10.1002/stc.2816.

[213] A. R. Albrecht, P. G. Howlett, P. J. Pudney, and X. Vu, "Energy-efficient train control: From local convexity to global optimization and uniqueness," *Automatica,* vol. 49, no. 10, pp. 3072-3078, 2013.

[214] D. He, L. Zhang, S. Guo, Y. Chen, S. Shan, and H. Jian, "Energy-efficient train trajectory optimization based on improved differential evolution algorithm and multi-particle model," *Journal of Cleaner Production,* vol. 304, p. 127163, 2021/07/01/ 2021, doi: https://doi.org/10.1016/j.jclepro.2021.127163.

[215] X. Yan, B. Cai, B. Ning, and W. ShangGuan, "Online distributed cooperative model predictive control of energy-saving trajectory planning for multiple high-speed train movements," *Transportation Research Part C: Emerging Technologies,* vol. 69, pp. 60-78, 2016/08/01/ 2016, doi: https://doi.org/10.1016/j.trc.2016.05.019.

[216] W. ShangGuan, X. H. Yan, B. G. Cai, and J. Wang, "Multiobjective Optimization for Train Speed Trajectory in CTCS High-Speed Railway With Hybrid Evolutionary Algorithm," *IEEE Transactions on Intelligent Transportation Systems,* vol. 16, no. 4, pp. 2215-2225, 2015, doi: 10.1109/TITS.2015.2402160.

[217] I.-S. Sorlei *et al.*, "Fuel Cell Electric Vehicles—A Brief Review of Current Topologies and Energy Management Strategies," *Energies,* vol. 14, no. 1, p. 252, 2021. [Online]. Available: https://www.mdpi.com/1996-1073/14/1/252.

[218] E. Kamal and L. Adouane, "Optimized EMS and a Comparative Study of Hybrid Hydrogen Fuel Cell/Battery Vehicles," *Energies,* vol. 15, no. 3, p. 738, 2022. [Online]. Available: https://www.mdpi.com/1996-1073/15/3/738.

[219] W. Zhang *et al.*, "Comparison of daily operation strategies for a fuel cell/battery tram," *International Journal of Hydrogen Energy,* vol. 42, no. 29, pp. 18532-18539, 2017/07/20/ 2017, doi: https://doi.org/10.1016/j.ijhydene.2017.04.151.

[220] Q. Li *et al.*, "Online extremum seeking-based optimized energy management strategy for hybrid electric tram considering fuel cell degradation," *Applied Energy,* vol. 285, p. 116505, 2021/03/01/ 2021, doi: https://doi.org/10.1016/j.apenergy.2021.116505.

[221] Y. Yan, Q. Li, W. Chen, B. Su, J. Liu, and L. Ma, "Optimal Energy Management and Control in Multimode Equivalent Energy Consumption of Fuel Cell/Supercapacitor of Hybrid Electric Tram," *IEEE Transactions on Industrial Electronics,* vol. 66, no. 8, pp. 6065-6076, 2019, doi: 10.1109/TIE.2018.2871792.

[222] Y. Yan, Q. Li, W. Chen, W. Huang, and J. Liu, "Hierarchical Management Control Based on Equivalent Fitting Circle and Equivalent Energy Consumption Method for Multiple Fuel Cells Hybrid Power System," *IEEE Transactions on Industrial Electronics,* vol. 67, no. 4, pp. 2786-2797, 2020, doi: 10.1109/TIE.2019.2908615.

[223] Y. Yan, Q. Li, W. Huang, and W. Chen, "Operation Optimization and Control Method Based on Optimal Energy and Hydrogen Consumption for the Fuel Cell/Supercapacitor Hybrid Tram," *IEEE Transactions on Industrial Electronics,* vol. 68, no. 2, pp. 1342-1352, 2021, doi: 10.1109/TIE.2020.2967720.

[224] D. Sofía Mendoza, J. Solano, and L. Boulon, "Energy management strategy to optimise regenerative braking in a hybrid dual-mode locomotive," *IET Electrical Systems in Transportation,* vol. 10, no. 4, pp. 391-400, 2020, doi: https://doi.org/10.1049/iet-est.2020.0070.

[225] Q. Li, W. Huang, W. Chen, Y. Yan, W. Shang, and M. Li, "Regenerative braking energy recovery strategy based on Pontryagin's minimum principle for fell cell/supercapacitor hybrid locomotive," *International Journal of Hydrogen Energy,* vol. 44, no. 11, pp. 5454-5461, 2019/02/26/ 2019, doi: https://doi.org/10.1016/j.ijhydene.2018.10.115.

[226] D. Chen, N. Prakash, A. Stefanopoulou, M. Huang, Y. Kim, and S. Hotz, "Sequential optimization of velocity and charge depletion in a plug-in hybrid electric vehicle," in *14th International Symposium on Advanced Vehicle Control*, 2018.

[227] Y. V. Bocharnikov, A. M. Tobias, and C. Roberts, "Reduction of train and net energy consumption using genetic algorithms for Trajectory Optimisation," in *IET Conference on Railway Traction Systems (RTS 2010)*, 13-15 April 2010 2010, pp. 1-5, doi: 10.1049/ic.2010.0038.

[228] J. C. J. Goodwin, D. I. Fletcher, and R. F. Harrison, "Multi-train trajectory optimisation to maximise rail network energy efficiency under travel-time constraints," *Proceedings of the Institution of Mechanical Engineers, Part F: Journal of Rail and Rapid Transit*, vol. 230, no. 4, pp. 1318-1335, 2016/05/01 2015, doi: 10.1177/0954409715593304.

[229] H. A. Hamid, G. L. Nicholson, H. Douglas, N. Zhao, and C. Roberts, "Investigation into train positioning systems for saving energy with optimised train trajectories," in *2016 IEEE International Conference on Intelligent Rail Transportation (ICIRT)*, 23-25 Aug. 2016 2016, pp. 460-468, doi: 10.1109/ICIRT.2016.7588769.

[230] Y. V. Bocharnikov, A. M. Tobias, C. Roberts, S. Hillmansen, and C. J. Goodman, "Optimal driving strategy for traction energy saving on DC suburban railways," *IET Electric Power Applications*, vol. 1, no. 5, pp. 675-682. [Online]. Available: https://digital-library.theiet.org/content/journals/10.1049/iet-epa_20070005

[231] A. P. Cucala, A. Fernández, C. Sicre, and M. Domínguez, "Fuzzy optimal schedule of high speed train operation to minimize energy consumption with uncertain delays and driver's behavioral response," *Engineering Applications of Artificial Intelligence*, vol. 25, no. 8, pp. 1548-1557, 2012/12/01/ 2012, doi: https://doi.org/10.1016/j.engappai.2012.02.006.

[232] C. S. Chang and S. S. Sim, "Optimising train movements through coast control using genetic algorithms," *IEE Proceedings - Electric Power Applications*, vol. 144, no. 1, pp. 65-73. [Online]. Available: https://digital-library.theiet.org/content/journals/10.1049/ip-epa_19970797

[233] N. Zhao, C. Roberts, S. Hillmansen, and G. Nicholson, "A Multiple Train Trajectory Optimization to Minimize Energy Consumption and Delay," *IEEE Transactions on Intelligent Transportation Systems*, vol. 16, no. 5, pp. 2363-2372, 2015, doi: 10.1109/TITS.2014.2388356.

[234] N. Zhao *et al.*, "Train trajectory optimisation of ATO systems for metro lines," in *17th International IEEE Conference on Intelligent Transportation Systems (ITSC)*, 2014: IEEE, pp. 1796-1801.

[235] N. Zhao, C. Roberts, and S. Hillmansen, "The application of an enhanced Brute Force algorithm to minimise energy costs and train delays for differing railway train control systems," *Proceedings of the Institution of Mechanical Engineers, Part F: Journal of Rail and Rapid Transit*, vol. 228, no. 2, pp. 158-168, 2014, doi: 10.1177/0954409712468231.

[236] F. De Cuadra, A. Fernandez, J. De Juan, and M. Herrero, "Energy-saving automatic optimisation of train speed commands using direct search techniques," *WIT Transactions on The Built Environment*, vol. 20, 1970.

[237] K. K. Wong and T. K. Ho, "Coast control for mass rapid transit railways with searching methods," *IEE Proceedings - Electric Power Applications*, vol. 151, no. 3, pp. 365-376. [Online]. Available: https://digital-library.theiet.org/content/journals/10.1049/ip-epa_20040346

[238] A. Ben-Tal and A. Nemirovski, "Robust Convex Optimization," *Mathematics of Operations Research*, vol. 23, no. 4, pp. 769-805, 1998, doi: 10.1287/moor.23.4.769.

[239] Y. Wang, B. Ning, T. Tang, T. J. Van Den Boom, and B. De Schutter, "Efficient real-time train scheduling for urban rail transit systems using iterative convex programming," *IEEE Transactions on Intelligent Transportation Systems*, vol. 16, no. 6, pp. 3337-3352, 2015.

[240] G. Maróti, "A branch-and-bound approach for robust railway timetabling," *Public Transport*, vol. 9, no. 1, pp. 73-94, 2017/07/01 2017, doi: 10.1007/s12469-016-0143-x.

[241] W. ShangGuan, X. Yan, B. Cai, and J. Wang, "Multiobjective Optimization for Train Speed Trajectory in CTCS High-Speed Railway With Hybrid Evolutionary Algorithm," *IEEE Transactions on Intelligent Transportation Systems*, vol. 16, no. 4, pp. 2215-2225, 2015, doi: 10.1109/TITS.2015.2402160.

[242] S. van Dooren, C. Balerna, M. Salazar, A. Amstutz, and C. H. Onder, "Optimal Diesel engine calibration using convex modelling of Pareto frontiers," *Control Engineering Practice*, vol. 96, p. 104313, 2020/03/01/ 2020, doi: https://doi.org/10.1016/j.conengprac.2020.104313.

[243] S. Makkonen and R. Lahdelma, "Non-convex power plant modelling in energy optimisation," *European Journal of Operational Research*, vol. 171, no. 3, pp. 1113-1126, 2006/06/16/ 2006, doi: https://doi.org/10.1016/j.ejor.2005.01.020.

[244] H. A. L. Thi, H. M. Le, and T. P. Dinh, "Fuzzy clustering based on nonconvex optimisation approaches using difference of convex (DC) functions algorithms," *Advances in Data Analysis and Classification*, vol. 1, no. 2, pp. 85-104, 2007/08/01 2007, doi: 10.1007/s11634-007-0011-2.

[245] E. S. Riis, M. J. Ehrhardt, G. R. W. Quispel, and C.-B. Schönlieb, "A Geometric Integration Approach to Nonsmooth, Nonconvex Optimisation," *Foundations of Computational Mathematics*, 2021/07/29 2021, doi: 10.1007/s10208-020-09489-2.

[246] J. Bernstein, Y.-X. Wang, K. Azizzadenesheli, and A. Anandkumar, "signSGD: Compressed Optimisation for Non-Convex Problems," presented at the Proceedings of the 35th International Conference on Machine Learning, Proceedings of Machine Learning Research, 2018. [Online]. Available: https://proceedings.mlr.press/v80/bernstein18a.html.

[247] O. Karakuş, P. Mayo, and A. Achim, "Convergence Guarantees for Non-Convex Optimisation With Cauchy-Based Penalties," *IEEE Transactions on Signal Processing*, vol. 68, pp. 6159-6170, 2020, doi: 10.1109/TSP.2020.3032231.

[248] S. Uebel, N. Murgovski, C. Tempelhahn, and B. Bäker, "Optimal Energy Management and Velocity Control of Hybrid Electric Vehicles," *IEEE Transactions on Vehicular Technology*, vol. 67, no. 1, pp. 327-337, 2018, doi: 10.1109/TVT.2017.2727680.

[249] Y. Kim, M. Figueroa-Santos, N. Prakash, S. Baek, J. B. Siegel, and D. M. Rizzo, "Co-optimization of speed trajectory and power management for a fuel-cell/battery electric vehicle," *Applied Energy*, vol. 260, p. 114254, 2020/02/15/ 2020, doi: https://doi.org/10.1016/j.apenergy.2019.114254.

[250] H. Peng *et al.*, "Co-optimization of total running time, timetables, driving strategies and energy management strategies for fuel cell hybrid trains," *eTransportation*, vol. 9, p. 100130, 2021/08/01/ 2021, doi: https://doi.org/10.1016/j.etran.2021.100130.

[251] R. Jibrin, S. Hillmansen, C. Roberts, N. Zhao, and Z. Tian, "Convex optimization of speed and energy management system for fuel cell hybrid trains," in *2021 IEEE Vehicle Power and Propulsion Conference (VPPC)*, 2021: IEEE, pp. 1-6.

[252] M. H. Zafar, N. M. Khan, A. F. Mirza, and M. Mansoor, "Bio-inspired optimization algorithms based maximum power point tracking technique for photovoltaic systems under partial shading and complex partial shading conditions," *Journal of Cleaner Production*, vol. 309, p. 127279, 2021.

[253] M. R. Bonyadi and Z. Michalewicz, "Particle swarm optimization for single objective continuous space problems: a review," *Evolutionary computation,* vol. 25, no. 1, pp. 1-54, 2017.
[254] M. H. K. Roni, M. Rana, H. Pota, M. M. Hasan, and M. S. Hussain, "Recent trends in bio-inspired meta-heuristic optimization techniques in control applications for electrical systems: A review," *International Journal of Dynamics and Control,* pp. 1-13, 2022.
[255] H. Rosenbrock, "An automatic method for finding the greatest or least value of a function," *The computer journal,* vol. 3, no. 3, pp. 175-184, 1960.
[256] S. Dasgupta and B. Saha, "HMA-ID mechanism: a hybrid mayfly optimisation based apriori approach for intrusion detection in big data application," *Telecommunication Systems,* vol. 80, no. 1, pp. 77-89, 2022.
[257] G. Shruthi, M. R. Mundada, B. Sowmya, and S. Supreeth, "Mayfly taylor optimisation-based scheduling algorithm with deep reinforcement learning for dynamic scheduling in fog-cloud computing," *Applied Computational Intelligence and Soft Computing,* vol. 2022, 2022.
[258] A. Jain and A. Gupta, "Review on Recent Developments in the Mayfly Algorithm," in *Proceedings of the International Conference on Paradigms of Communication, Computing and Data Sciences: PCCDS 2021*, 2022: Springer, pp. 347-357.
[259] S. Mizzi, "Improved Mayfly Algorithm for Optimal Design of Hybrid PV/Diesel Generator along with Battery: Application to Shilisha Village in Maowusu Desert, China," *Journal of Smart Systems and Stable Energy,* vol. 1, no. 4, pp. 333-348, 2022.
[260] R. Rajabioun, "Cuckoo optimization algorithm," *Applied soft computing,* vol. 11, no. 8, pp. 5508-5518, 2011.
[261] V. Veerakumaran and A. Rajini, "An Energy-Efficient Adaptive Mayfly Optimization Algorithm Based Optimal Routing in Wireless Sensor Network for Military Application," in *2021 International Conference on Advancements in Electrical, Electronics, Communication, Computing and Automation (ICAECA)*, 2021: IEEE, pp. 1-6.
[262] O. Ferreira, A. Iusem, and S. Németh, "Concepts and techniques of optimization on the sphere," *Top,* vol. 22, no. 3, pp. 1148-1170, 2014.
[263] Y. Huang, J.-p. Li, and P. Wang, "Unusual phenomenon of optimizing the Griewank function with the increase of dimension," *Frontiers of Information Technology & Electronic Engineering,* vol. 20, no. 10, pp. 1344-1360, 2019.
[264] M. Molga and C. Smutnicki, "Test functions for optimization needs," *Test functions for optimization needs,* vol. 101, p. 48, 2005.
[265] G. Zhu and S. Kwong, "Gbest-guided artificial bee colony algorithm for numerical function optimization," *Applied mathematics and computation,* vol. 217, no. 7, pp. 3166-3173, 2010.
[266] Y. Shang and Y. Qiu, "A Note on the Extended Rosenbrock Function," *Evolutionary Computation,* vol. 14, no. 1, pp. 119-126, 2006, doi: 10.1162/evco.2006.14.1.119.
[267] S. Motiian and H. Soltanian-Zadeh, "Improved particle swarm optimization and applications to hidden markov model and ackley function," in *2011 IEEE International Conference on Computational Intelligence for Measurement Systems and Applications (CIMSA) Proceedings*, 2011: IEEE, pp. 1-4.
[268] D. U. Sauer, "BATTERIES | Charge–Discharge Curves," in *Encyclopedia of Electrochemical Power Sources*, J. Garche Ed. Amsterdam: Elsevier, 2009, pp. 443-451.

[269] L. Wang, "Research and Implementation of Machine Learning Classifier Based on KNN," *IOP Conference Series: Materials Science and Engineering*, vol. 677, p. 052038, 2019/12/10 2019, doi: 10.1088/1757-899x/677/5/052038.
[270] X. Lin, P. Bogdan, N. Chang, and M. Pedram, "Machine learning-based energy management in a hybrid electric vehicle to minimize total operating cost," *2015 IEEE/ACM International Conference on Computer-Aided Design (ICCAD)*, pp. 627-634, 2015.
[271] X. Hu, S. E. Li, and Y. Yang, "Advanced Machine Learning Approach for Lithium-Ion Battery State Estimation in Electric Vehicles," *IEEE Transactions on Transportation Electrification*, vol. 2, no. 2, pp. 140-149, 2016, doi: 10.1109/TTE.2015.2512237.
[272] E. Alpaydin, "Introduction to machine learning," in *Adaptive computation and machine learning*, 2004.
[273] G. Krummenacher, C. S. Ong, S. Koller, S. Kobayashi, and J. M. Buhmann, "Wheel Defect Detection With Machine Learning," *IEEE Transactions on Intelligent Transportation Systems*, vol. 19, no. 4, pp. 1176-1187, 2018, doi: 10.1109/TITS.2017.2720721.
[274] A. Rageh, S. Eftekhar Azam, and D. G. Linzell, "Steel railway bridge fatigue damage detection using numerical models and machine learning: Mitigating influence of modeling uncertainty," *International Journal of Fatigue*, vol. 134, p. 105458, 2020/05/01/ 2020, doi: https://doi.org/10.1016/j.ijfatigue.2019.105458.
[275] H. Tsunashima, "Condition Monitoring of Railway Tracks from Car-Body Vibration Using a Machine Learning Technique," *Applied Sciences*, vol. 9, no. 13, p. 2734, 2019. [Online]. Available: https://www.mdpi.com/2076-3417/9/13/2734.
[276] L. Dai, "A machine learning approach for optimisation in railway planning," 2018.
[277] V. S. Dave and K. Dutta, "Neural network based models for software effort estimation: a review," *Artificial Intelligence Review*, vol. 42, no. 2, pp. 295-307, 2014.
[278] H. He and E. A. Garcia, "Learning from imbalanced data," *IEEE Transactions on knowledge and data engineering*, vol. 21, no. 9, pp. 1263-1284, 2009.
[279] A. Mozaffari, M. Emami, and A. Fathi, "A comprehensive investigation into the performance, robustness, scalability and convergence of chaos-enhanced evolutionary algorithms with boundary constraints," *Artificial Intelligence Review*, vol. 52, no. 4, pp. 2319-2380, 2019.
[280] N. Izeboudjen, C. Larbes, and A. Farah, "A new classification approach for neural networks hardware: from standards chips to embedded systems on chip," *Artificial Intelligence Review*, vol. 41, no. 4, pp. 491-534, 2014.
[281] M. Saki, M. Abolhasan, and J. Lipman, "A Novel Approach for Big Data Classification and Transportation in Rail Networks," *IEEE Transactions on Intelligent Transportation Systems*, vol. 21, pp. 1239-1249, 2020.
[282] O. I. Abiodun, A. Jantan, A. E. Omolara, K. V. Dada, N. A. Mohamed, and H. Arshad, "State-of-the-art in artificial neural network applications: A survey," *Heliyon*, vol. 4, no. 11, p. e00938, 2018/11/01/ 2018, doi: https://doi.org/10.1016/j.heliyon.2018.e00938.
[283] A. J. Mehta, H. A. Mehta, T. Manjunath, and C. Ardil, "A multi-layer artificial neural network architecture design for load forecasting in power systems," *International Journal of Electrical and Computer Engineering*, vol. 5, no. 2, pp. 207-220, 2008.
[284] V. Khryashchev, L. Ivanovsky, V. Pavlov, A. Ostrovskaya, and A. Rubtsov, "Comparison of different convolutional neural network architectures for satellite image segmentation," in *2018 23rd conference of open innovations association (FRUCT)*, 2018: IEEE, pp. 172-179.

[285] P. Benardos and G.-C. Vosniakos, "Optimizing feedforward artificial neural network architecture," *Engineering applications of artificial intelligence,* vol. 20, no. 3, pp. 365-382, 2007.
[286] G. Bebis and M. Georgiopoulos, "Feed-forward neural networks," *IEEE Potentials,* vol. 13, no. 4, pp. 27-31, 1994.
[287] B. Warsito, R. Santoso, and H. Yasin, "Cascade forward neural network for time series prediction," in *Journal of Physics: Conference Series*, 2018, vol. 1025, no. 1: IOP Publishing, p. 012097.
[288] S. Gündoğdu and T. Elbir, "Application of feed forward and cascade forward neural network models for prediction of hourly ambient air temperature based on MERRA-2 reanalysis data in a coastal area of Turkey," *Meteorology and Atmospheric Physics,* vol. 133, no. 5, pp. 1481-1493, 2021.
[289] R. Rojas, "The backpropagation algorithm," in *Neural networks*: Springer, 1996, pp. 149-182.
[290] Y. Xinghuo, M. O. Efe, and O. Kaynak, "A general backpropagation algorithm for feedforward neural networks learning," *IEEE Transactions on Neural Networks,* vol. 13, no. 1, pp. 251-254, 2002, doi: 10.1109/72.977323.
[291] B. Ozkaya, A. Demir, and M. S. Bilgili, "Neural network prediction model for the methane fraction in biogas from field-scale landfill bioreactors," *Environmental Modelling & Software,* vol. 22, no. 6, pp. 815-822, 2007/06/01/ 2007, doi: https://doi.org/10.1016/j.envsoft.2006.03.004.